Spring 2012

Investigation of electrical and impact properties of carbon fiber reinforced polymer matrix composites with carbon nanotube buckypaper layers

Christopher Brandon Hill
University of Iowa

INVESTIGATION OF ELECTRICAL AND IMPACT PROPERTIES OF CARBON FIBER REINFORCED POLYMER MATRIX COMPOSITES WITH CARBON NANOTUBE BUCKYPAPER LAYERS

by

Christopher Brandon Hill

A thesis submitted in partial fulfillment
of the requirements for the Master of
Science degree in Mechanical Engineering
in the Graduate College of
The University of Iowa

May 2012

Thesis Supervisor: Assistant Professor Olesya I. Zhupanska

Graduate College
The University of Iowa
Iowa City, Iowa

CERTIFICATE OF APPROVAL

_____

MASTER'S THESIS

_____

This is to certify that the Master's thesis of

Christopher Brandon Hill

has been approved by the Examining Committee
for the thesis requirement for the Master of Science
degree in Mechanical Engineering at the May 2012 graduation.

Thesis Committee: _____
Olesya I. Zhupanska, Thesis Supervisor

_____
Sharif Rahman

_____
Albert Ratner

To My Family

ACKNOWLEDGMENTS

I would like to thank Professor Olesya Zhupanska for her support and guidance through this research and my graduate education. Both my experimental work and studies have been rewarding and enjoyable experiences. I also thank Professors Sharif Rahman and Albert Ratner for serving on my thesis committee. Lastly I would like to express gratitude to Yeqing Wang for his assistance with the present work and Robert Hart for his invaluable teachings in the past.

TABLE OF CONTENTS

LIST OF TABLES

LIST OF FIGURES

CHAPTER 1

INTRODUCTION

1.1 Motivation

Composite materials in general and carbon fiber (CF)/carbon nanotube (CNT) buckypaper polymer matrix composites specifically derive their properties from a complex hierarchical material structure, in which a matrix phase is combined with reinforcement phases (e.g. carbon fibers, aramid fibers, carbon nanotube buckypaper, etc.) to achieve desirable mechanical and functional responses. These desired properties can include stiffness, thermal behavior, electrical behavior, and strength to weight ratios among many others. Historically, the primary developments in composites were motivated by enhancing a singular capacity of the material. Examples of this include the improvement of electrical conductivity and magnetic properties for the use of composites in EMI shielding, increased heat operating capacity in composites designed for thermal protection systems, and improved structural capabilities such as in the use of fiber reinforced laminate materials in aerospace structures. Due to these singular motivations a majority of the theoretical and experimental developments have been strictly limited to the investigation of the properties that were dictated by the specific applications of the composites. Though this strategy has led to great achievements in the field of composites in the past, future technological advancements will demand materials with multifunctional capabilities which will be required to provide one or more additional functions beyond their primary role or be able to adapt performance wise in response to

their operating environment. Composite materials lend themselves naturally to the concept of multifunctionality, where a material or structure performs more than one function. A multifunctional material could be designed for structural support as well as a variety of other functions such as energy storage, actuation, damage sensing, etc. Therefore, studies of coupled electrical, magnetic, thermal, and mechanical properties among other fields in composites are critical in moving towards their multifunctional use.

In the research for this thesis the electrical and impact properties of carbon fiber reinforced polymer matrix composites with carbon nanotube buckypaper layers are investigated. This has been inspired by the work of past researchers who investigated carbon fiber reinforced polymer matrix composites and their changes in impact resistances with electrification (Sierakowski et al., 2008; Telitchev et al., 2008; Telitchev et al., 2008a). The results of their research showed that the impact resistance of carbon fiber reinforced composites can be improved by subjecting them to an electrical load coinciding with the moment of impact. It was also noticed that the magnitude of the applied electrical current had a considerable effect on the propagation of impact damage on the composite: the stronger the applied current, the less impact damage was observed in the experiments. Furthermore, the research demonstrated that the duration of the current application and current-induced heating played an important role in the impact behavior of the electrified composites. It was found that while a short-term current application benefits the impact resistance of the composites, a prolonged application of electrical current appeared to have detrimental effects. Reduction in the electrical current duration and increase in the current magnitude motivated this work in exploring the effects of pulsed electrical currents. Moreover, the addition of carbon nanotube

buckypaper layers to conventional carbon fiber reinforced polymer matrix composites enabled the increase in overall conductivity of such composites, and thus, responsiveness of the composites to the application of electromagnetic fields.

The main goal of this thesis was to investigate the effect of the addition of carbon nanotube buckypaper on the electrical and impact behavior of carbon fiber polymer matrix composite laminates. This thesis is separated into multiple sections, the first of which are background information and literature review which are followed by the thesis objectives. The materials used in this work and composite sample manufacturing are discussed in Chapter 2. The experimental studies and results obtained in this work are reported in Chapters 3, 4, 5, and 6. Lastly a summary of all work and recommendations for future work are given in Chapter 7.

1.2 Background Information

The term composite material covers a very broad group. At its core, a composite material can be defined as a material that consists of at least two independent constituents and that those elements are combined on a macroscopic level (Jones, 2009). The types of materials and manufacturing methods of composites are practically limitless. Composites can contain metals, ceramics, or polymers and come in fiber, whisker, particle, or strips. Materials can be combined by using many forms as well, including being laminated, suspended, vapor deposited, or clad. An example of a laminated fiber reinforced composite material is shown below in Figure 1.1.

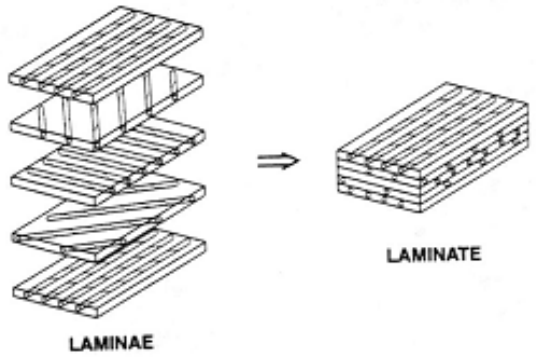

Figure 1.1: Laminas being combined into a Laminate (Food and Agriculture Organizations of the United Nations, 2003)

Composite materials are both naturally occurring, such as wood or bone, and manufactured, such as fiberglass and carbon fiber. The intent of a composite is to have a material that displays all properties favorable to its use and minimizes all others. By combining two or more materials it is possible to produce make a material that displays the most beneficial properties of one material while eliminating its weaker ones (Jones, 2009). It is even possible to produce a composite that displays better properties than any of its constituents (Jones, 2009). These beneficial properties could include strength, stiffness, wear resistance, weight, or electrical and thermal properties among many others.

There are numerous examples of products that have been made better through the use of composites. These include sporting good products such as golf clubs and hockey sticks that now use fiber reinforced composites instead of traditional materials such as metals and woods. The newer designs of these products are stronger, longer lasting, and much lighter than their previous models. Another example of composite materials being

used is in aerospace applications. Newer aircraft are using larger and larger percentages of composite materials for their structural components including wings, landing gear, and engine support structure. An example of this is the Bell Boeing V-22 Osprey which is produced with approximately 50 percent of its weight as composites (Deo et al., 2001). This is because the components can be made much lighter which directly correlates to fuel savings for the purchasers of the aircraft. Another example of aerospace applications for composite materials is shown in Figure 1.2 with a Lockheed F-35 Lightning II fighter jet. It can be seen that major components including the upper and lower wing skins and nacelle are produced using composite materials.

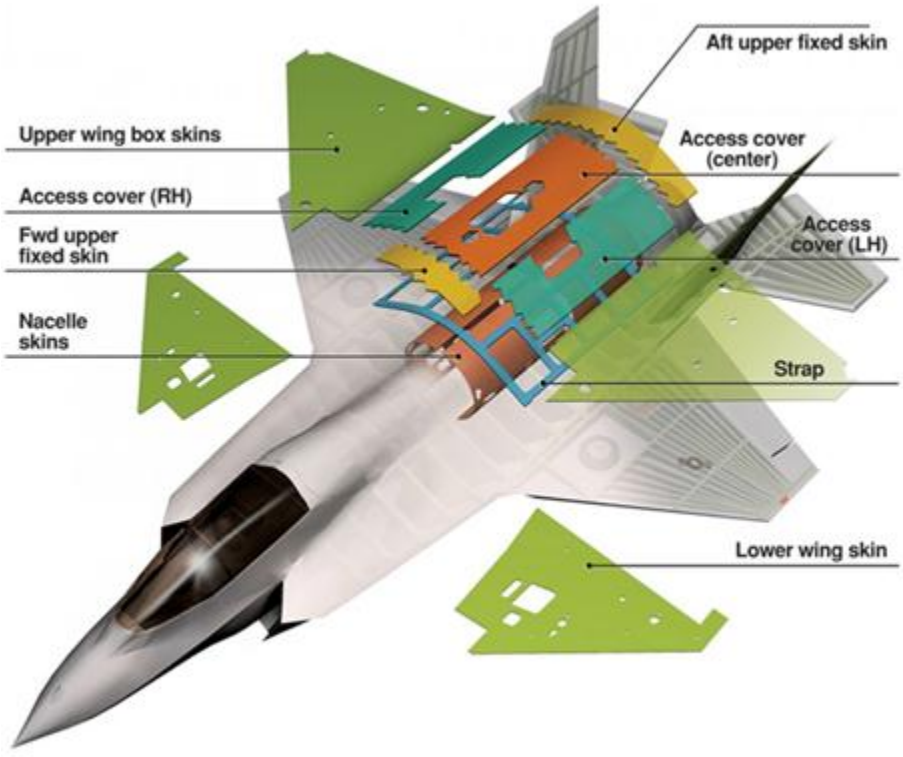

Figure 1.2: Composite components on Lockheed Martin F-35 Lightning II (Shaw, 2011)

1.3 Literature Review

As the applications for composite materials, and specifically carbon fiber reinforced composites, have continued to expand so has the technical research allowing composites to be used to their full potential. Several research areas that have been highly focused include damage detection, electrical characterization, and the relationships between the electrical and mechanical properties of the composites. The researchers focused on damage detection in composite materials have investigated the failure modes of composites and devised methods for both periodically and dynamically testing composite components for strength degradation. The electrical characterization work has been applied to real world situations such as lightning strikes on an aircraft with composite components. The electrical and mechanical properties research has led to the understanding of principals such as the Lorentz force as it applies to composite materials and has shown promises in increased impact resistance of composites when electrical fields are applied.

1.3.1 Carbon Fiber Reinforced Polymer Composites

Carbon fibers reinforced polymer composites are widely used in many applications from advanced aerospace equipment, to high performance racing cars, to reinforcement of concrete structures (Fortress Stabilization Systems, 2011). Properties that make carbon fiber materials so widely used include high strength, low density, and low coefficient of thermal expansion (JCMA, 2011). Thermosetting epoxy resins are the

most prevalent matrix material in carbon fiber composites with over 90 percent of materials using them (Stenzenberger, 1993).

Carbon fibers can be made from a variety of precursors including PAN (polyacrylonitrile) based, pitch based, and rayon based materials, with PAN based being the most common (JCMA, 2011). To make carbon fiber several steps are required, first of which includes preparing the precursor by heating it to 200 to 300 degrees Celsius. Next the material is transferred to an oxygen free environment and heated further to 1000 to 3000 °C. Because there is no oxygen the fibers cannot burn and instead carbonize by releasing all of their non-carbon atoms. The remaining carbon items crystallize that are aligned parallel to the axis of the fiber. The last step involves slightly oxidizing and coating the surface to ensure proper adhesion to epoxies and overall protection. A finished carbon fiber will be between 0.005 and 0.01 mm (How Products are Made, 2011).

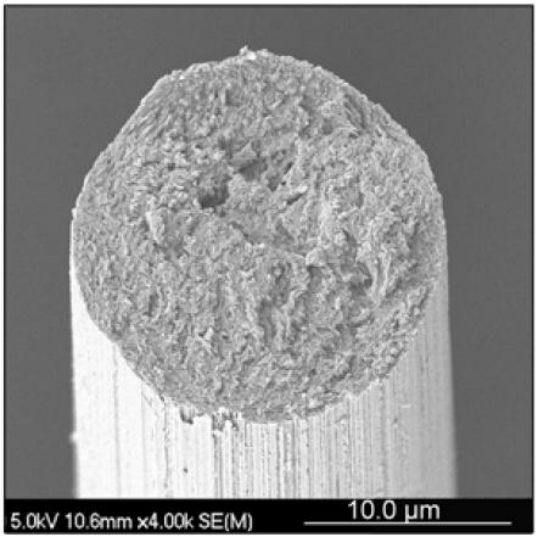

Figure 1.3: Magnified view of an end of a carbon fiber carbonized at 1000 °C (Wazir and Kakakhel, 2009)

Epoxide resins are a large group of thermosetting matrix products each with unique strengths, weaknesses, and applications. The main groups of epoxy resins include Bisphenol resins, Novalac resins, Trifunctional resins, Tetrafunctional resins, and Cycloaliphatic resins, each with their own constituents and chemical structure (Morgan, 2005). What defines a thermosetting resin as an epoxy is a reaction group consisting of two carbon atoms and one oxygen atom. Resins with more epoxy groups per molecule have higher temperature ranges and lower toughness while fewer groups leads to the opposite, with lower temperature ranges and higher toughness (McCarvill and Strong, 2005).

Combined carbon fibers and epoxy matrices can produce truly impressive materials. Many characteristics that make carbon fiber reinforced composites attractive for many structural applications include low density, high strength and stiffness, good damage and toughness tolerances. They also are very electrically conducive along the directions of the fibers as well as provide great shielding of components from electromagnetic interference (Chung, 2010). As production and cost factors for carbon fiber reinforced polymers are continued to be improved so will the number of products that they will be used in.

1.3.2 Carbon Nanotubes and Buckypaper Material

Carbon nanotubes have held many promises since their inception for a wide array of applications including structural and electrical components as well as for specialized equipment such as tips for atomic force microscopy (Harris, 2009). Though known about

prior, the first physical carbon nanotubes were discovered in 1991 by Sumio Iijima at the NEC Corporation in Japan. There he found that needles were growing on the negative end of an electrode that was being used for an arc-discharge evaporation method and that these needles were circular tubes made of carbon atoms (Iijima, 1991). After their first discovery thousands of researchers turned their attention to the production and investigation of carbon nanotubes resulting in many breakthroughs. One of which is the production of nanotube by not only arc-discharge evaporation but also chemical vapor deposition which has allowed for large scale production of the materials (Harris, 2009).

Carbon nanotubes can grow in practically unlimited different sizes and configurations. They can be produced as single walled nanotubes (SWNTs), where there is only one coaxial carbon structure or multi-walled nanotubes (MWNTs), where two or more nanotubes are nested into each other. An example of a multi-walled carbon nanotube is shown in Figure 1.4. The three structures that categorize carbon nanotubes are the armchair form, zigzag form, and helical form each depicting how the carbon nanotubes are structured (Iijima, 2002). The three forms are shown in Figure 1.5. Carbon nanotubes can also differ on how their ends are structured with some nanotubes having caps on their ends while others remain as was seen in the MWNT image in Figure 1.4 (Harris, 2009). The experimental testing of multi-walled carbon nanotubes have shown tensile strengths of 0.15 TPa and a Young's modulus of 0.8 TPa (Demczyk et al., 2001). Other researchers have found the resistivity of single carbon nanotubes to be as low as 0.051 micro ohm meters (Ebbesen et al., 1996). With these attractive properties it is easy to understand why many researchers and corporations have spent so much energy into understanding carbon nanotubes.

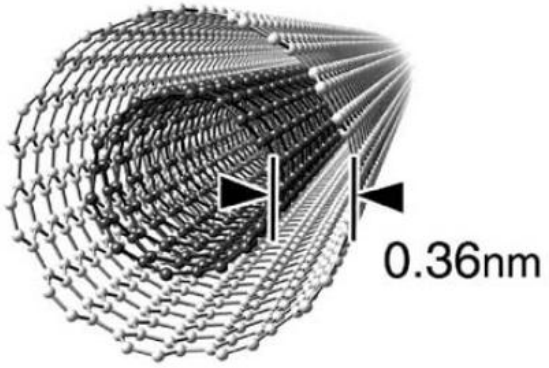

Figure 1.4: Two layer MWNT (Iijima, 2002)

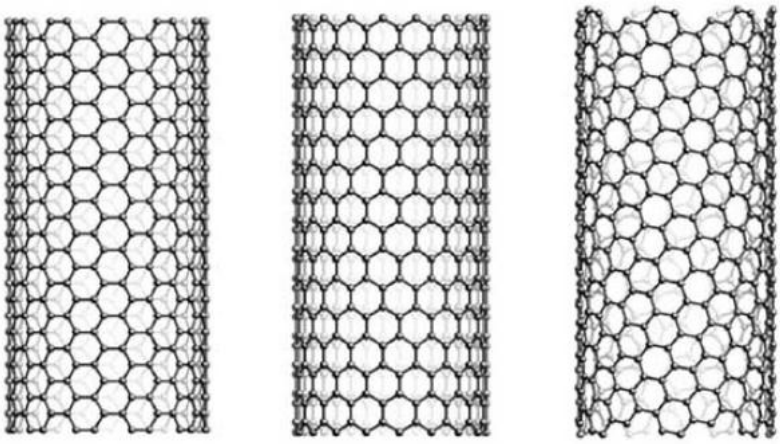

Figure 1.5: SWNTs in the armchair form (left), zigzag form (center), and helical form (right) (Iijima, 2002)

The processing of carbon nanotubes for use in laminate composites can take several forms, one of which is being produced as what is called buckypaper materials. Buckypaper is a thin film with much the same look as tissue paper and is made of many individual carbon nanotubes. Buckypaper was first produced in 1998 by researchers at

Rice University who purified material containing carbon nanotubes by a process beginning “with a 45-h reflux in 2-3 M nitric acid” after which the material was centrifuged and cleaned with deionized water multiple times (Rinzler et al., 1998). Lastly the remaining material was vacuum filtered and the dried material could be pulled off of the membrane in sheets. Buckypaper can be produced in multiple forms including using single or multi-walled carbon nanotubes (Harris, 2009). The nanotubes can also be aligned in specific directions through multiple methods including the introduction of strong magnetic fields (Fischer et al., 2002). A magnified view of MWNT buckypaper showing individual carbon nanotubes is shown in Figure 1.6.

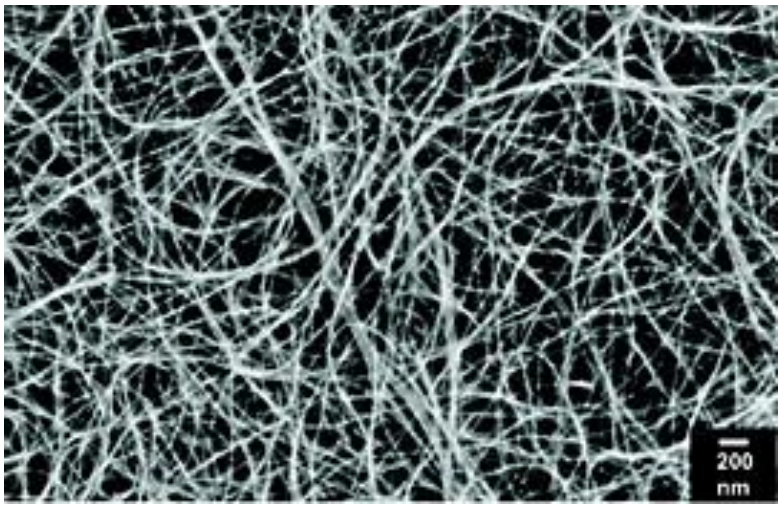

Figure 1.6: Image of MWNT buckypaper taken with an electron microscope (The University of Texas at Dallas, 2010)

1.3.3 Electrical Properties Characterization

The electrical properties of carbon fiber reinforced composites and carbon nanotube buckypaper have intrigued researchers just as much as their mechanical ones. That being said, researchers have taken their studies into a wide array of topics, those of which include damage detection and structural health monitoring through electrical resistance measurements (Schulte and Baron, 1988). Also studied have been structural degradation of composites due to electrical events such as lightning strikes as well as the use of composites and nanotubes for electromagnetic interface shielding (Hirano et al., 2010: Park et al., 2009). This research has provided a thorough understanding of many of the electrical properties of these materials and has led to the investigations performed for this thesis.

As was described previously, both carbon fibers and carbon nanotubes are highly conductive. When applied into materials such as carbon fiber reinforced polymers or carbon nanotube buckypaper the alignments and volume fractions of these materials can have a great effect on their conductivity. As these materials are electrically anisotropic the conductivity effects can be much greater in on one material direction compared to others. This can be seen in carbon fiber polymer materials where the epoxy matrices are extremely insulating and can have a resistivity on the order of 10^{20} ohm meters (Abry et al., 1998). For unidirectional samples the large resistivity of these epoxies has a proportional effect on the electrical conductivity of the material in the direction of the carbon fibers. By using the rule of mixtures and the percent volume of non-conducting epoxy and carbon fibers the fiber direction conductivity can easily be determined

(Todoroki et al., 2002). The same is not true in the directions perpendicular to the fiber direction as well as through the thickness of the composite. Research has shown that for unidirectional carbon fiber reinforced polymers the electrical conductivities in these two directions are 10^{-3} and 10^{-4} times less that in the fiber direction respectively (Todoroki and Yoshida, 2004). This is because; while the epoxy is non-conducting the carbon fibers are not perfectly straight and have some contact with each other in both the transverse and thickness directions. It has been found that as long as the carbon fiber volume percentage is above what is called the percolation threshold (30 – 40%) this inter-touching between fibers will remain true (Angelidis et al., 2006).

The relationship between alignment and electrical conductivity is also true for the carbon nanotubes in buckypaper material. Researchers at Florida State University have discovered that the increase in alignment of carbon nanotubes in buckypaper material through the use of a strong magnetic field is directly related to the resistivity of that material. It was found the unaligned buckypaper had a resistivity of 0.00186 ohm centimeters in all directions while buckypaper aligned in a five Tesla magnetic field had a resistivity of 0.00172 ohm in the magnetized direction and 0.00556 ohm centimeters in the perpendicular direction. This trend continued with 17.3 Tesla aligned buckypaper where the parallel resistivity was 0.00113 and perpendicular was 0.00725 ohm centimeter (Wang, 2006). These results show both an increase in conductivity in the magnetized direction as the nanotubes are more aligned as well as an increase in anisometric electrical properties.

Many different methods have been developed for measuring the electrical properties of laminated composite materials, two of which are a potential difference

method and electrical resistance method. Both methods have been used extensively in damage detection in carbon fiber reinforced composites and both have their advantages and limitations. The potential difference method involves a series of point electrodes located at various positions on a composite sample surface and are not all collinear. A constant current is than applied through the entire sample with all of the electrodes located between the positive and negative terminals of the current supply. The potential magnitudes are then measured at each electrode location and damage can be detected by comparing the potential field to that of an undamaged sample (Angelidis and Irving, 2007). The potential difference method is very effective at detecting damage in carbon fiber reinforced polymers but is limited to laminates that are less than eight layers thick (Wang et al., 2006).

The electrical resistance method is similar in many ways to the potential difference method. Like the potential method a series of electrodes are placed on the surfaces of the samples but unlike the first one, the electrodes in the resistance method are placed so that the electrical current path coincides with the electrodes of which the potential is to be measured (Wang et al., 2006). Electrical current is then applied on the outermost electrodes and the potential can be measured on any of the outer or inner electrodes. Measuring the potential on the outer electrodes is considered a two probe electrical resistance measurement where the same electrodes are used both as the current source and voltage sensing. Measuring the potential at points in between the two source electrodes is a four probe resistance test and the resistance calculated is the resistance between the two potential measuring electrodes. The four probe method is considered

more accurate compared to the two probe method because it eliminates the contact resistances between the electrodes and samples (Wang et al., 2006).

The electrical resistance method is better suited for composite samples with more than eight layers than the potential method previously discussed. One disadvantage of the electrical resistance method is that when a composite sample is damaged the electrical current path changes which results in less damage sensitivity than the potential method (Wang et al., 2006). One advantage of both methods is that many electrodes can be placed between the current source electrodes which in turn allows for damage detection to be spread across a more broad area than just having two sensing electrodes. Also, electrodes can be placed on both the upper and lower surfaces of the composite samples allowing for the resistance and potential differences through the thicknesses of the samples. An example of these advantages is shown in Figure 1.1 where many sensing electrodes have been placed between the source electrodes on both upper and lower surfaces for four probe electrical resistance testing.

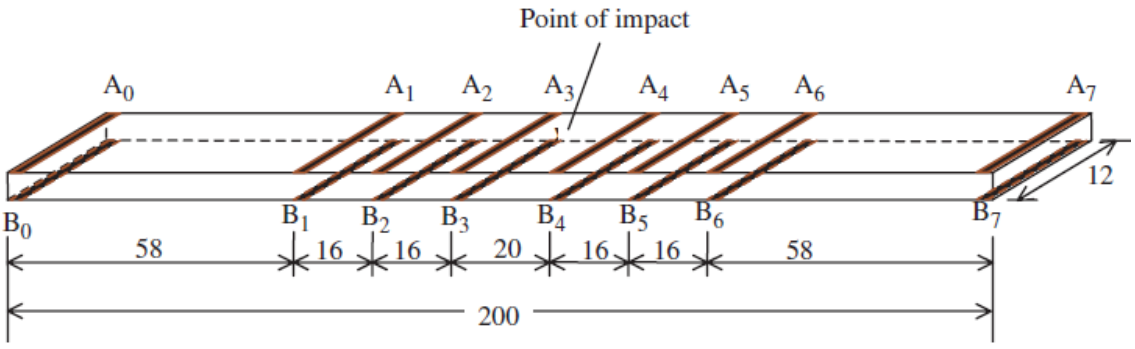

Figure 1.7: Electrode placement for four probe electrical resistance testing (Wang et al., 2006)

1.3.4 Mechanical and Electrical Property Coupling in Composite Materials

The electrical properties of carbon fiber reinforced composite materials are not only limited to low current, damage detection applications. Much research has been conducted on the coupling relationship between the electrical and mechanical properties of composite materials (Snyder et al., 2001: Zhupanska and Sierakowski, 2007: Sierakowski et al., 2008). It has been found that the strength and impact resistance of a composite material are increased when electrical current is applied to the composite during an impact (Snyder et al., 2001). In fact it was later observed by Sierakowski et al. that the greater the current applied the greater the load that a composite sample could carry prior to failure (Sierakowski et al., 2008). Their results are shown in Figure 1.8 which includes a sample with 25 A current carrying more load than a sample with no electrical current and a sample with 50 A carrying more mechanical load than the other two samples. This motivated further experimental (Zantout, 2009; Deierling, 2010; Hart, 2011) and theoretical (Barakati and Zhupanska, 2011) studies of electrified composites.

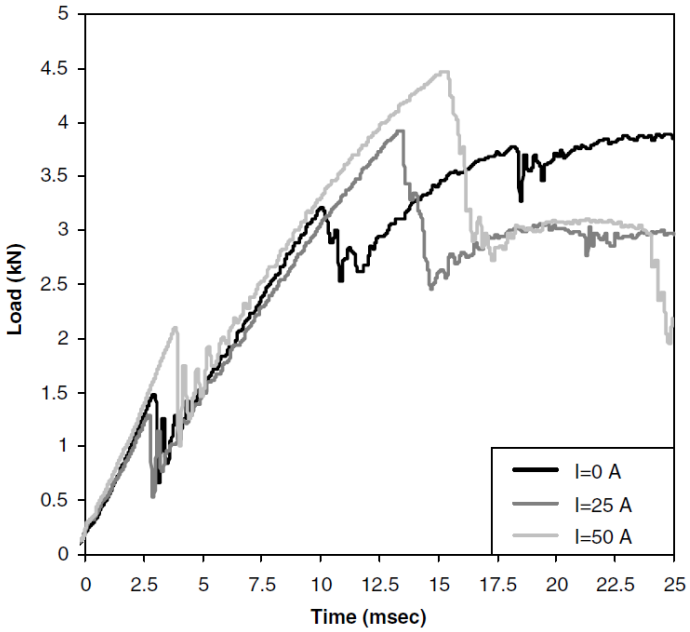

Figure 1.8: Impact load over time for composite samples with electrical current loads between zero and 50 amps (Sierakowski et al., 2008)

From the theoretical standpoint, one of the coupling mechanisms is the action of the Lorentz force that is exerted in the electrified composite by the application of an electromagnetic field. The mathematical equation for the Lorentz force in an electrically anisotropic but magnetically isotropic composite material was derived by Zhupanska and Sierakowski (2007) and is shown Equation 1.1, where **E** is the electric field vector, u is the displacement vector, **B** is the magnetic induction vector, **J*** is the external electric current density, ρ_e is the charge density, σ is the conductivity tensor, and ε and ε_0 are the electrical permittivities of the standard conditions and conditions in a vacuum respectively.

Equation 1.1: Lorentz force for anisometric composites with no magnetization

$$\mathbf{F}^{L} = \rho_e \left(\mathbf{E} + \frac{\partial \boldsymbol{u}}{\partial t} \times \mathbf{B}\right) + \left(\boldsymbol{\sigma} \cdot \left(\mathbf{E} + \frac{\partial \boldsymbol{u}}{\partial t} \times \mathbf{B}\right)\right) \times \mathbf{B} + (((\varepsilon - \varepsilon_o \cdot \mathbf{1}) \cdot \mathbf{E}) \times \mathbf{B})_{\alpha} \nabla \left(\frac{\partial \boldsymbol{u}}{\partial t}\right)_{\alpha} + (\mathbf{J}^{*} \times \mathbf{B})$$

The Lorentz force enters the equations of motion as a body force and leads to a mutual coupling between the mechanical and electromagnetic fields. The result of this coupling is manifested by the change in the stressed state of the electrified structure as compared to the non-electrified one. The effects of a pulsed electric current of large magnitude but short duration on the impact response of composites were investigated by Barakati and Zhupanska (2011), who showed that the characteristics of the electromagnetic field can significantly reduce or enhance the stressed and deformed state of the electrically conductive composite. Figure 1.9 shows the middle plane transverse deflection of the electrified composite plate subjected to an impact load and varying electromagnetic loads.

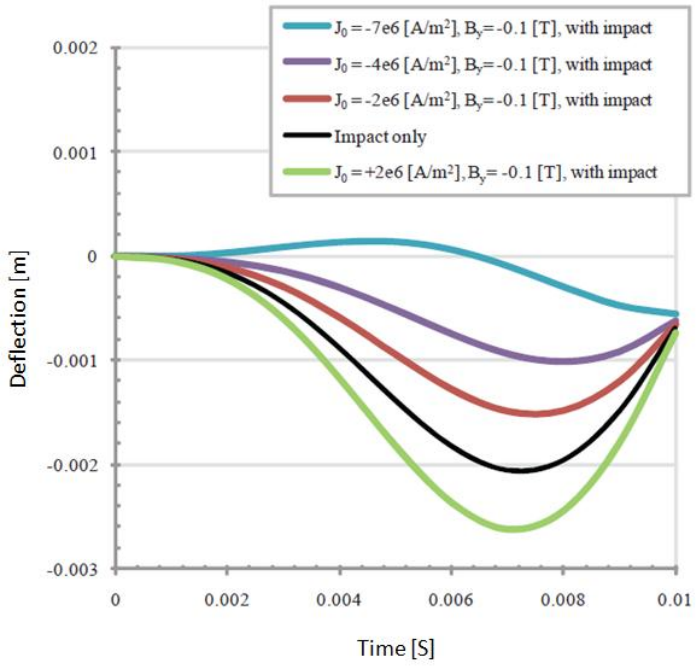

Figure 1.9: Effect of different current magnitudes on composite deflection during impact (Barakati and Zhupanska, 2011)

From this work it was also determined that to achieve the greatest benefit from the electromagnetic load (maximum reduction in the plate deflection and stress), the application of the mechanical load must be coordinated with the application of the pulsed electric current, i.e. the maximum current should coincide with the maximum mechanical load. Overall the study of Barakati and Zhupanska demonstrated that the application of a pulsed electromagnetic load concurrently with an impact event can effectively mitigate its damaging effects in electrically conductive composite plates.

1.3.5 Electrical Current Pulse

While it was observed that the application of electrical current can be beneficial in increasing the impact resistance of carbon fiber reinforced composite materials, limitations have also been found. These restrictions include Joule heating and contact resistance heating produced in the composite-electrode electric contact. To apply electrical current through the carbon fibers in a laminate composite it is easiest to attach two electrodes, one on each side of the laminate, in contact with the edges in which fiber ends are exposed. This method provides a direct electrical current path as well as allows for experimentation such as impact tests to occur without the hindrance of having the electrodes in the way of the striking mechanism. In the past experiments performed by Zantout (2009), Deierling (2010), and Hart (2011) large copper electrodes were used due to coppers high electrical conductivity and use in a wide array of electrical applications. One issue that arises when connecting any two materials for electrical current applications is the contact resistance. Contact resistance occurs because the two surfaces, in this case the composite laminate samples and copper electrodes, cannot ever be perfectly smooth. Therefore only small portions of the total contact area between the two surfaces is actually capable of passing electrical current. The contact resistance is increased even further in fiber-polymer composites by the fact that the polymer matrix is dielectric and therefore only a portion of the composites surface is capable of making an electrical contact with the electrodes (Sierakowski et al., 2008). An image of how surfaces of two solids come in contact with each other is shown in Figure 1.10.

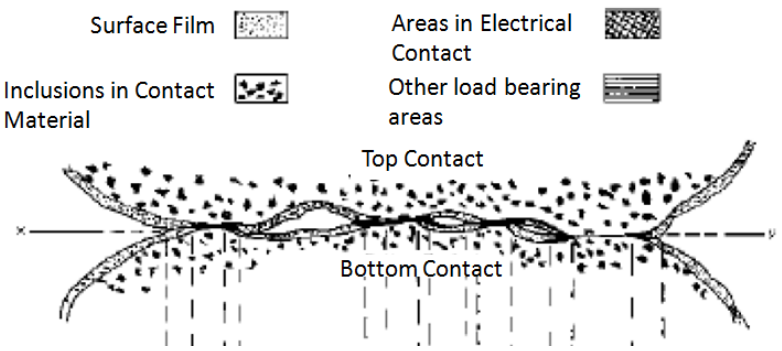

Figure 1.10: Contact surfaces between two materials (Copper Development Association, 1997)

The contact resistance between the composites and electrodes is important because of two reasons. One of which is the heating created in the contact region when electrical current is passed through it, the other is the increased possibility of electrical arcing occurring. The heat created through contact resistance is the amount of current squared multiplied by the magnitude of the contact resistance. This creates a limit for the amount of current than can be passed through a composite because the contact region can become hot enough to degrade the polymer matrix. The potential for arcing to occur between the gaps of the two materials, as was shown in Figure 1.10, also becomes much greater the rougher the two surfaces are and the greater the electrical current used.

For these two reasons researchers have attempted many solutions to reduce the contact resistance between composite materials and electrodes. These attempts have included increasing the force between the composite and copper to reduce resistance as is done in some metal-metal electrical contacts (Anway et al., 2010). Some have also removed the epoxy close to the edge of the composite using aluminum oxide powder to

allow only the carbon fibers to contact the electrodes (Schulte and Baron, 1989). Though these methods have had some success many researchers have relied on a method that includes very fine sanding of the composites and electrodes as well as the application of a highly conductive paste or resin between the two prior to joining (Sierakowski et al., 2008). An experiment determining the benefits of each of these steps was performed by Zantout (2009) and is shown in Figure 1.11. It can be observed that each step of sanding led to a reduction in electrical contact resistance and that the application of a silver based resin reduced it a great deal further.

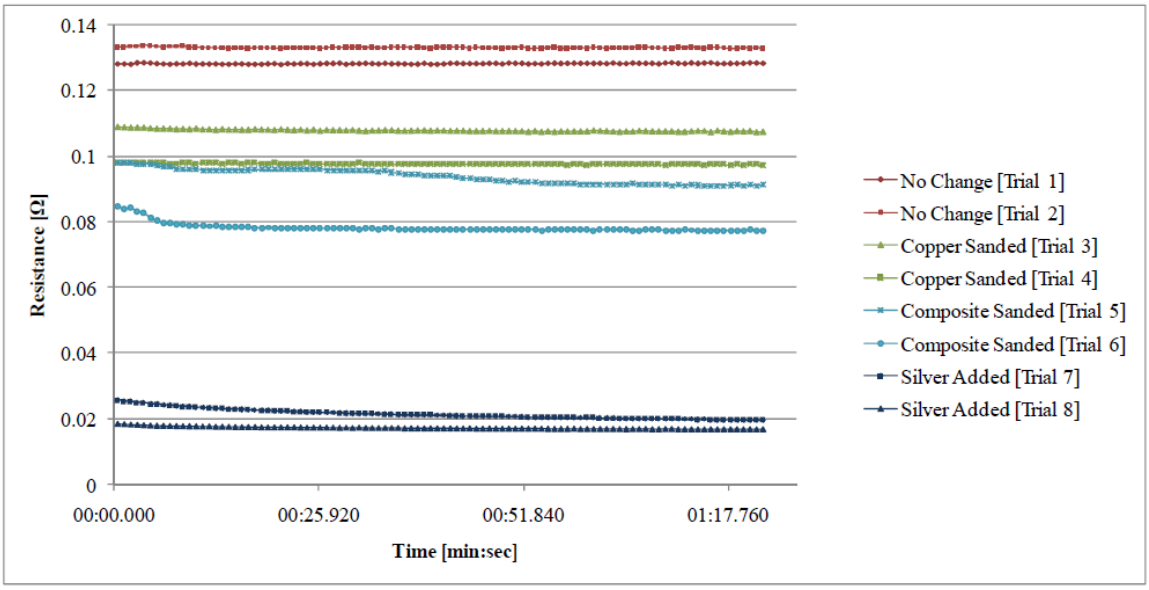

Figure 1.11: Reduction of contact resistance between composites and copper electrodes (Zantout, 2009)

The duration of time that the electrical current is applied is also a contributing factor to the Joule heating in the carbon fiber reinforced composite materials. It was

found that a composite sample under an electrical current load for a long period of time (24 minutes) absorbed less energy than that of a sample that was only briefly induced with an electrical current (Sierakowski et al., 2008). This was attributed back to the Joule heating generated over the long period of time that the electrical current was applied. This heat provides thermal loading to the composites which can have many negative effects including "strength degradation, physical appearance change and structural integrity loss" (Ankara et al., 2003). The research of Deierling and Hart took this understanding into effect and developed methods of coordinating the application of electrical current with impacts to limit the length of time that the composite samples were exposed to high current levels (Hart, 2011).

1.3.6 Impact Tests on Electrified Composites

The application of electrical current during impact events on carbon fiber reinforced polymer composites has been performed by researchers in the past to investigate the electro-mechanical coupling properties previously described. In these experiments ASTM standards D5728-07 and D3763-06 as well as the Standard Tests for Toughened Resin Composites developed by NASA were used in developing proper test fixtures and experimental procedures (Zantout, 2009). Impact tests on electrified composites consisted of using standard engineering drop test equipment with several important modifications. As with standard drop tests, the impact energy to be applied to the specimen was dictated by the starting height of the tup as well as the quantity of weight added. The energy to be used for each type of composite sample was determined

experimentally to find the V_{50} which is the velocity in which 50 percent of non-electrified samples would break (Sierakowski et al., 2008). This energy was then used on electrified samples to measure the differences in impact resistance. One difference between a standard drop test and an electrified one was that instead of a standard metal tup being used one was produced out of a nonconductive plastic preventing any electrical current from passing through the impact equipment.

The test fixture holding the composite specimens was also designed with specific requirements. One such requirement included having the composite specimen being restrained by compression that was in the perpendicular direction to the laminae (ASTM, 2006). The composites also had to have a minimum of one half inch of material to be clamped on all parameters and a five inch by five inch area unsupported for impact (ASTM, 2006: ASTM, 2007). Much like the tup all fixture materials that were in contact with the composite samples had to be nonconductive. One additional requirement that arose due to the electrification was that the test fixture had to have additional space included to incorporate the copper electrodes used to pass current through the specimen. The copper electrodes also had to be restrained so that no separation between the composite and electrodes could occur during impact. A diagram of the previous experimental setup is shown in Figure 1.12.

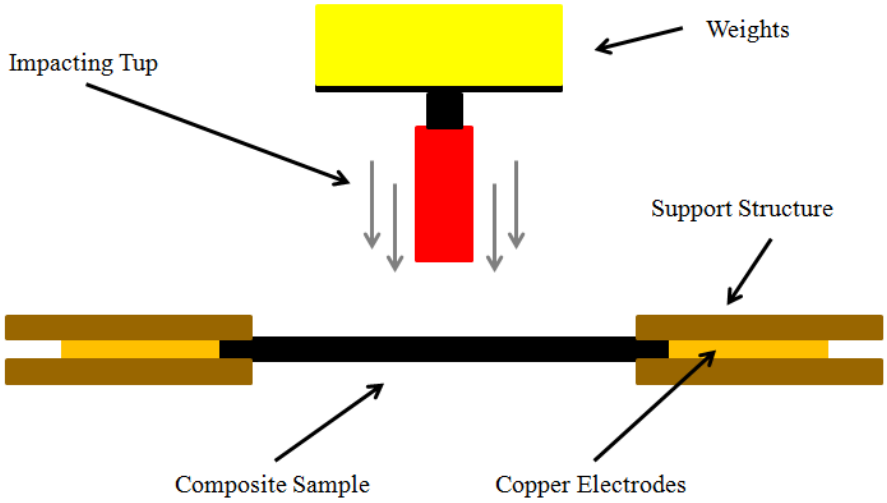

Figure 1.12: Experimental setup for electrified impact experiments

Hart's research (Hart, 2011) expanded upon this experimental setup and developed a means of coordinating high current pulse applications to composite samples with the already described impact events. By allowing the current application to occur only during the fractions of a second that the impact force was acting on the composite sample much larger currents could be used without the risk of Joule heating causing the burning of the samples. Hart's coordinated timing with the current pulse peak coinciding with the maximum impact load is shown in Figure 1.13. Through this research some promising results were discovered including increased absorbed energy for 32-ply composite samples which were electrified with a current pulse compared to non-electrified samples (Hart, 2011). Building upon these results would prove to be important in understanding the changes in electrical and impact properties in carbon fiber reinforced polymer materials as layers of buckypaper were added to enhance the overall electrical properties of the carbon fiber reinforced composites.

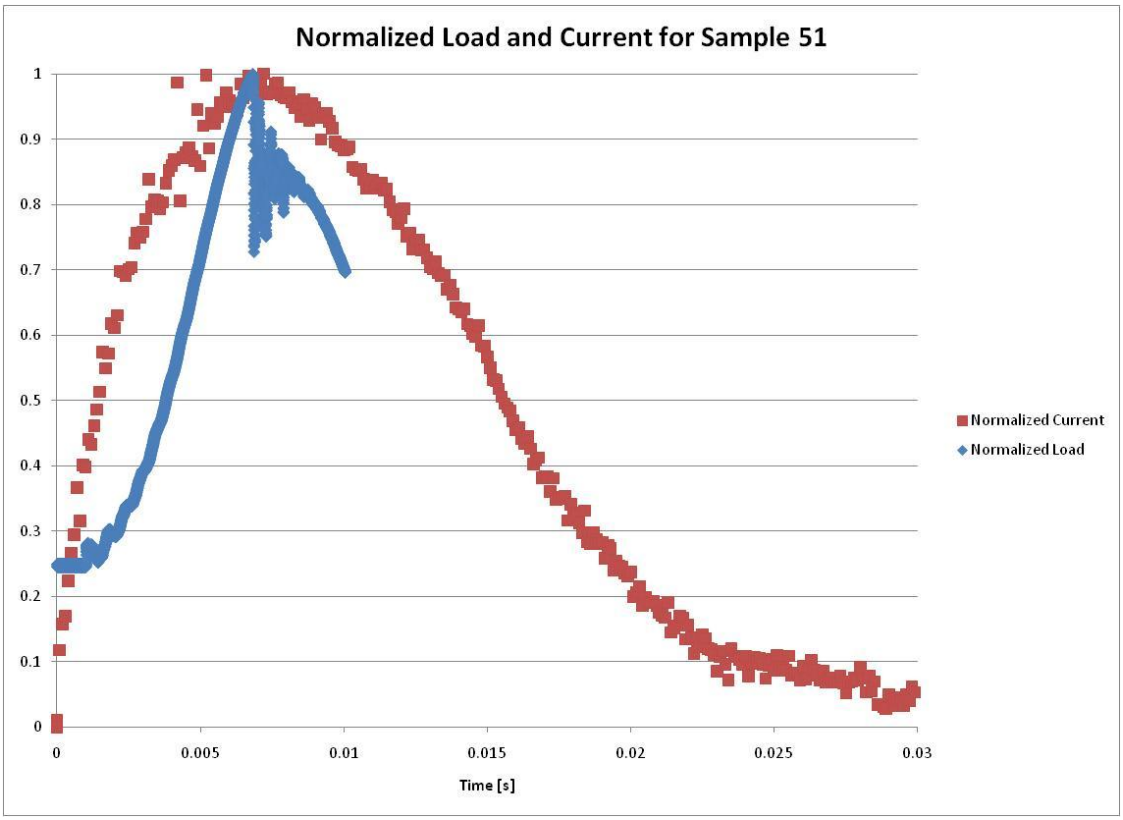

Figure 1.13: Normalized current and impact loads for a coordinated impact (Hart, 2011)

1.4 Thesis Objectives

The main goal of this thesis was to investigate the effect of the addition of varying quantities of carbon nanotube buckypaper on the electrical and impact response of carbon fiber reinforced polymer matrix composite laminates. Specific research objectives included the following: (1) to determine the electrical resistance of 16-ply unidirectional IM7/977-3 carbon fiber reinforced polymer matrix composites with zero, four, and seven carbon nanotube buckypaper layers using two and four probe electrical resistance

measurements; (2) to determine the response of these composites to the application of electric current pulses of varying magnitudes; (3) to determine the effects of the application of an electric current pulse coordinated with a low velocity impact on the impact resistance of these composites.

These research objectives were accomplished using four separate experimental setups and procedures including four probe electrical resistance testing through multiple planes of the samples; two probe electrical resistance testing in the carbon fiber directions; electrical current pulse testing; and coordinated current low velocity impact-electrical current pulse experimentation. Development of the fully-automated experimental setups constituted a secondary objective of this work.

CHAPTER 2

COMPOSITE SAMPLE MATERIALS AND PRODUCTION

2.1 Constituent Materials of Composite Samples

As discussed in the literature review section, composite materials are non-homogenous by nature and can consist of two or more different materials depending on the application that the composite will be used in. Examples of this can be seen in every day products such as the cermets, metal-matrix composites used on drill bits and saw blades, as well as exotic applications such as the carbon-matrix composites used in high temperature aerospace applications (Chung, 2010). The laminated composites used in the experimentation for this thesis were produced by The High-Performance Materials Institute at Florida State University. The composite prepreg material used for manufacturing of the laminates was supplied by the Air Force Research Laboratory. The samples contained three constituents, Hexel-IM7 carbon fibers, Cytec 977-3 polymer epoxy, and carbon nanotube buckypaper layers. Each material has substantially different mechanical and electrical properties which are discussed in the following subsections.

2.1.1 IM7 Carbon Fibers

IM7 carbon fibers are produced by the Hexcel Corporation as one of their HexTow® branded products. IM7 is available for use as both continuous fibers, which were used in the creation of the samples used for these experiments, and chopped fiber forms. The HexTow® fibers are produced from a PAN precursor which is further

modified through "Successive surface treatment and sizing stages…" (Hexcel, 2010). IM7 has many physical properties that have made them ideal for aerospace applications such as high tensile strength and low density, which can be seen in Table 2.1 (Hexcel, 2010). Also worth noting is the very low electrical resistance reported by Hexcel as 0.0015 Ohm-cm in the fiber direction.

Table 2.1: Hexcel IM7 carbon fiber properties

(Hexcel, 2010)

Yarn/Tow Characteristics	
Tensile Strength [MPa]	
6K	5,310
12K	5,670
Electrical Resistivity [ohm-cm]	1.5×10^{-3}
Density [g/cm^3]	1.78
Thermal Conductivity [W/mK]	5.40

2.1.2 977-3 Polymer Matrix

The epoxy matrix used in conjunction with the IM7 carbon fiber material was CYCOM® 977-3 produced by Cytec Industries. 977-3 is a toughened epoxy material that has found many applications in United States combat aircraft including the F/A-18E/F. This is due to the fact that CYCOM® 977-3 is less sensitive to impact damage than typical epoxy systems (Deo et al., 2001). 977-3 is also capable of being using in many hotter applications that typical epoxy materials which is an advantage for the experiments conducted in this thesis as will be described later (Koo et al., 2004). Important physical

and mechanical properties for 977-3 are in Table 2.2. It is noted that no information is available on the electrical properties of 977-3 as it is not intended to be used as an electrically conductive material and acts as a dielectric in the composite.

Table 2.2: Cytec CYCOM® 977-3 epoxy base resin

(Grimsley et al., 2001)

977-3 Neat Resin	
Glass Transition Temp [C]	232
Density [g/cc]	1.28
Tensile Strength [MPa]	6.9
Tensile Modulus [GPa]	3.6

The CYCOM® 977-3 epoxy was combined with the HexTow® IM7 carbon fibers into a unidirectional prepreg by Cytec Industries. Prepregs are sheets of composite material that have been created by impregnating fibers with an epoxy matrix. The final product is flexible and tacky so that it can be shaped and layered as desired by the customer (Chung, 2010). The advantages of purchasing prepreg versus the carbon fiber and epoxy separate include lower fabrication cost, higher control of the orientations and material content, and better weight to performance ratios (Hexcel, n.d.). Strength and electrical properties of IM7/977-3 are shown in Table 2.3.

Table 2.3: Properties of IM7/977-3 composite material (Grimsley et al., 2001; Todoroki et al., 2002)

IM7/977-3	
Tensile Strength [GPa]	1.8
Tensile Modulus [GPa]	152
Electrical Conductivity [S/m]	
- Fiber Direction	41000
- Transverse Direction	41
- Thickness Direction	4.1

2.1.3 Carbon Nanotube Buckypaper Layers

The Carbon Nanotube Buckypaper layers used in the creation of the current composite samples were produced at Florida State University (FSU). The carbon nanotubes were SWeNT® SMW100 multiwall nanotubes (MWNT) produced by SouthWest NanoTechnologies Inc. Typical properties of SWeNT® MWNTs reported by the manufacturer include a bulk density of 0.22 g cm^{-3}, median diameter of 6.6 nm, typical number of walls from 3-6, and aspect ratio of `1,000 (SouthWest NanoTechnologies, 2010). The finished buckypaper material had a pre-cure weight of 19.3 milligrams per square inch and each sheet had a thickness between 41 and 43 micrometers. Nanotube layers were added in between IM7/977-3 prepreg layers with three samples containing four layers of buckypaper and three samples containing seven layers of buckypaper. A layer of buckypaper being added to the carbon fiber composite can be seen in Figure 2.1 which was provided by FSU.

Figure 2.1: Buckypaper layer being added to CFRP sample at the HPMI at FSU

2.2 Sample Production

Nine composite plates were acquired for testing all measuring eight inches wide by eight inches tall. Three samples were 16-ply IM7/977-3 unidirectional carbon fiber polymer matrix composites and are denoted as CF_{16}. Three samples had four layers of buckypaper (BP) and 12 unidirectional IM7/977-3 carbon fiber polymer matrix layers arranged as $CF_2/BP/CF_4/BP/CF_4/BP/CF_4/BP/CF_2$. Three remaining samples had seven layers of buckypaper and nine unidirectional IM7/977-3 carbon fiber polymer matrix layers arranged as $[CF_2/BP]_7CF_2$. Here the subscripts in the layup annotation indicate the number of corresponding layers. For example the script CF_2 specifies two layers of carbon fiber. Also important was that the samples were produced in three separate batches that were cured at different times and that each batch consisted of one of each

type of sample (i.e. with no buckypaper, with four layers of buckypaper, and with seven layers of buckypaper). The weight and thickness properties of each sample are shown in Table 2.4, Table 2.5, and Table 2.6 for batches one, two, and three respectively.

Table 2.4: Sample and buckypaper properties for batch one samples (FSU)

Sample	Pre-Cure Weight	Final Weight	Final Thickness
1	142.4 g	140.0 g	2.2 mm
2	195.3 g	182.7 g	2.24-2.28 mm
3	199.0 g	186.4 g	2.29-2.38 mm

Table 2.5: Sample and buckypaper properties for batch two samples (FSU)

Sample	Pre-Cure Weight	Final Weight	Final Thickness
1	140 g	130.1 g	1.60-2.12 mm
2	145 g	140.5 g	1.96-2.12 mm
3	148.6 g	144.1 g	2.13-2.22 mm

Table 2.6: Sample and buckypaper properties for batch three samples (FSU)

Sample	Pre-Cure Weight	Final Weight	Final Thickness
1	140 g	138.3 g	2.04-2.12 mm
2	145 g	145 g	2.20-2.22 mm
3	148.6 g	148 g	2.40-2.42 mm

2.3 Sample Preparation

It would later be required to know which batch each sample came from to compare electrical resistance properties from batch to batch. To track the samples through the preparation and testing process a three number identification system was utilized and is used in this thesis. The first number of the system represents the batch of samples that it was produced in, the second contained the sample number as provided by the manufacturers, and the third was the number of buckypaper layers in the sample. Each sample had its identification number written onto its lower left corner as well as an arrow indicating the carbon fiber direction. An example of this is shown in Figure 2.2.

Figure 2.2: Identification number for sample 3-3-7

2.3.1 Waterjet Cutting

As mentioned previously the composite plates were delivered with eight inch by eight inch dimensions. The standard specimen size for low velocity impact testing is 6 inches by 6 inches. Thus, it was decided to cut each of the original plate sizes into three smaller samples, one that was 6 inches by 6 inches and two other narrow beam samples. This resulted in two cuts being required to the original composite plates as is seen in Figure 2.3. The sample for the four probe test was chosen to have its fiber direction be

along the long length of the sample therefore having the electrodes being perpendicular to the carbon fibers. The size of this sample was 2 inches wide by 8 inches long. The remaining beam sample was used for additional two probe electrical characterization tests.

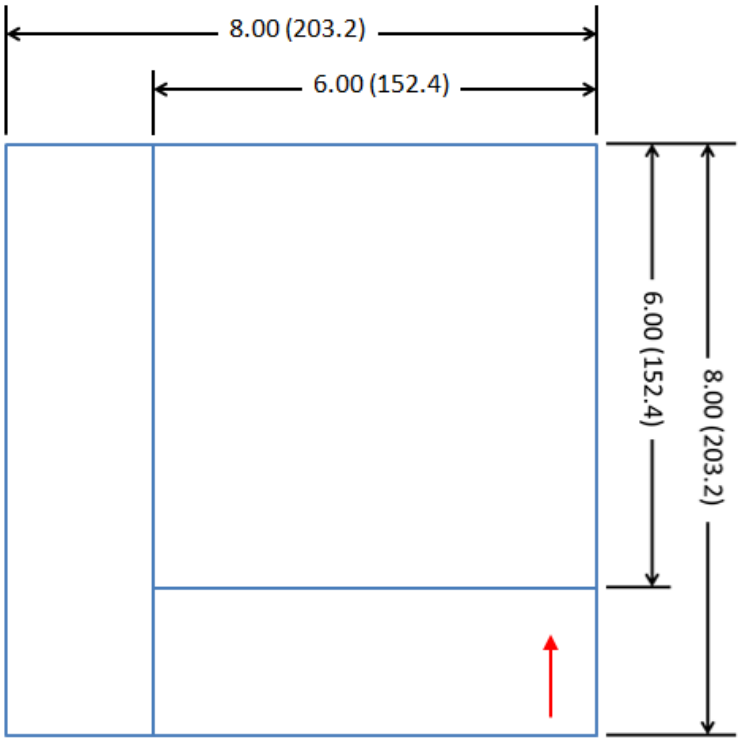

Figure 2.3: Original composite plate as well as cut lines required and orientation of fibers (red arrow indicates the fiber direction)

The next step was to cut the composite samples. The quality requirements of the cutting of the plates included excellent surface finishes and no edge delamination which is known to cause samples to have high electrical contact resistance in the subsequent electrical characterization tests.

Much research has been conducted in previous decades on successful methods of cutting and machining cured carbon fiber reinforced polymer (CFRP) composite components. The difficulty in the machining of CFRPs versus standard engineering materials is their brittleness and the complicated fracture mechanisms when the fibers aren't perfectly aligned (Rahman et al., 1999). Methods of cutting that have been used have included tungsten carbide tools, water jet cutting, and even ND:YAG lasers (Lau, 1990). Results from poor cutting of CFRPs are delamination and poor surface finishes both of which were not acceptable for the experiments. For this reason the water jet cutting method was chosen for the composite plates. For these samples a 60,000 psi waterjet was used in conjunction with an 80 mesh crushed garnet abrasive (Galen Thomson, n.d.). A diagram of the nozzle used in the water jet cutting process is shown in Figure 2.4. The results of the cutting of composite samples using a table saw versus the water jet cutting can be seen in Figure 2.5 and Figure 2.6. It can be seen that the water jet cutting produced a very good surface finish as well as no delamination as had occurred with the table saw.

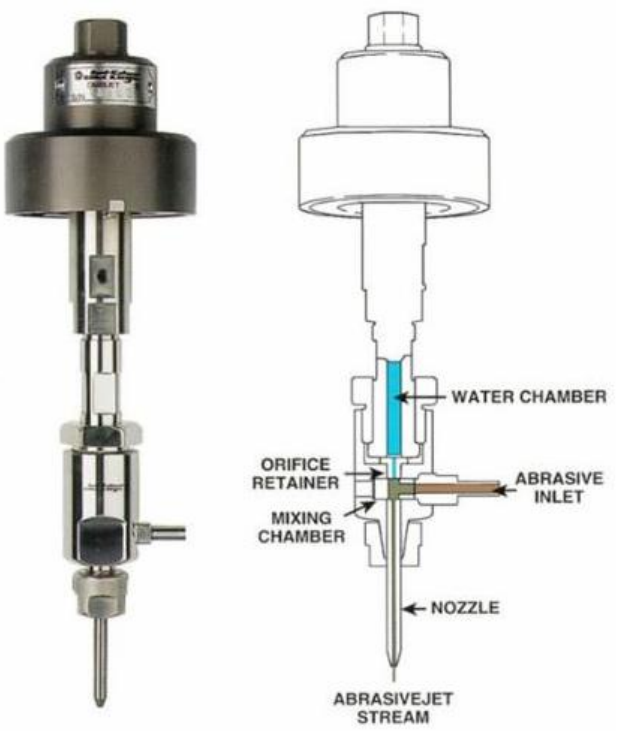

Figure 2.4: Schematic of water jet cutting nozzle (Water Jet Cutting World, 2011)

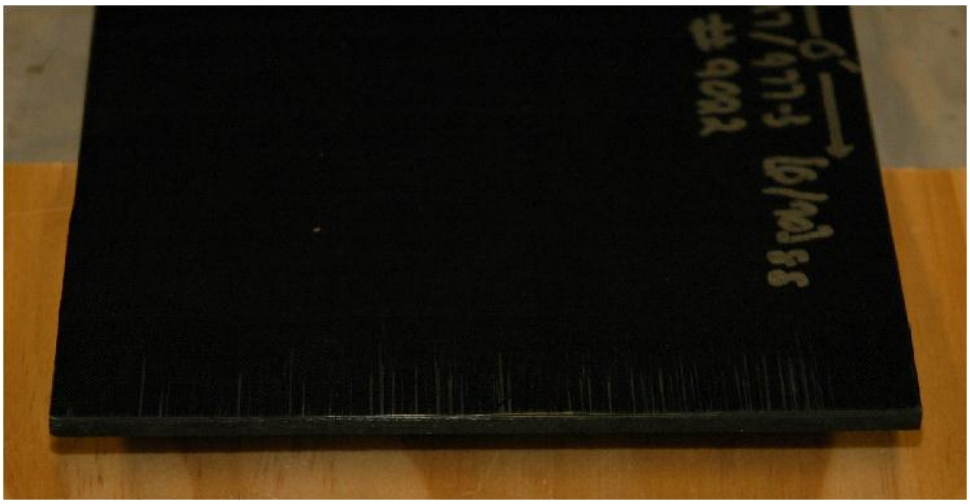

Figure 2.5: Image of a sample cut using table saw

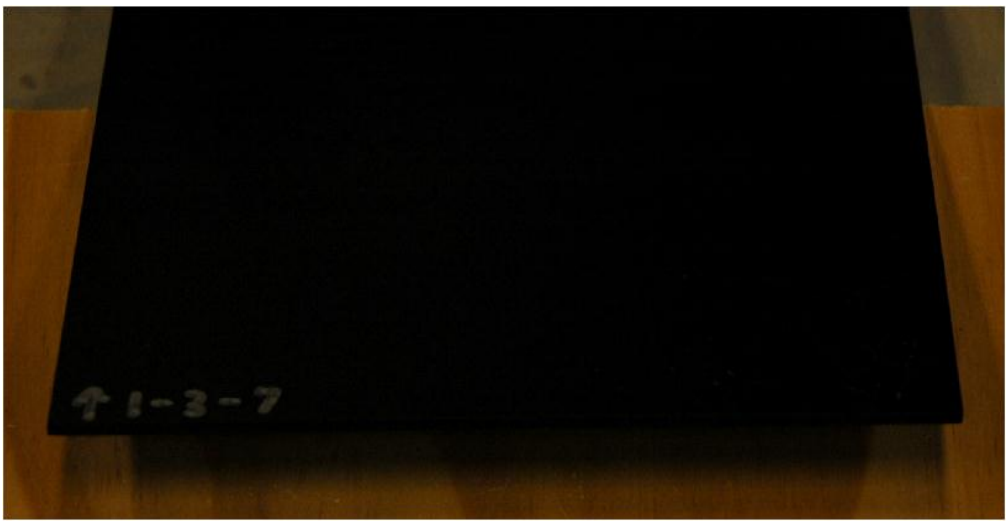

Figure 2.6: Image of a sample cut using water jet technology

CHAPTER 3

FOUR PROBE METHOD FOR ELCETRICAL CHARACTERIZATION OF BUCKYPAPER AND CARBON FIBER POLYMER MATRIX COMPOSITES

3.1 Experimental Considerations

One method that has been used by past researchers for characterizing the electrical properties of fiber reinforced composite materials has been to perform four probe electrical resistance measurements across different planes of the materials. The advantages to these tests are the elimination of the measurement of the contact resistance in the sensing electrodes as well as the ability to fairly easily take measurements of the materials in multiple directions which is beneficial due to their anisotropic properties. In this work four probe electrical resistance measurements have been performed on carbon fiber reinforced polymer composite samples and CFRP samples consisting layers of carbon nanotube buckypapers. The goal was to determine the effect of addition of the buckypaper layers on the overall electrical properties of CFRP composites.

To perform the four probe experiment a previously developed experimental set-up was taken and modified (McAndrew, 2009). The modification included a new controller program being written as well as the use of new data collection hardware which could allow for dynamic resistance measurements for use during impact tests. Also completed were computational models of the resistance problem which were compared to the experimental results and further used to understand the current flow and voltage potential trends in the composite materials.

3.2 Previous Experimental Set-up

The previous experimental was developed by McAndrew (2009). This setup utilized an Agilent 34420A ohm meter as well as an Agilent 34970A Data acquisition and channel switching unit as hardware for measuring and communicating the resistances of composite samples across their top, bottom, and oblique planes. In this setup the composite sample was connected to this equipment with twelve wires through the use of an Agilent 34901A multiplexer. Four wires were connected to electrodes evenly spaced across the top of the composite, four located directly opposite on the bottom surface, and four connected opposite to each other on the top and bottom surfaces. The multiplexer with all twelve wires connected can be seen in Figure 3.1 and a prepared sample with four electrodes attached to the top and bottom surfaces is shown in Figure 3.2.

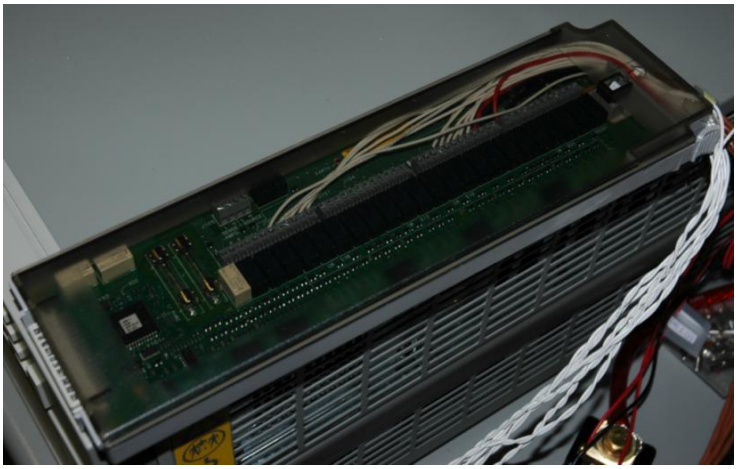

Figure 3.1: Agilent 34901A multiplexer with wire leads connected (McAndrew, 2009)

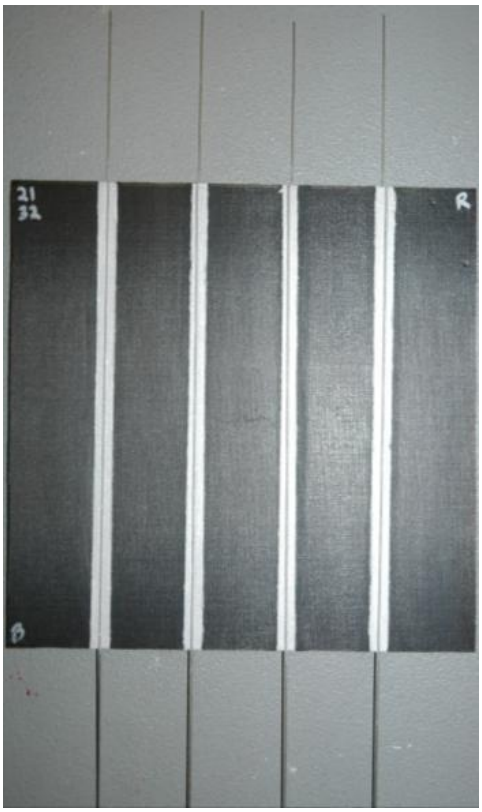

Figure 3.2: Prepared sample with four electrodes attached to each surface (McAndrew, 2009)

The twelve wires in conjunction with the Agilent switching unit allowed for the electrical resistance of all three planes of the composite to be measured with no need for the electrical leads to be adjusted. Lastly both the Agilent 34420A ohm meter and 34970A DAQ were connected to a desktop computer through a series of GPIB/USB cables completing the setup. To perform the actual measurements the desktop computer was used to execute a control program written using the Agilent VEE Pro software package. Figure 3.3 shows the main setup used for all previous four probe electrical resistance measurements.

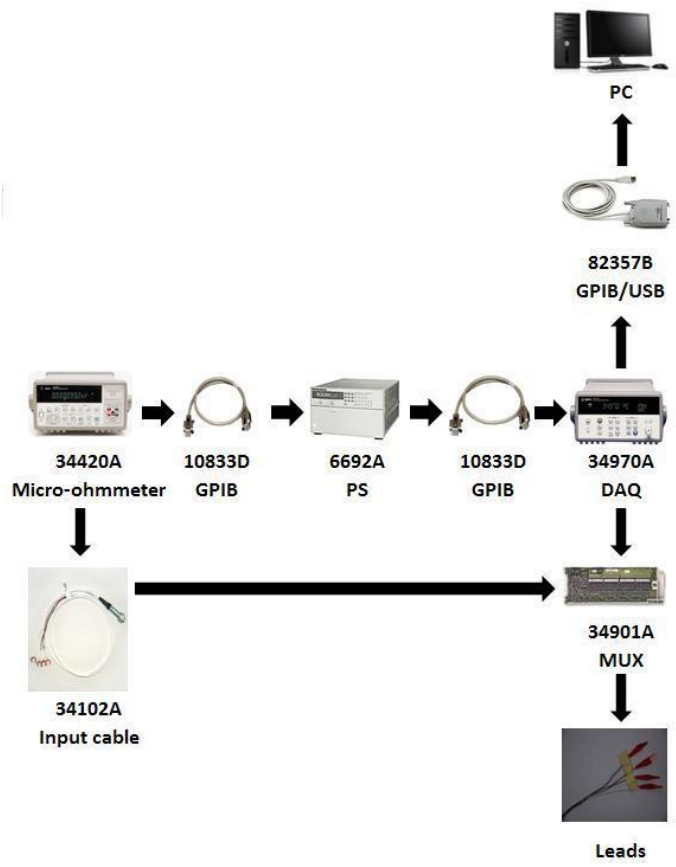

Figure 3.3: Previous experimental setup for electrical resistance measurement (McAndrew, 2009)

The benefits of this previous experimental setup was the ability to completely connect a composite sample to the equipment for all needed recordings with no adjustments when, for example, switching between reading the top and bottom plane resistances. The hardware used in measuring the composite resistance could also be set for very accurate readings with the Agilent 34420A ohm meter having a resolution of seven and a half digits (Agilent, 2003, p.58). Also the VEE Pro program allowed for full

control of the Agilent hardware in use as well as for all data to be recorded in an easy to use spreadsheet format.

The limitations of the hardware used in the setup was that, while it could be very precise in its resistance measurements, it also required long periods of time to record to produce those results. To record results to the seven and a half digits capable of the ohm meter readings could only be taken every thirteen and one third seconds (Agilent, 2003, p.278). While this was acceptable for stationary composite characterization it could not allow for recording during events such as physical impacts which can occur over only several milliseconds. Another limitation of the ohm meter was the limited source current settings using in measuring electrical resistances which prevented any testing of resistances with currents higher than 10 milliamps. The new experimental setup developed in this work overcame these limitations.

3.3 New Experimental Setup

The new experimental setup was developed from the knowledge gained from the previous one as well as goals for added functions and uses. The added functionalities include being able to measure the changes in electrical resistance during impact with a much higher sampling rate as well as vary the source current to allow for resistance measurements through different composite layers than was done previously. For the new experimental setup, first addressed was the hardware used for producing the source current in the two outer electrodes as well as the voltage measuring of the two inner electrodes in the composite samples. As mentioned in section 2.2 an Agilent 34420A ohm meter was used previously for both of these functions. For the new setup two

separate pieces of equipment were chosen with one being dedicated to providing the source current while one measured the voltage difference across electrodes.

3.3.1 Hardware Selection

Chosen to supply the source current to the outer two electrodes was a HP 6612C direct current power supply. The power supply allowed for output current to be controlled from zero to two amps rather than the 10 milliamps of the Agilent ohm meter (Agilent, 2004). The operating characteristics of the power supply also allowed for precise readings with accuracies of 2.5 microamps when used to supply low current, ranging between zero and 20 milliamps, and 0.25 milliamps when supplying 20 milliamp current and above (Agilent, 2004). Also the power supply could be automatically controlled using a software program and a GPIB/USB cable with allowed for it to be integrated with any other hardware to be used. A front panel view of the 6612C power supply is shown in Figure 3.4.

Figure 3.4: HP 6612C DC Power Supply (Axiom, 2011)

With the selection of the HP 6612C power supply as the source current in the four probe electrical resistance measurements, next needed was an ability to measure the voltage differences between the two inner electrodes. For this task the Agilent U2531A data acquisition unit (DAQ) was chosen. This DAQ has a significant increase in measuring capabilities when compared to the previous ohm meter used. Its operating specifications include a resolution of 14 bits and a maximum sampling rate of two million samples per second (Agilent, 2007). With these specifications it could be possible to record changes in resistances during impact events. An image of the Agilent U2531A DAQ is shown in Figure 3.5.

Figure 3.5: Agilent U2531A DAQ used in new setup (Agilent, 2007)

3.3.2 Setup Completion

By combining the features of the HP 6612C power supply and Agilent U2531A DAQ a complete setup could be developed with the ability of extremely fast measurements along with the control over inputs such as source current. To complete the setup an electrical harness consisting of four 22 gauge insulated copper wires was created for the purpose of connecting the composite sample to the experimental hardware. For ease of identification each wire was selected with a different colored insulation material. The four wires were then all cut to a length of four feet and all ends were striped, exposing approximately a half an inch of copper. Next alligator clips were crimped onto one end of each wire and protective rubber sleeves were slid over the exposed connection between the wires and the clips. Two of the completed wires were then connected to the HP 6612C power supply via the positive and negative terminals seen on the bottom right portion of the front face in Figure 3.4. The remaining two wires were connected to the positive and negative terminals of channel four on an Agilent U2901A terminal block. The terminal block is an accessory of the Agilent U2531A DAQ which allows connections from single wires to be conformed to the standard SCSI-2 68 pin configuration used (Agilent, 2007). The remainder of the setup was completed by connecting the HP 6612C to the computer using a GPIB/USB cable and the Agilent U2531A by the use of a mini USB cable. A Diagram of the new experimental setup is shown in Figure 3.6.

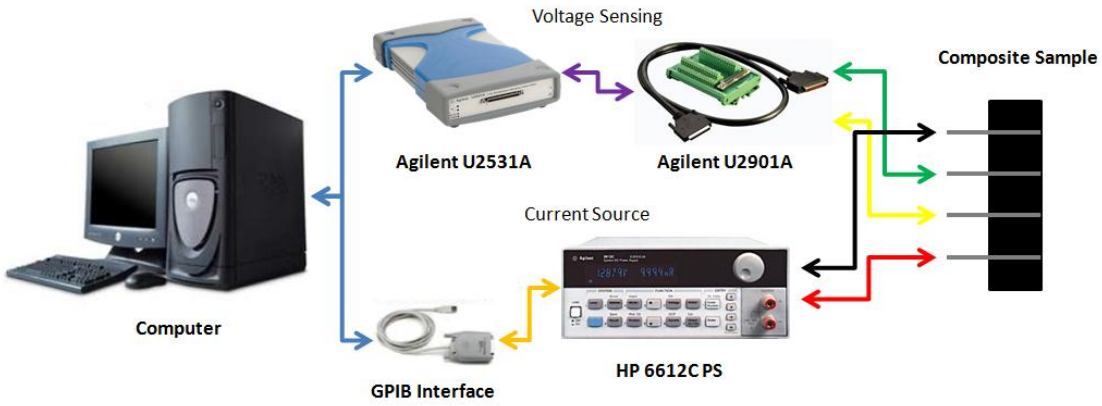

Figure 3.6: New four probe experimental setup

3.3.3 Agilent VEE Pro Software Program

To control the operating parameters of the selected hardware as well as record the measured results, a program was developed using Agilent's VEE Pro version 8.5 software. The basic functions of this program included directly communicating the desired input current to the HP 6112C power supply as well as the correct voltage reading range to the Agilent U2531 DAQ. Also controlled was the number of readings taken for each four probe electrical resistance test as well as the period of time between each reading. A basic diagram of the program's logic can be seen in Figure 3.7.

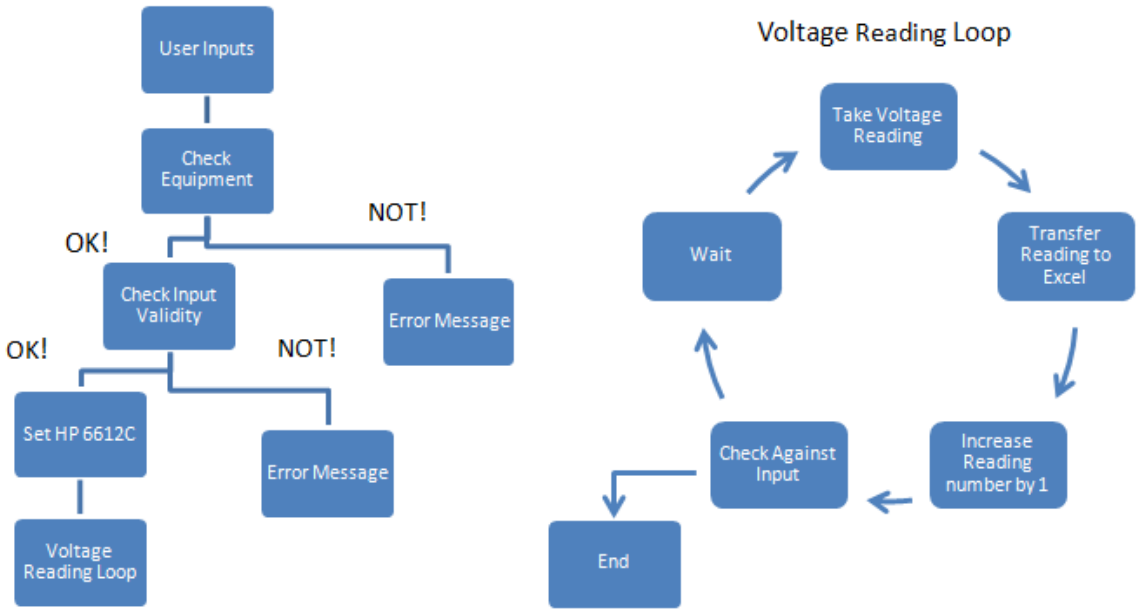

Figure 3.7: Logic diagram of four probe VEE Pro program

3.4 Composite Sample Preparation

3.4.1 Sample and Electrode Preparation

Once cut, the portions of the composite plates that were chosen for the four probe electrical resistance testing were next prepared to have electrodes attached to both their top and bottom surfaces. The procedure for accomplishing this was replicated from the previous work of McAndrew (2009). This first consisted of accurately measuring all samples and recording their lengths, widths, and thicknesses, which can be observed in Table 3.1. Next the composite samples were marked using a silver Sharpie and carpenter's square for the locations of the four electrodes on both the top and bottom

surfaces with the electrodes being placed perpendicular to the fiber direction. The distance between the electrodes was set at intervals of 4 cm with the pattern being symmetric along the center of the sample. The composite samples were then sanded at the locations determined for attaching the electrodes. This was done using 600 grit sand paper and a small eight millimeter thick plywood sanding block. By sanding the sample the top layer of the polymer epoxy could be removed so that the carbon fiber layer would be more greatly exposed to the electrode (Wang, 2006). As described by Wang et al. "The sanding step is not essential, but it helps the electrical measurements by increasing the accuracy and decreasing the noise" (Wang, 2006).

Table 3.1: Physical characteristics of four probe composite samples

Sample	Width (mm)	Length (mm)	Thickness (mm)
1-1-0	47	204	2.23
1-2-4	48	204	2.27
1-3-7	50	204	2.35
2-1-0	49	201	2.26
2-2-4	49	202	2.22
2-3-7	48	201	2.29
3-1-0	48	202	2.19
3-2-4	49	202	2.29
3-3-7	49	203	2.49

The method for preparing the electrodes for the electrical resistance testing was also identical to experimentation that had been conducted previously (McAndrew, 2009). First 72 electrodes were produced by slicing 22 gauge bus wire into 80 mm lengths. Because the bus wire was packaged in a spool the cut electrodes were slightly curved and could not lay flat on the surface of the composite samples as desired. To straighten the

electrodes a large table top vice was used along with a pair of needle nose pliers. Each electrode was individually clamped on one end to the vice in a vertical position then the pliers were used to stretch the wire until it became straight. In the process of straightening the electrodes approximately five millimeters of both ends of the wires would become crushed and had to be removed. Once all electrodes were straightened the process of attaching them to the prepared samples could be conducted.

3.4.2 Attachment of Electrodes

To attach the wire electrodes to the sanded portions of the composite samples a two stage process was used. This consisted of bonding the electrodes to the surfaces and securing them so that no movement or separation between the electrodes and samples could occur during testing. The boding process was done using a highly conductive silver paint product produced by Structure Probe, Inc and sold under the model number 05002. The paint was ideal for this application due to its low bulk resistivity of $3 * 10^{-5}$ Ω-cm and typical adhesion tensile strength of 1000 N/cm^2 (Structure Probe, Inc., 2005-2009). The first step of the application process was to tape off the composite samples using blue painter's tape so that only the potions that were sanded were left exposed for the electrode attachment. This was done so that a thin layer of the silver paint could be applied along the marked and sanded lines of the samples without paint accidently being placed in locations other than those intended for electrode attachment. This was done using a small brush attached to the cap of the paint jar. After the first layer of paint was applied an electrode was placed on top of the paint layer and was positioned so that one

end of the electrode was directly lined up with an edge of the sample while the other end was allowed to extend off of the samples surface. To ensure that the electrode was in strong contact with the sample along its entire surface length an additional paint layer was applied over the initial on as well as the placed electrode. This process was repeated until all nine samples had four electrodes placed along their top surfaces. Once this was finished the blue tape was removed and the paint was allowed to air dry for two hours prior to proceeding.

The second step of the electrode attachment process was to ensure that strong contact made between the electrodes and composite would not be compromised during the experimental process. This was accomplished by applying a layer of non-conductive, high strength epoxy over the already attached electrodes. The epoxy chosen was the LOCTITE® branded Hysol® E-120HP. E-120HP had been used previously due to its long workable time as well as its low viscosity and high strength (LOCTITE®, 2008). The epoxy was applied to the composite using an applicator which dispensed the correct 2:1 ratio of resin to hardener through a mixing nozzle which can be seen in Figure 3.8. A layer of epoxy was placed over the four electrodes on each sample's top surface and allowed to dry for a period of 24 hours.

Figure 3.8: Epoxy application system (McAndrew, 2009)

Once the Hysol® epoxy had completely cured over the electrodes on the top surface the samples were flipped over so their bottom surfaces were facing upwards and the process of electrode attachment and epoxy application could be repeated. Additionally after the samples were tested once for their electrical resistances along the top, bottom, and oblique surfaces it was decided that two additional electrodes would be applied to each surface of all the samples. The rational for the additional electrodes was to validate the results found from the initial testing as well as to investigate the electrical resistance changes due to wider separation between the sensing electrodes. An example of a sample with the original eight electrodes is shown in Figure 3.9 while a sample with the additional four electrodes is shown in Figure 3.10.

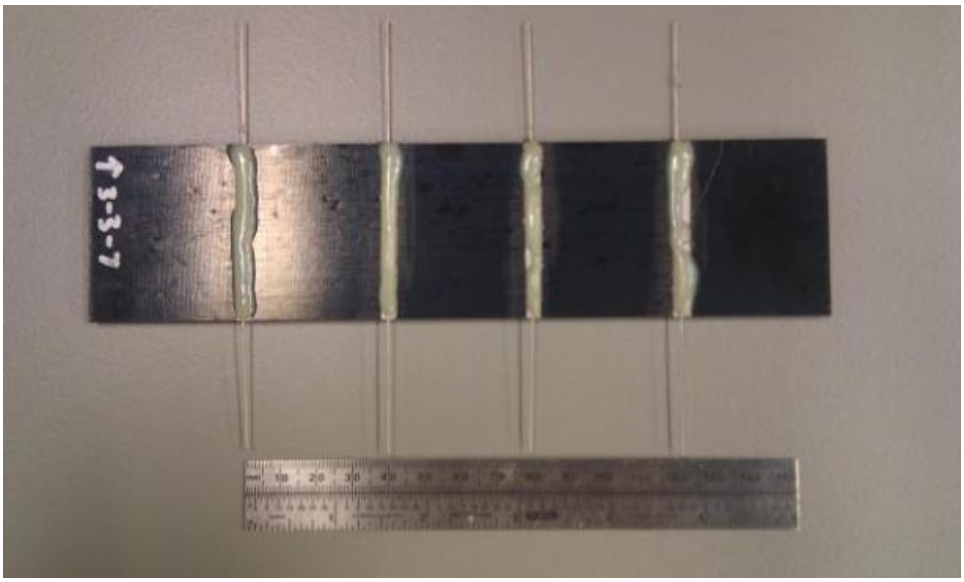

Figure 3.9: Completed probe sample with original eight electrodes

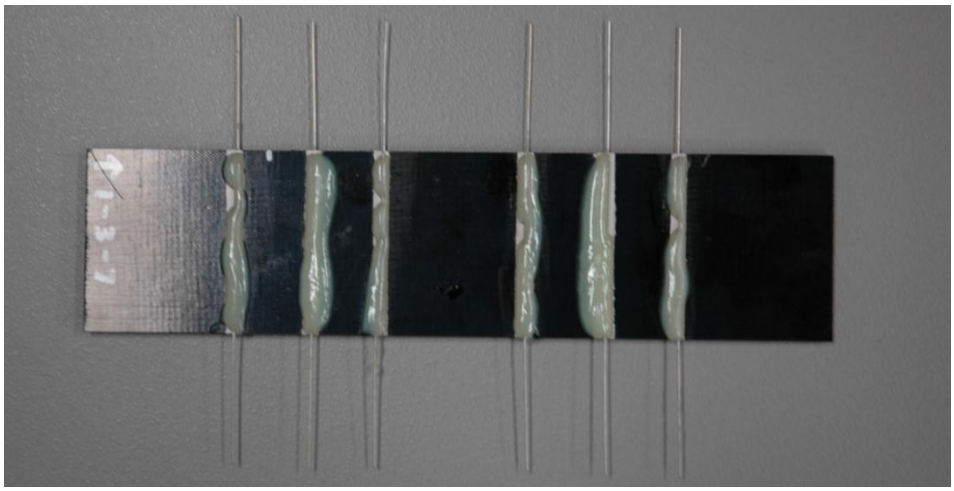

Figure 3.10: Composite sample with additional four electrodes attached

3.5 Four Probe Experimental Procedure

The twelve electrode placement, with six electrodes on each face of the composite sample, allowed for the electrical resistance testing of multiple different planes of each sample through the variation of source and sensing electrode selections. These different planes included the electrical resistance along each of the outer surfaces of the composite as well as through the thickness of the samples in the transverse direction of the composite fibers. The three types of resistance measurements were categorized separately so that they could later be compared type to type and sample to sample. Resistance measurements along the upper surfaces of the samples were labeled top measurements while those measured along the lower surface were labeled bottom measurements. Those measurements that were through the thickness of the composite samples were labeled oblique plane measurements.

To perform the electrical resistance measurements using the new experimental setup each sample was taken individually and connected to the hardware via the electrical alligator clip connectors. The first measurements taken were those of the top surface where the positive output of the HP 6612C power supply was connected to one of the outer most electrodes on the samples upper surface while the negative output was connected to the electrode on the opposite side of the upper surface. Next the positive terminal of the Agilent U2531A data acquisition unit was connected to the top surfaces innermost electrode on the same side as the positive power supply connection. Lastly the negative terminal of the data acquisition unit was connected to the remaining inner most sample electrode on the top surface. After the sample was fully connected the VEE pro software program was started and the HP power supply and Agilent data acquisition unit were turned on. Because all hardware was controlled through the VEE pro program only the desired current level, number of readings, and time between each reading needed to be inputted into the desktop computer before the start button was pressed. For each samples top surface 10 resistance measurements were than taken with source currents of 10, 30, 50, 70, 90, and 110 mA. The multiple current levels were used do to the fact that the larger the source current used the greater the current spreading through the thickness of the composite sample. This allowed for full analysis of resistance of the samples and more data to compare by.

After the top surfaces of all of the samples were measured the bottom surfaces were tested in an identical manner. This included connecting the outer bottom surface electrodes to the HP power supply and the inner most electrodes to the Agilent data acquisition unit. The last of the electrical resistances to be measured were the oblique

surfaces. These were done in a slightly different manner than those of the top and bottom surfaces. First the positive terminal of the power supply was connected to one of the outermost electrodes on the top surface of the samples. Then the power supply's negative output was connected to outermost electrode on the bottom surface of the composite on the opposite side of the sample from the connection on the top surface. The connections to the data acquisition unit were done in a similar manner with the terminals being connected to the innermost electrode on the top and bottom surfaces of the sample on the same sides as the power supply connections. For both the bottom and oblique surfaces of all the samples the same number of readings and source current levels were used as in the top surface measurements.

To allow for further investigation into the electrical resistance of the different types of composite samples top, bottom, and oblique measurements were also taken using the wider sense electrodes. This allowed for a greater understanding into how the electrical resistance values would change as the width between the sense electrodes was changed. To perform these experiments the electrode setups were identical to the original ones except instead of connected the positive and negative terminals of the data acquisition unit to the innermost electrodes they were connected to the inner electrodes that were closer to the source electrodes. The process for running the VEE pro program and recording the results also remained the same.

3.6 Four Probe Experimental Results

Results for both the initial sensing electrode width as well as the later explored wider width were all compiled into separated into individual tables for analysis. These

tables are shown in Appendix A with the initial electrode widths in section A.1 and the wider widths in section A.2. Each table shows the resistance found for each plane of the samples at each current level. Also the determined standard deviation of each of the results is reported.

3.6.1 Sample Comparison: Batch Variability

After all of the data was collected it could be organized and compared by like samples. First compared were the three samples that contained no buckypaper, 1-1-0, 2-1-0, and 3-1-0. The results of the top, bottom, and oblique surfaces resistances for these three samples are shown in Figure 3.11, Figure 3.12, and Figure 3.13.

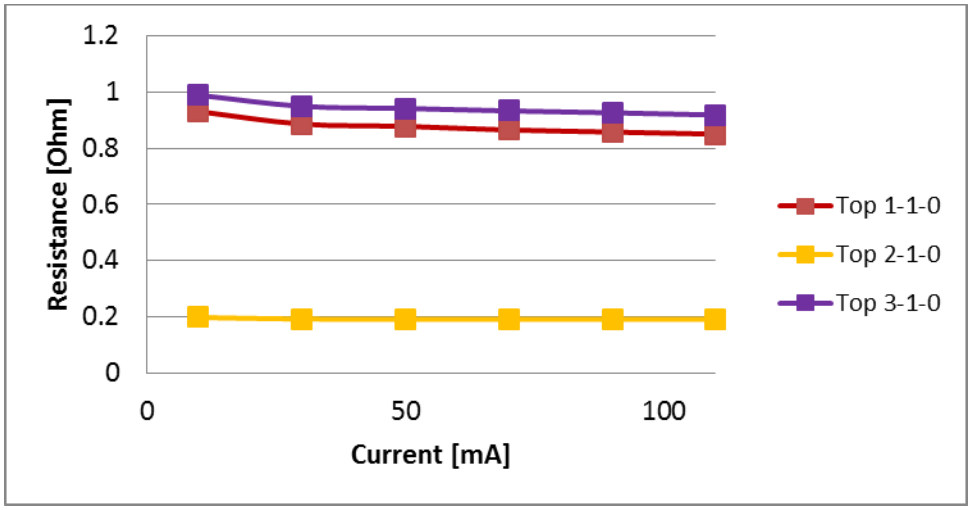

Figure 3.11: Top surface resistances for samples with no buckypaper

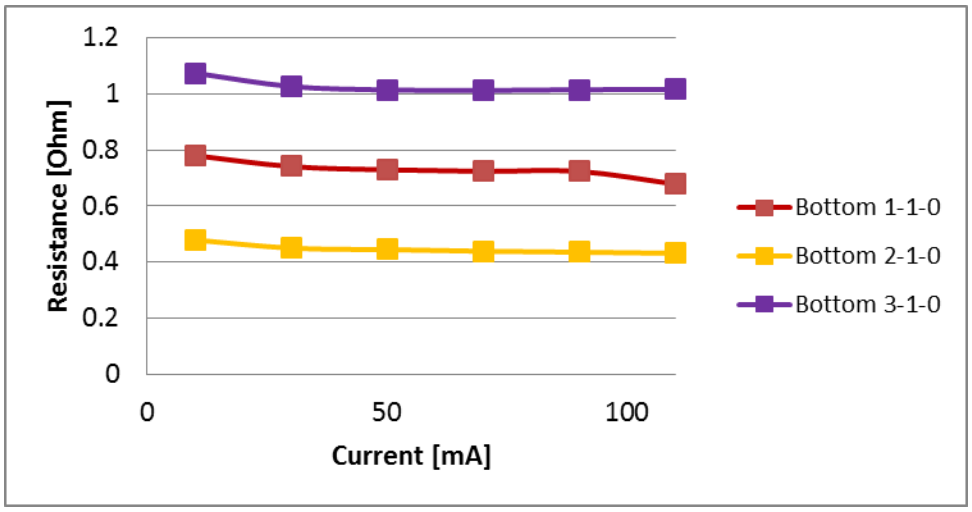

Figure 3.12: Bottom surface resistances for samples with no buckypaper

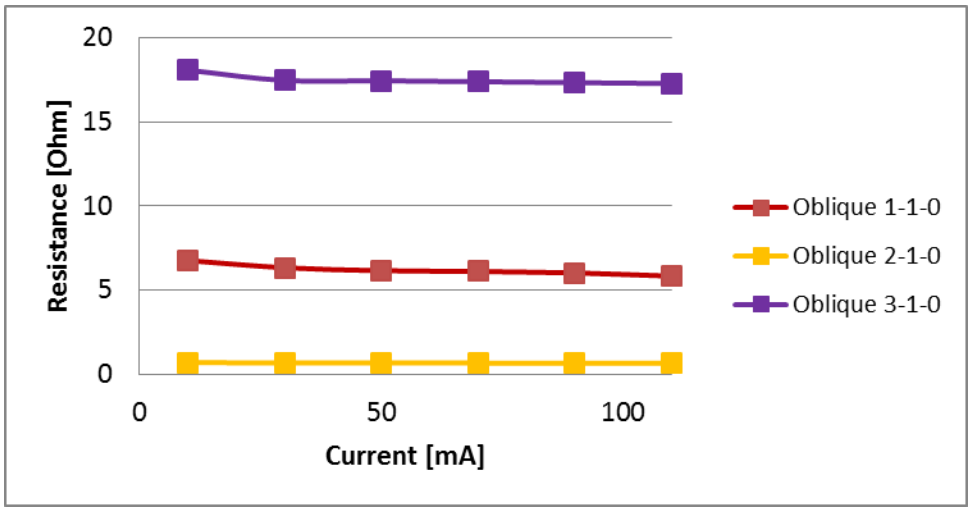

Figure 3.13: Oblique surface resistances for samples with no buckypaper

It was observed from the results that the resistances of the three samples varied widely. The results for the top resistances showed samples 1-1-0 and 3-1-0 being similar while 2-1-0 is much lower at approximately 0.2 ohms. The results of the bottom surfaces were different, with sample 3-1-0 having the highest resistance while the resistance of sample 2-1-0 was approximately 0.3 ohms lower and the resistance of sample 1-1-0 being

approximately 0.28 ohms below that. The resistant testing of the oblique surfaces provided trends very similar to that of the bottom surface in that 3-1-0 was the highest with 1-1-0 in the middle and 2-1-0 having the lowest resistance. Worth noting for the oblique surface testing was the extremely high resistance values found for samples 2-1-0 and 1-1-0. In fact all resistance values were much higher than would be expected from past experimentation for a carbon fiber composite at the widths used.

Next compared were the samples that had four layers of buckypaper. The plots of samples 1-2-4, 2-2-4, and 3-2-4 are shown in Figure 3.14, Figure 3.15, and Figure 3.16 respectively.

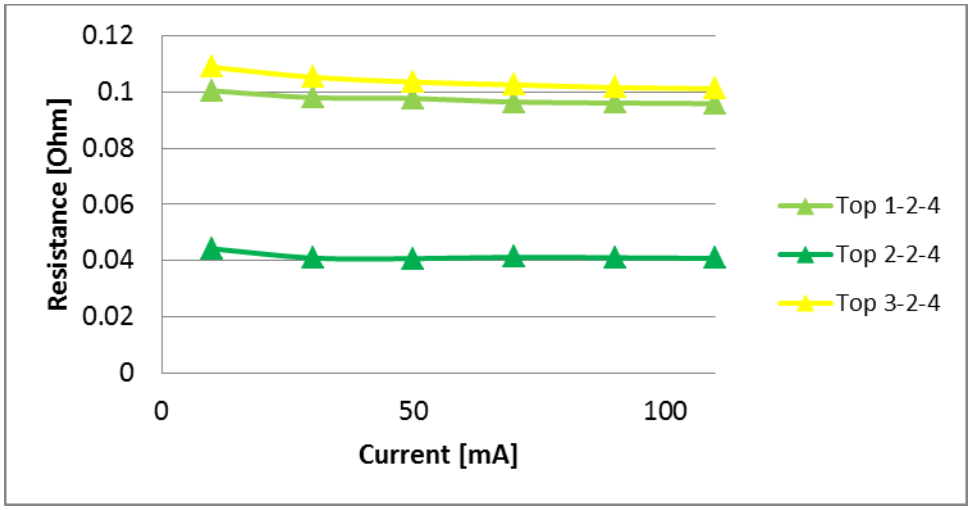

Figure 3.14: Top surface resistances for samples with four layers of buckypaper

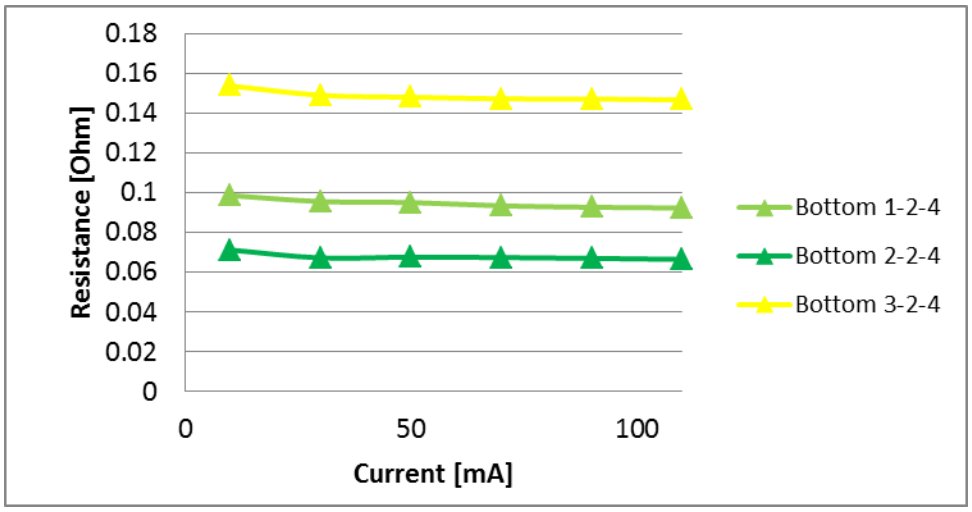

Figure 3.15: Bottom surface resistances for samples with four layers of buckypaper

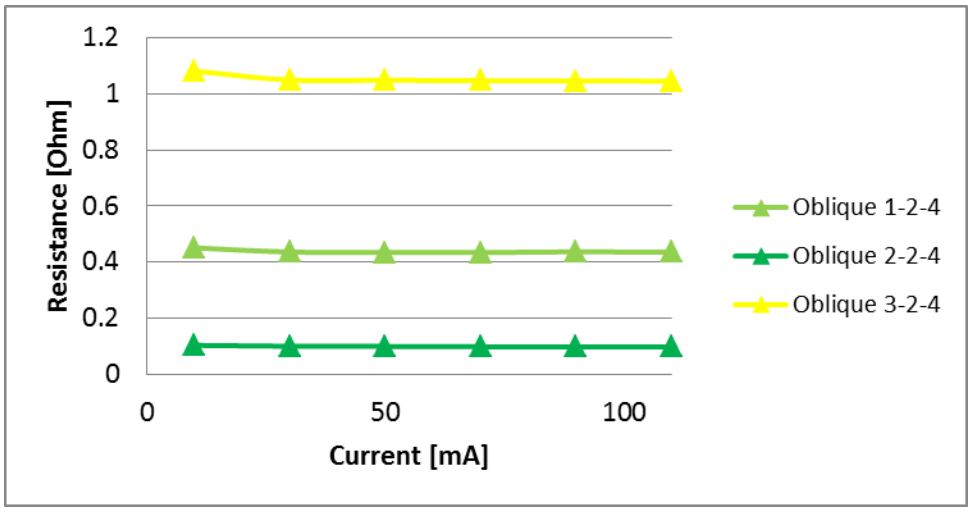

Figure 3.16: Oblique surface resistances for samples with four layers of buckypaper

In a similar manner to the measured resistances of the samples with no buckypaper material, the samples with four layers of buckypaper had one sample with much lower resistance values than the other two. Unlike the first set of samples with no buckypaper layers, the samples with four layers of buckypaper had resistances much closer in values to what would be expected of composite materials. Analyzing the bottom

and oblique surfaces resistances also showed much lower values that were seen for the first set samples as well a continuing trend of batch three producing the highest resistances followed by batch one and batch two with the lowest resistance values.

With the samples containing no buckypaper and four layers of buckypaper analyzed, the last set of samples to investigate were those with seven layers of buckypaper. The results of their electrical resistance tests are shown in Figure 3.17, Figure 3.18, and Figure 3.19 respectively.

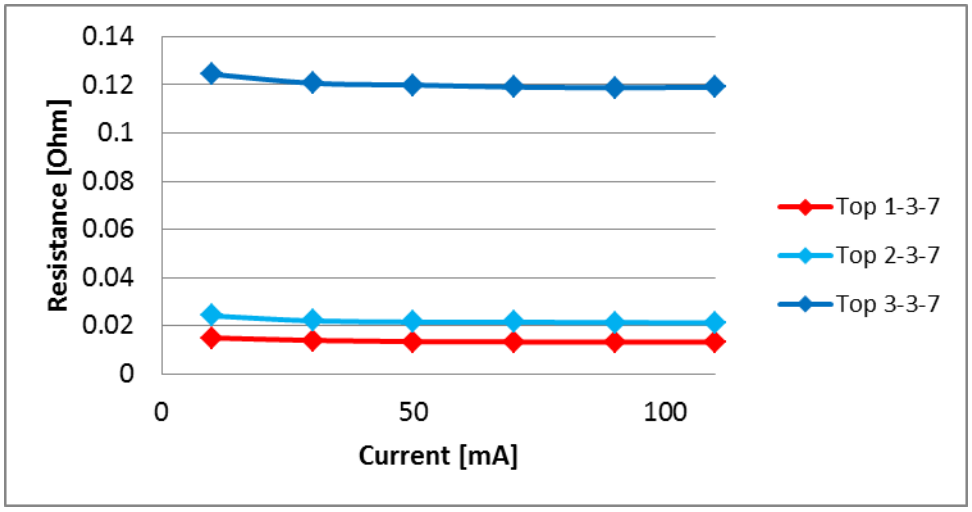

Figure 3.17: Top surface resistances for samples having seven layers of buckypaper

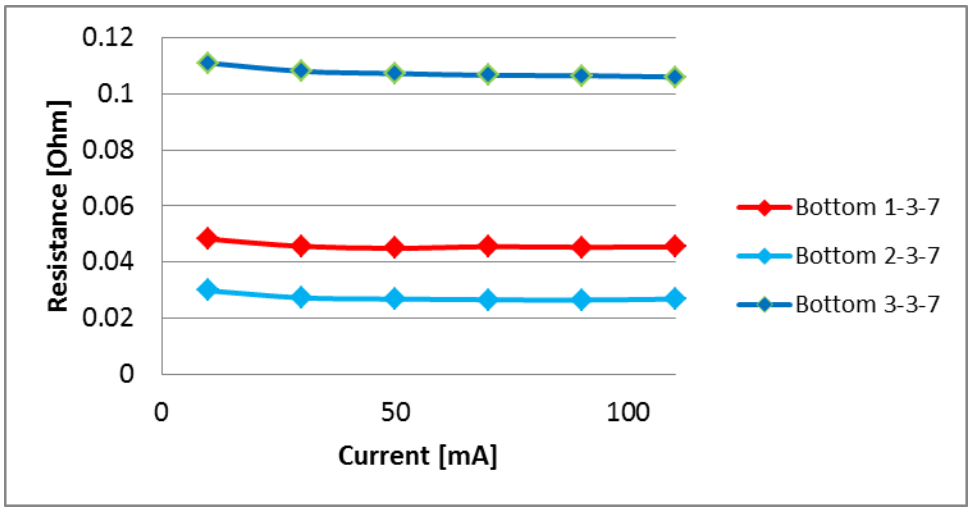

Figure 3.18: Bottom surface resistances for samples having seven layers of buckypaper

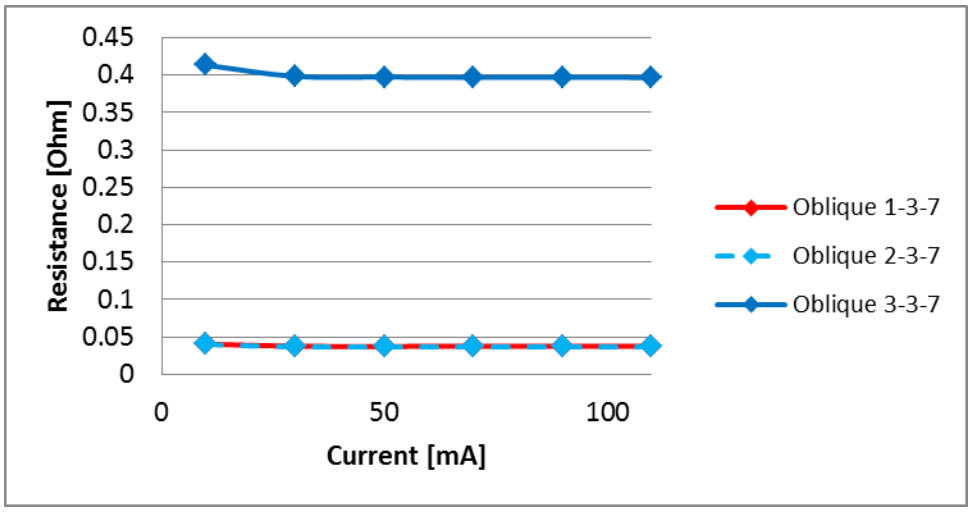

Figure 3.19: Oblique surface resistances for samples having seven layers of buckypaper

For the top surface resistances the batch three samples showed the greatest resistance followed by batch two and batch one which were fairly close. The same trends held true for the bottom and oblique surfaces as well. In fact it can be seen that samples 2-3-7 and 1-3-7 had nearly identical results for the oblique surface.

The analysis of all nine samples grouped by the number of buckypaper layers they contain showed some common trends. The most prominent of these was that for every plot, with the exception of the seven layer bottom resistance, the batch three samples had the highest electrical resistance followed by batch one samples in the middle and batch two samples with the lowest resistance. Also observed were the very high resistance values recorded for all surfaces of the samples with no buckypaper. These values are much larger than would be expected and that have been recorded in previous experiments (McAndrew, 2009). A final trend seen in the plots in Figure 3.11 through Figure 3.19 were the large differences in resistances for samples that had the same makeup which leads back to the issue of batch variation.

3.6.2 Sample Comparison: Effects of Buckypaper on the Electrical Resistance of Composites

To investigate the effect of the addition of the buckypaper layers on the electrical resistance of carbon fiber polymer matrix composites, the samples were grouped by batch number and plotted. The results of this analysis are shown for batch one in Figure 3.20, Figure 3.21, and Figure 3.22.

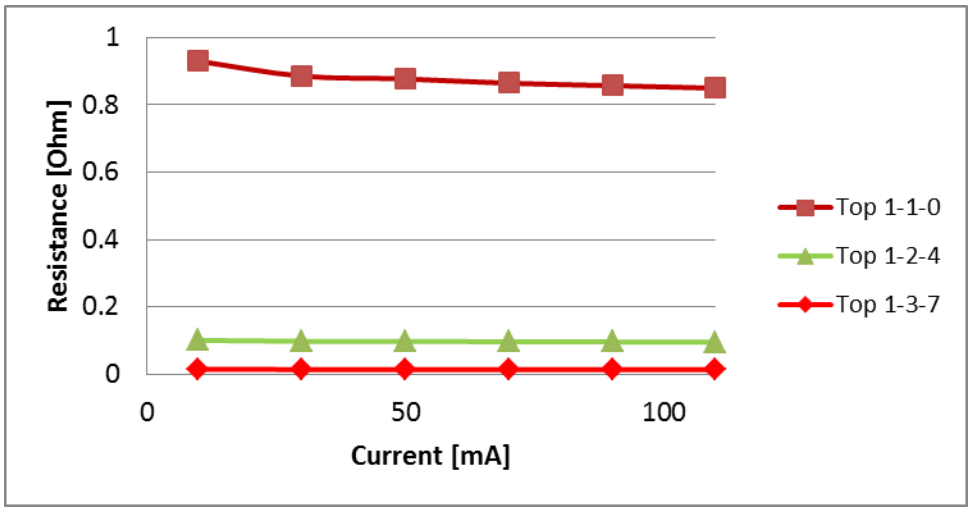

Figure 3.20: Top surface resistances for batch one samples

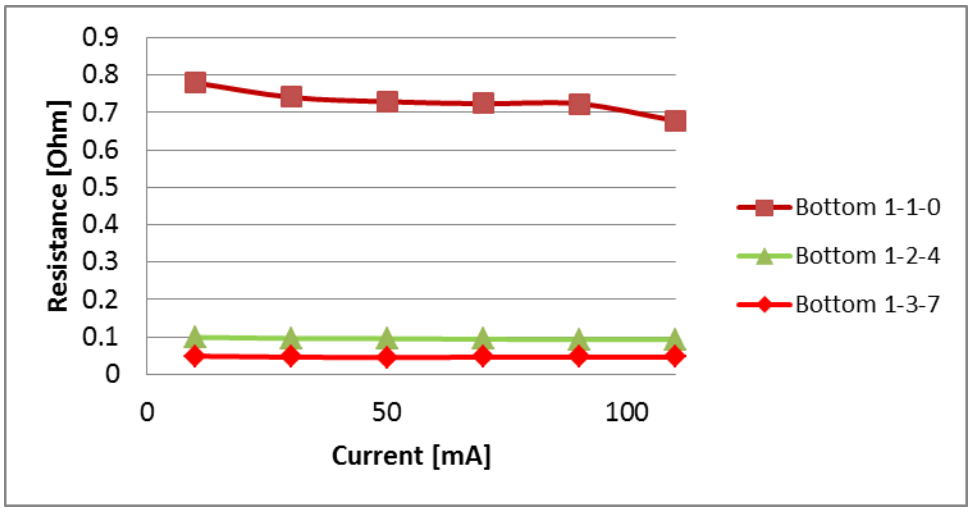

Figure 3.21: Bottom surface resistances for batch one samples

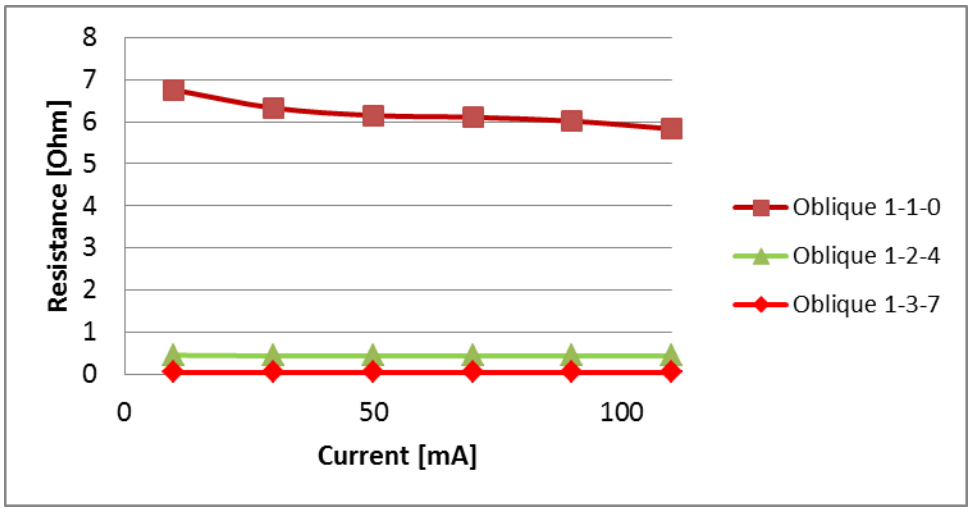

Figure 3.22: Oblique surface resistances for batch one samples

As expected, sample 1-1-0 with no buckypaper had the highest resistance for all surfaces followed by 1-2-4 with four layers of buckypaper and 1-3-7 with seven. This trend of decreasing resistance with increased amounts of buckypaper is due to buckypaper's high electrical conductivity. Also worth noting is the magnitude of the resistances found. Sample 1-1-0 showed much greater resistances than the other two samples while 1-2-4 and 1-3-7 were much smaller in magnitude and in differences between each other.

Batch two was also analyzed similarly to batch one. The results of that investigation are shown in Figure 3.23, Figure 3.24, and Figure 3.25 for the top, bottom, and oblique surface respectively.

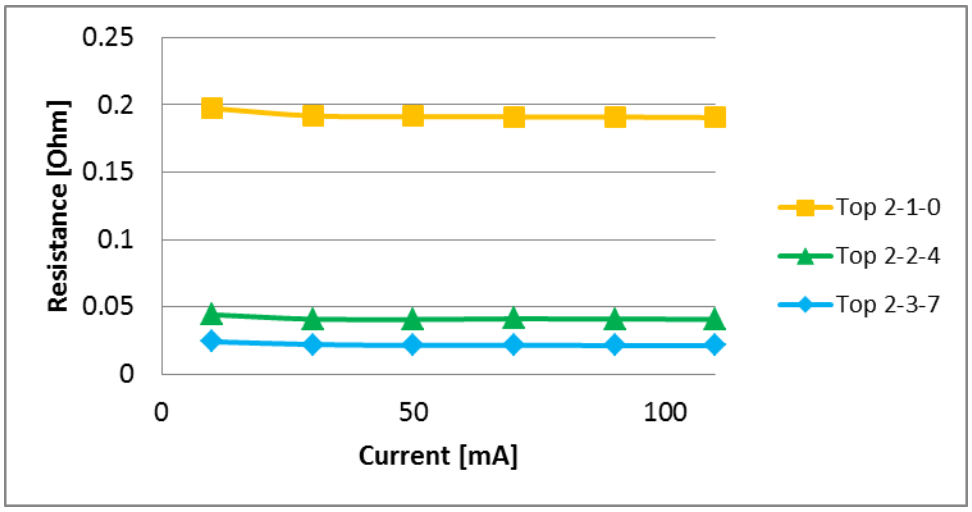

Figure 3.23: Top surface resistances for batch two samples

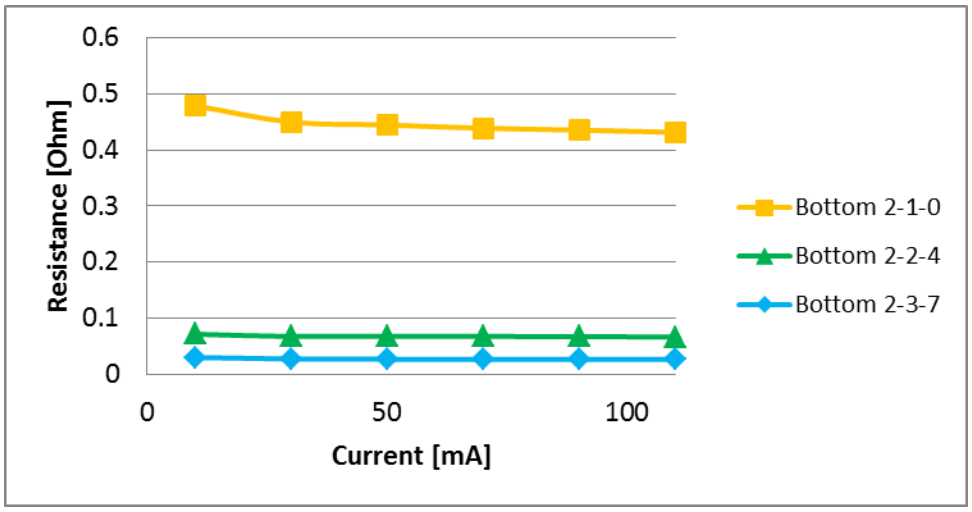

Figure 3.24: Bottom surface resistances for batch two samples

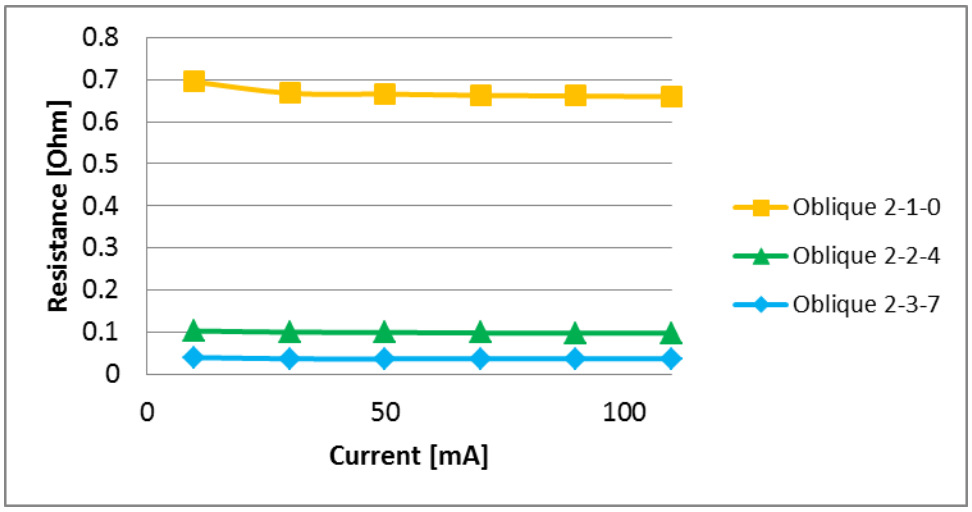

Figure 3.25: Oblique surface resistances for batch two samples

From the batch two analysis it can be observed that a similar trend was found to the samples of batch one where the greater the number of buckypaper layers the lower the resistance. Also the same was that the samples that contained buckypaper had much lower resistance values than the one that didn't as well as resistance values that were much closer together.

The last analysis was performed on the samples of batch 3. Figure 3.26, Figure 3.27, and Figure 3.28 show the results of this for all three surfaces investigated.

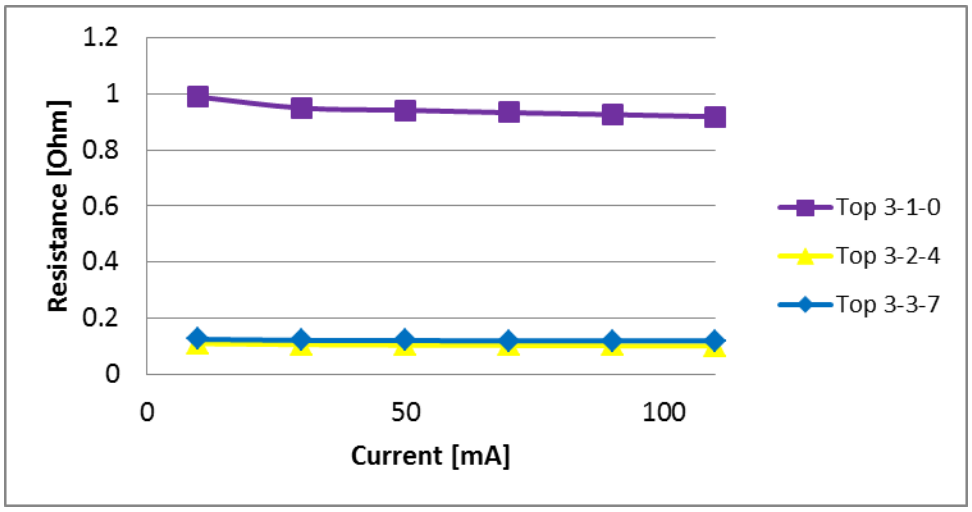

Figure 3.26: Top surface resistances for batch three samples

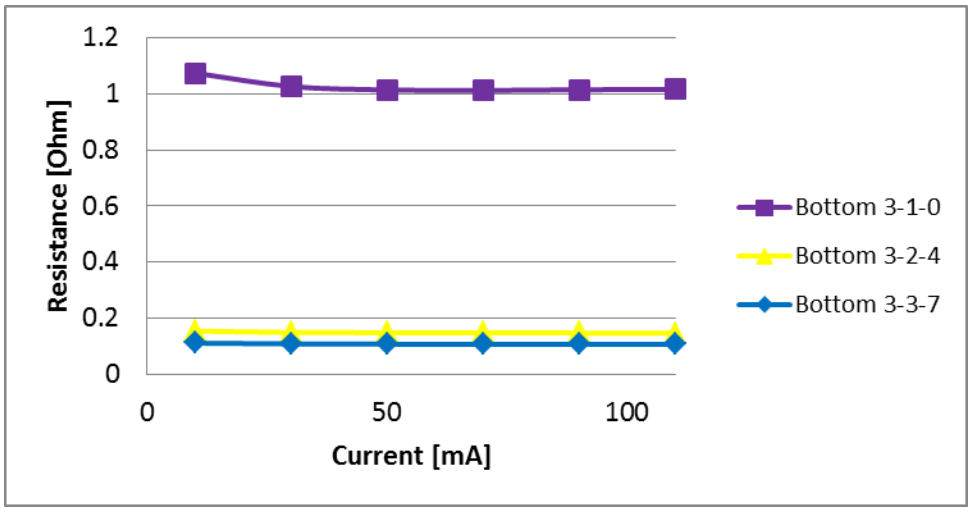

Figure 3.27: Bottom surface resistances for batch three samples

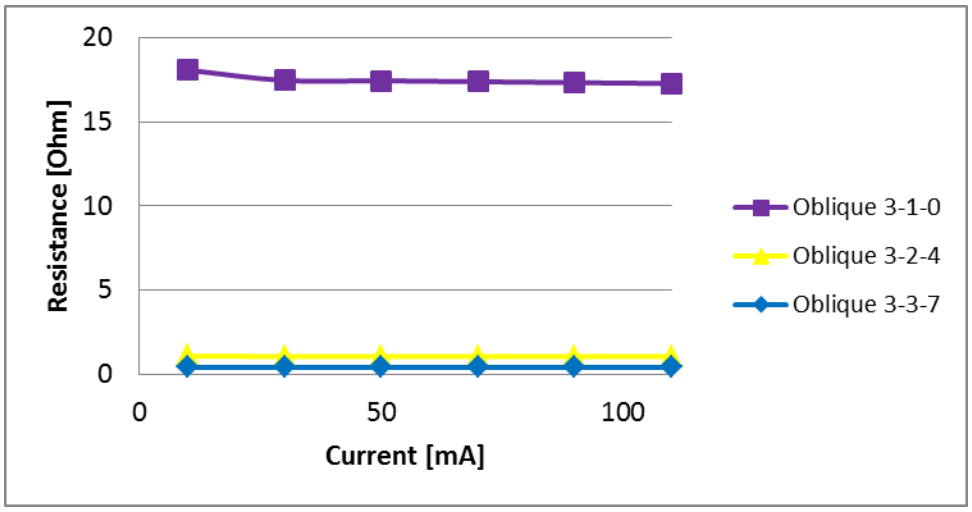

Figure 3.28: Oblique surface resistances for batch three samples

Much like the previous two batches the bottom and oblique surfaces for batch three had the same order of makeup with respect to resistance magnitude. Worth noting is the extremely high resistance values for the oblique surface of sample 3-1-0. The top surface plot in Figure 17 is slightly different from all other batch surface comparisons in that the sample with seven layers of buckypaper had lower resistance values than the sample with four layers thought they are very close in value for all current levels.

The experiment and subsequent analysis has allowed for some conclusions to be drawn about the resistance values of composite samples and how the introduction of buckypaper affects those resistances. It was shown that the greater the amount of buckypaper, the lower the resistance. It was also shown that there was a much larger resistance magnitude decrease from no buckypaper to four layers of buckypaper than from the latter to samples with seven layers of buckypaper. Also found was that batch three had the highest resistance values for all surfaces followed by batch one and lastly batch two.

3.6.3 Validation Using Wider Electrode Placement

The samples were again connected to the Agilent DAQ and HP power supply, this time with the wider sensing electrodes being used for voltage measurements. For these tests the same source current levels of 10, 30, 50, 70, 90, and 110 mA were used. The results were then compared by batch and number of buckypaper layers before being analyzed against the previous results. Figure 3.29, Figure 3.30, and Figure 3.31 display the results for the resistance measurements of samples containing no buckypaper. The results from the original tests showed that the batch three sample had the highest electrical resistance followed by batch one and batch two with the lowest.

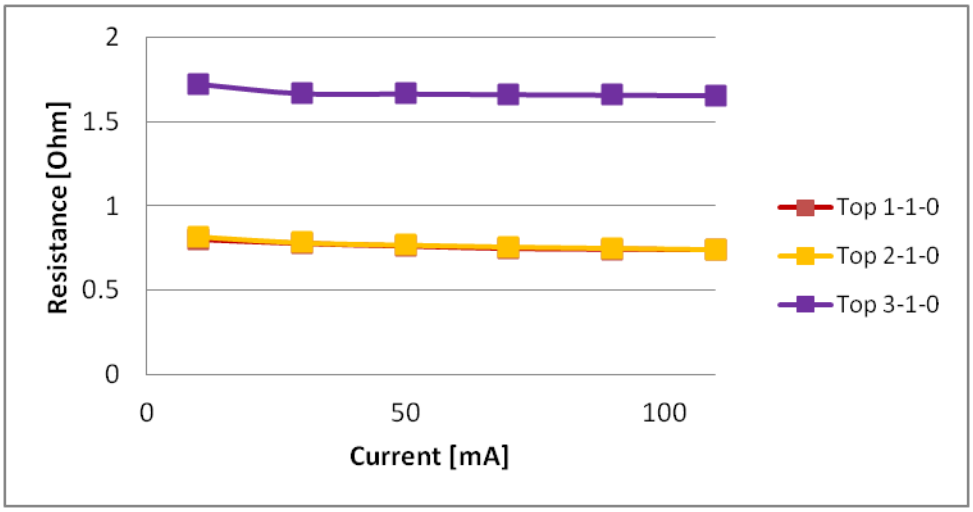

Figure 3.29: Wider top surface resistances for samples with no buckypaper

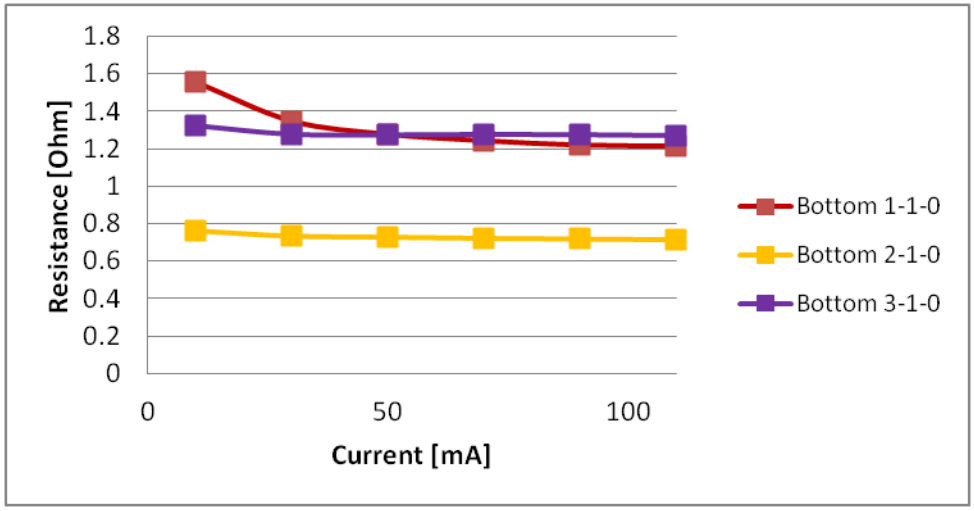

Figure 3.30: Wider bottom surface resistances for samples with no buckypaper

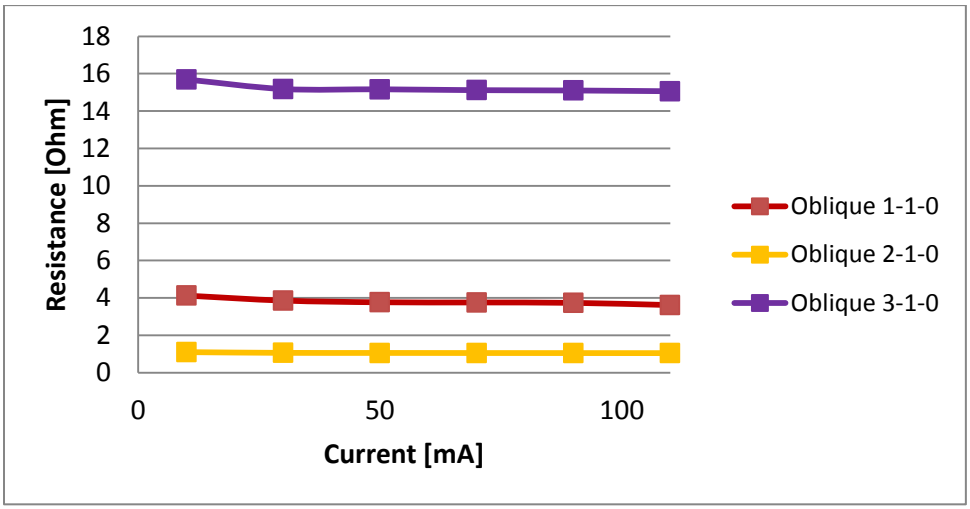

Figure 3.31: Wider oblique surface resistances for samples with no buckypaper

Among the figures the oblique results show the most obvious trend with the third batch sample having the highest resistance followed by the first batch and lastly the second batch. The bottom plane resistances showed the same with batch three being much larger than the batch two sample but the batch one sample performed oddly and

could not be compared to the other two. The top plane resistances had the batch two and one samples so close together in their results that it could not be determined which had a higher resistance while the batch three was much higher.

Next compared were the samples that contained four layers of buckypaper. The initial testing had shown that for all planes the electrical resistance was highest in batch three and lowest in batch one with batch two being in between. Figure 3.32, Figure 3.33, and Figure 3.34 show the results of the wider resistance testing of these samples.

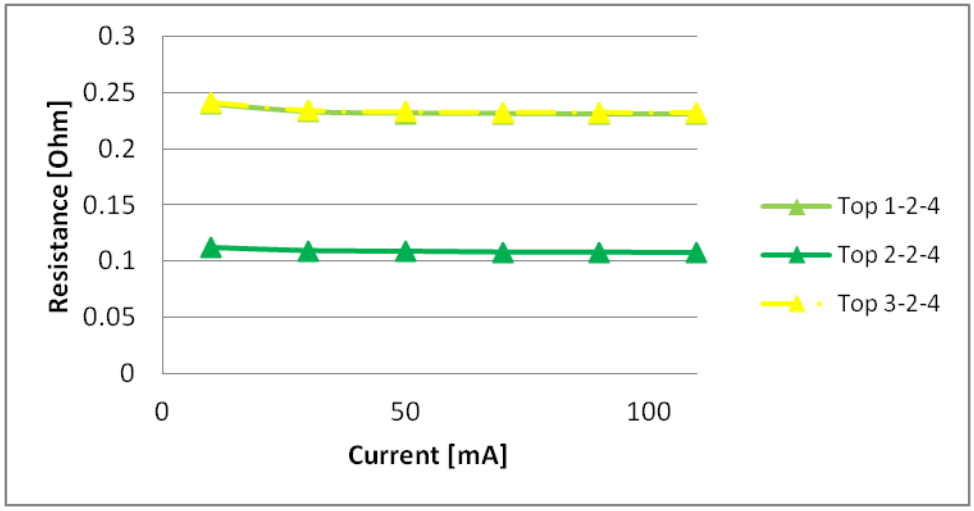

Figure 3.32: Wider top surface resistances for samples with four layers of buckypaper

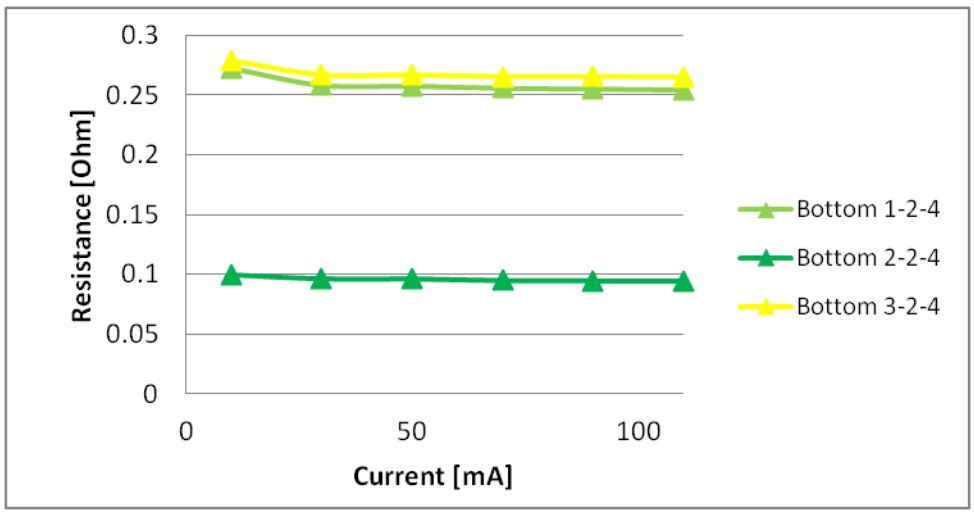

Figure 3.33: Wider bottom surface resistances for samples with four layers of buckypaper

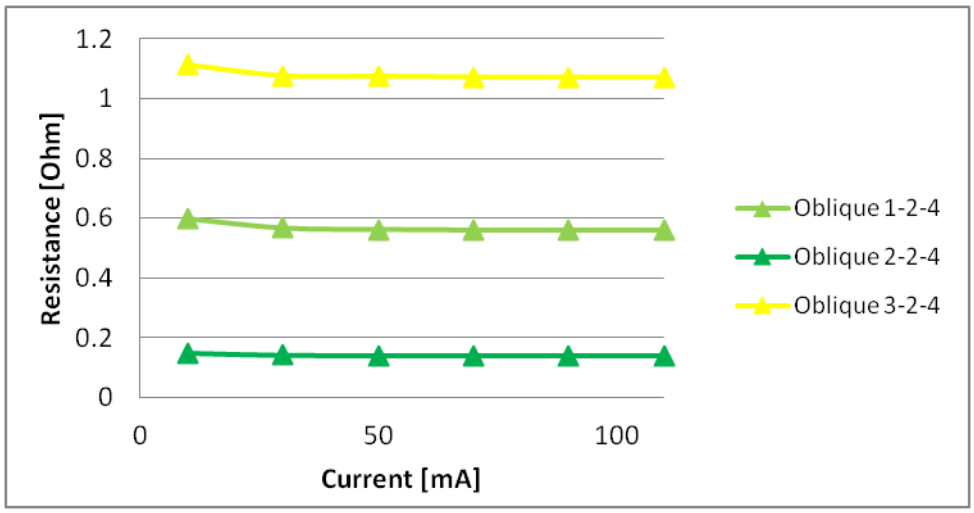

Figure 3.34: Wider oblique surface resistances for samples with four layers of buckypaper

Much like the initial measurements and plots show the wider electrode placement produced results with batch three having the highest resistance followed by batch one and

lastly batch two. The slight exception to this result was the top plane measurements which showed batch three and batch one samples with almost identical resistances.

The remaining samples, all of which contained seven layers of buckypaper, were compared lastly. In previous electrical resistance measurements these samples followed the trend of having the batch three sample with the highest resistance for all planes. Unlike the original testing of the samples with no buckypaper and four layers of buckypaper, the batch two sample did not have lower resistances than the batch one sample for the top and oblique planes in the initial results. The following in Figure 3.35, Figure 3.36, and Figure 3.37 show the results when the wider electrodes were used.

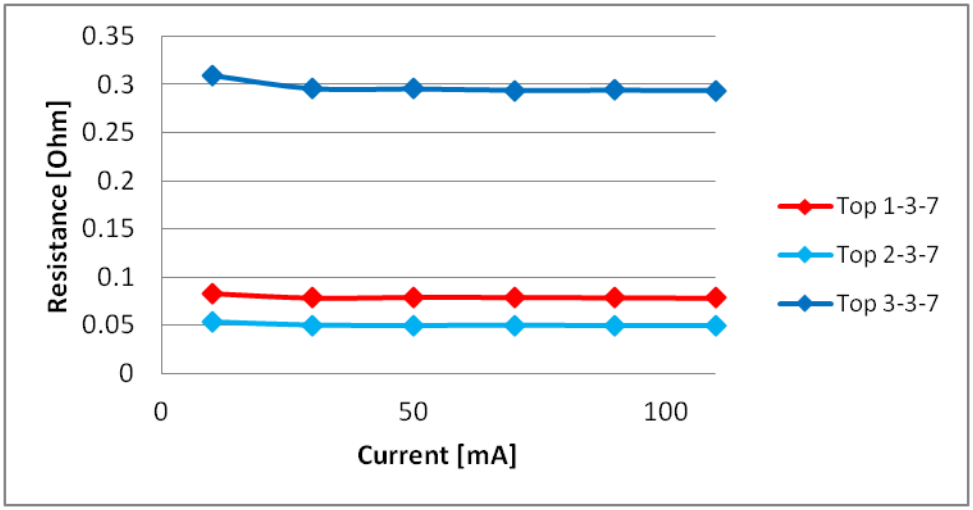

Figure 3.35: Wider top surface resistances for samples with seven layers of buckypaper

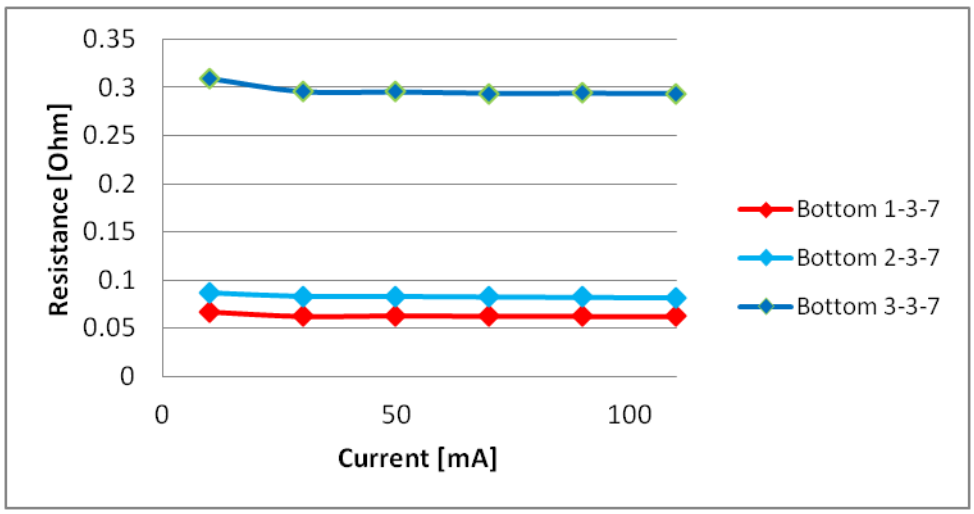

Figure 3.36: Wider bottom surface resistances for samples containing seven layers of buckypaper

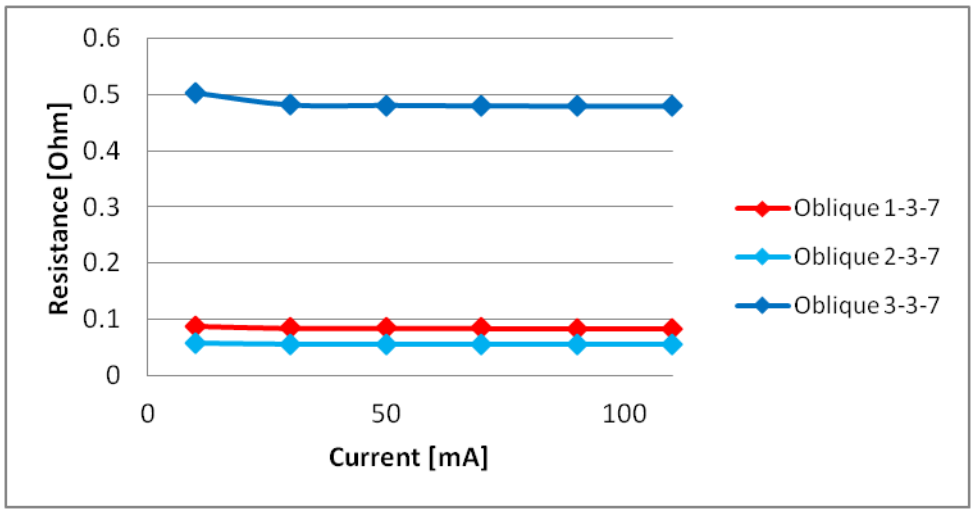

Figure 3.37: Wider oblique surface resistances for samples containing seven layers of buckypaper

Again batch three was the most resistive, far exceeding the values of both the batch one and two samples. Also similar to the testing of the original electrodes was that the batch two sample was not the least resistive for all planes with batch one's sample being less resistive for the bottom plane.

The conclusions of the electrical resistance testing with the wider electrodes was that no matter the buckypaper content of the sample, the samples from batch three were always the most resistive. Also continued was the trend of batch one having samples that were in the middle of the measurements and batch two having samples that were least resistive. That being said the wider electrodes did show some slight variations with the batch one samples being equal in resistance for some planes with the batch two and three samples.

3.7 Four Probe Computational Analysis

In order to better understand how the electrical resistance of the CFRP composite samples is affected be the addition of buckypaper layers, computational studies were performed using finite element analysis (FEA). Using COMSOL Multiphysics version 4.2 the physical sample and electrode geometry was created and material properties were applied. The electrical potential and current properties were added using the AC/DC physics library and meshing was achieved through various mapping and distribution techniques. Solutions were found using the parameter sweeping features of COMSOL and were analyzed in comparison with the experimental results and analytical solution.

3.7.1 Formation of COMSOL Model

To find an FEA solution of the electrical resistance in a composite sample using a four probe method three dimensional geometric models needed to first be created. This was done using the modeling package available in the COMSOL software. Measurements that were taken from the physical samples used in experimentation including thicknesses, widths, and lengths were used in the creation of the 3D model so that the results could be directly compared. The pure carbon fiber samples were modeled as a singular block in which their anisotropic electrical properties could be applied. Samples that contained buckypaper layers had to be modeled somewhat differently. For these samples 3D blocks were created directly on top of each other in the Z dimension with each layer being as thick as the number of carbon fiber or buckypaper layers it was to represent. This method of layer blocks would allow for the different material properties to be applied to the blocks representing different materials. Examples of the layering for each type of sample are shown in Figure 3.38.

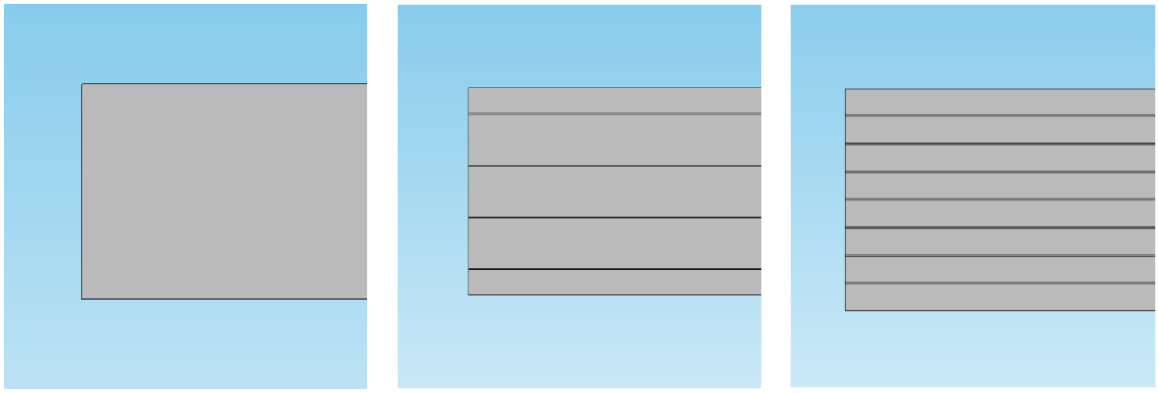

Figure 3.38: models of pure CF (left), 4 layers of buckypaper (middle), and 7 layers of buckypaper (right) in COMSOL

The electrodes were modeled as long rectangles with their width and height dimensions being the diameter of the 22 gauge wire used in the experimentation. The four electrodes were placed at even intervals along the surfaces of the samples with four centimeters of space between them. To allow for a conforming mesh between the electrodes and samples the composite samples were separated into sections the width of the electrodes directly under the electrodes locations. The completed geometry for the pure carbon fiber samples is shown in Figure 3.39.

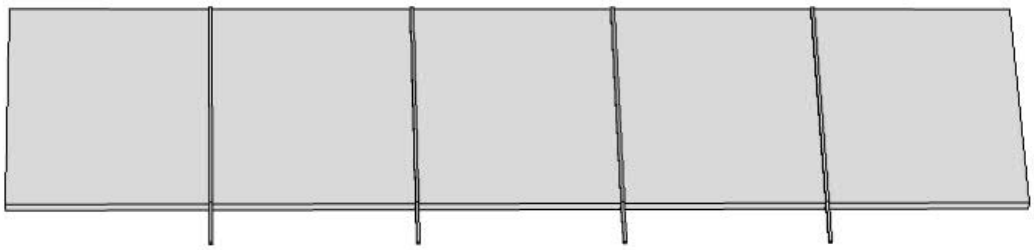

Figure 3.39: Completed model of pure CF sample in COMSOL

Once the geometry had been completed for all three types of composite samples the meshing could be addressed. It was decided to use a conforming hexahedral mesh for both the composite material as well the electrodes. To apply the mesh one of the long sides of the composite was selected as a mapping face. For the pure carbon fiber sample a distribution was created allowing for the mesh grid to be 16 equal elements in the height direction of the sample, the sample number as there are layers of carbon fiber. This was similar in the samples that contained buckypaper except the distribution was set so that

the number of elements along the vertical edge of each block was equal to the number of carbon fiber layers in that block. The buckypaper layers were all assigned one vertical element. The same horizontal distribution was set for all types of samples. Ten elements were assigned along the horizontal edge of each portion of the composite sample between the electrodes. Rather than a uniform distribution of nodes as was done in the vertical direction, the nodes were set so that each one was 20 times greater distance away from the previous one as the nodes moved away from the contact region between the electrodes and composite sample. This allowed for a concentration of elements near the contact regions. The last surfaces to be mapped were the composite sample areas directly under the electrodes as well as the electrodes themselves. The areas under the electrodes were assigned three equally spaced elements in the horizontal direction and the same vertical spacing as the rest of the composite. The electrodes were given a distribution of three equal elements in both the horizontal and vertical direction aligning the nodes exactly with those of the composite. With the mapping complete the node and element distribution could be swept through the thickness of the sample and electrodes. It was chosen to have the mesh be five elements wide through the thickness as well as one additional element width for the portion of the electrodes that extended beyond the composite sample.

The next step in the model building process was the application of the material properties of all materials used in the composite samples and test setup. The electrodes were assigned as a copper material from the COMSOL Material Library with an electrical conductivity of 5.9E7 siemens per meter (S/m). The IM7/977-3 composite material was applied as a diagonally anisotropic material with electrical conductivity in

the fiber direction being 9,000 S/m. The conductivity value was determined by using the rule of mixtures and Reuss estimate to predict bounds and adjusting accordingly based on the experimental data. The conductivities in the directions transverse the fibers and through the thickness were found to be 9 S/m and 0.37 S/m respectively using the same method. The relative permittivity of the composite was set to one as it had been determined by past researchers to not need to be defined for very good conductors (Seidel et al., 2010). Lastly the buckypaper material was applied with a resistivity of 100 micro ohm-cm which was determined experimentally by Florida State University researchers (Yeh, 2007).

After the materials had all been assigned properties, the physics constraints of the problem had to be applied. Using the AC/DC library built into COMSOL 4.2 electrical current conservation was applied to all materials. This included dictating the electrical conductivity parameters to be assigned by the applied materials which were discussed previously. Also added was a contact resistance between each of the composite layers of $2.9x10^{-5}$ ohm-m^2 which was found by Chung experimentally (Chung, 2000). After this an initial value parameter was set with all materials having initial electrical potentials of zero volts. The final step in the physics setup was to apply the electrical current sources to the two outer electrodes and voltage probes to the two inner electrodes. The source current was applied using COMSOL's Boundary Current Source feature. First the electrode geometry was split so that the portions of the electrodes that were directly in contact with the composite sample were separated from the portions that extended beyond the composite. This allowed for the contact surface between the electrode portions over the composite samples and the portions extending beyond the samples to be

selected. The boundary currents were applied to the two outer source electrodes with one electrode receiving a positive current value and one an equal but negative current value. This enforced the current flow pattern through the composite. The last constraints that were applied were two voltage probes to the inner two sensing electrodes. The probes allowed for the voltage potential to be determined between the two electrodes after the solver was ran.

To validate results from the experimental sample testing as well as investigate the electrical resistance changes when parameters that were not possible to test during experimentation were changed the COMSOL solver was ran in many different configurations. These included parameter sweeps changing properties such as sample thickness or width between electrodes as well as modifications to the mesh sizing to ensure results were consistent.

3.7.2 Validation of Computational Model

Several tests were performed on the COMSOL models before they were used to investigate the behaviors of the composite materials. First of which was a mesh quality examination. This was to ensure that too large of mesh elements had not been chosen for the models which would produce invalid results. This was performed by adding additional elements in different components of the models to see if any of the results would change. The results of these tests are shown in Table 3.2. As it can be seen no variation occurred to the electrical resistances of the samples when the mesh was modified.

Table 3.2: COMSOL mesh variation for validation

Modification	Element number	Resistance
Original pure carbon fiber mesh	5176	0.1913 Ω
Increased vertical mesh density	10136	0.1913 Ω
Increased horizontal mesh density	9176	0.1913 Ω
Concentrated elements closer to electrodes	9176	0.1913 Ω
Increased electrode elements	8824	0.1913 Ω
Original four BP layer mesh	6416	0.0459 Ω
Increased vertical BP mesh density	6726	0.0459 Ω
Increased horizontal BP mesh density	6466	0.0459 Ω

Once it was determined that the meshes contained the proper element resolution the computational electrical resistance results were compared to an analytical solution that had been previously developed by Park et al (2007). This analytical solution, shown in Equation 3.1, can be used to determine the voltage at any point of an electrically anisometric composite material which then easily be divided by the source current to find resistance:

Equation 3.1: Voltage distribution through a composite sample for a DC electrical resistance test (Park, 2007)

$$V\,(x,z) \approx \frac{-I}{b}(\rho_z\rho_x)^{1/2}\frac{\sin[\pi\frac{x}{L}]}{\sinh[(\pi\frac{t}{L})(\rho_z/\rho_x)^{1/2}}\cosh[\pi\frac{z}{L}\left(\frac{\rho_z}{\rho_x}\right)^{\frac{1}{2}}]$$

Here V is the voltage, ρ_z and $\rho_x$are the resistivities of the composite in the thickness and fiber directions respectively, I is the applied current, b is the width of the sample, t is the thickness, L is the total length, and x and z are the coordinates of the point where the voltage is to be found.

For both the COMSOL and the analytical solution tests both the thickness of the composite sample as well as the electrical conductivity ratio between the fiber direction and thickness directions were adjusted multiple times to ensure that both solutions converged to the same answers no matter what the input parameters were. An example of this is shown in Table 3.3 where an anisometric ratio of 100 was used and the thickness was varied as a function of the number of laminates in the sample from 2 to 16 by increments of 2. As can be observed the two solutions produce fairly close results with a percent difference of 5.22 percent for two laminae up to 8.65 percent for 16 laminae. This proved that the COMSOL model accurately predicted the voltage distributions through both the thickness and length of the composite samples.

Table 3.3: COMSOL versus analytical solution for a conductivity ratio of 100

Number of Layers	COMSOL Solution	Analytical Solution	% Difference
2	0.2909	0.3065	5.22
4	0.1456	0.1535	5.28
6	0.0971	0.1027	5.61
8	0.0728	0.0773	6.00
10	0.0583	0.0622	6.47
12	0.0486	0.0522	7.14
14	0.0416	0.0451	8.07
16	0.0365	0.0398	8.65

3.7.3 Results from Computational Model

With the problem setup and validations completed the FEM model could be used to investigate the effects of the addition of buckypaper on the electrical resistance of carbon fiber reinforced polymer composite laminates. As was discussed in the experimental setup many computational tests were run in determining the material properties of the IM7/977-3 and buckypaper materials. Table 3.4 shows the comparisons between the batch two samples which were used in determining the material properties and the COMSOL models. The values are also plotted and shown in the bar graph in Figure 3.40. From the table and graph it can be seen that the values are very similar for the pure carbon fiber and four layer buckypaper samples and associated COMSOL models but become more separated as the number of buckypaper layers was increased to seven. Both the experimental results and COMSOL model show a large resistance decrease between the pure carbon fiber samples and four buckypaper layer ones where as only small resistance decreases between the four and seven buckypaper layer samples. This was a trend that was observed throughout all of the experimental results.

Table 3.4: Top resistance variations with the addition of buckypaper layers

Sample type	Batch 2	COMSOL
Pure carbon fiber	0.1907 Ω	0.1913 Ω
Four layers of BP	0.0408 Ω	0.0459 Ω
Seven layers of BP	0.0212 Ω	0.0433 Ω

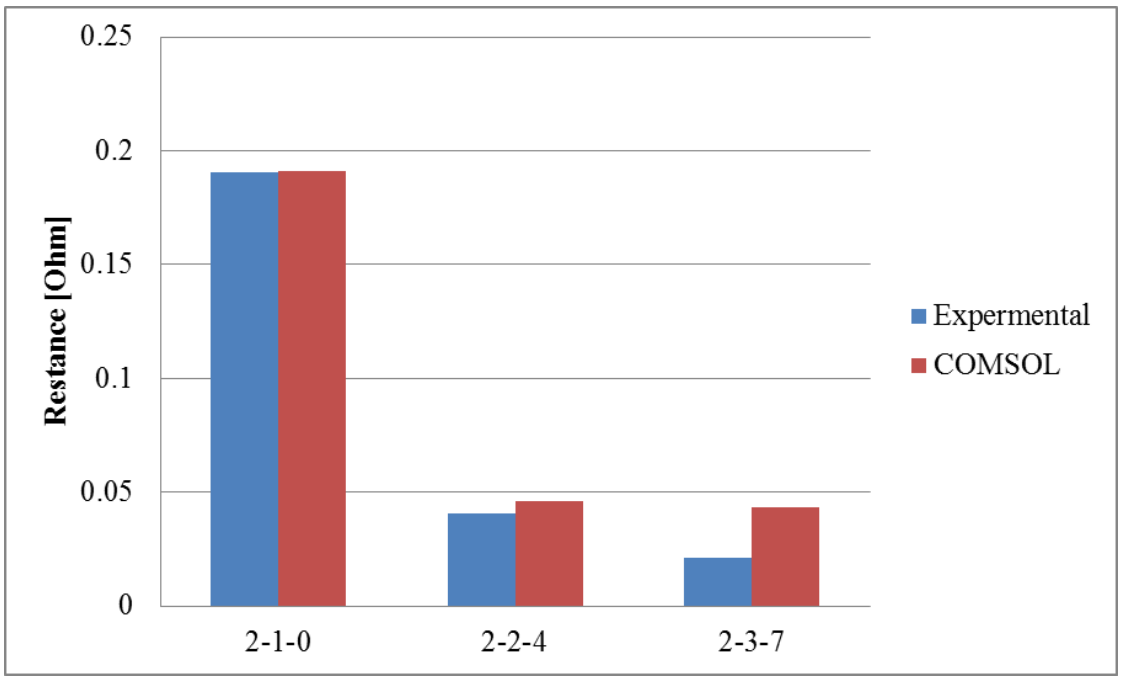

Figure 3.40: Comparisons between the batch two experimental results and COMSOL models

While the model is very close to the experimental results for sample 2-1-0, adjusting it to catch some of the other trends seen in the experimental results such as the three and four times greater top resistances of samples 1-1-0 and 3-1-0 was a challenge. Some changes can be made to the contact resistance between laminates with the understanding that all three patches were produced at different time potentially under different pressure and temperature conditions. Also, changes can be made to the conductivities of the buckypaper sheets as they were all made individually and have the potential to have many different properties depending on the nanotube alignment. What must remain the same are the material properties of the IM7/977-3 which would have been produced in a very controlled and uniform manner by its manufacturer. Further

refinement of this model and adjustment of these properties should in the future allow for a wider sample result range to be investigated.

3.8 Summary of the Electrical Characterization Results using the Four Probe Method

The four probe electrical resistance testing and subsequent computational model have identified many characteristics of the nine samples tested, the most obvious of these being the batch variability. It was determined that the batch three samples were more resistive in the top, bottom, and oblique planes than the samples from batches one and two. The samples from batch two were found to be the least resistive. This batch variability could be contributed to the manufacturing and/or material properties of the samples since every sample tested in this study was individually made.

Unlike the batch variability, the decrease in electrical resistance for all planes as buckypaper layers were added was consistent. It was found both experimentally and in the computational model that the addition of four layers of buckypaper to a pure carbon fiber reinforced sample will greatly reduce its electrical resistance along the outer surfaces as well as through the thickness. This decreasing resistance trend was also found to continue when three more buckypaper layers were added in making seven buckypaper layer samples but the magnitude of the resistance reduction was very small when compared to the differences between the pure carbon fiber and four buckypaper layer samples. This could be a trend of diminishing return where there is an optimal number of buckypaper layers which should be used in maximizing the resistance decrease needed for the cost.

CHAPTER 4

TWO PROBE METHOD FOR ELCETRICAL CHARACTERIZATION OF BUCKYPAPER AND CARBON FIBER POLYMER MATRIX COMPOSITES

4.1 Experimental Considerations

To further investigate the electrical resistivity properties of the carbon fiber reinforced polymer composite samples with varying number of buckypaper layers a two probe electrical resistance experiment was performed. The intent of the two probe test was to validate the results found from the four probe plane tests as well as to investigate the composite samples properties as well as contact resistance as electrical current was passed directly in the carbon fiber direction. The experimental setup was based on the work of Zantout (2009) with variations being made for the change in sample size as well as equipment available.

4.2 Previous Experimental Set-up

As with the four probe electrical resistance testing, the two probe method had been used in similar forms for past experimentation with different CFRP materials (Zantout, 2009). In the two probe method the same pair of contacts is used for applying the electrical current and measuring voltage. Therefore, the electrical resistance measured includes contact resistance between the composite sample and electrode. In the experiments of Zantout (2009) an Agilent 6692A power supply was used in producing a constant source current across the composite sample. During experimentation the output

levels of the power supply were adjusted manually using the equipment's front panel interface. A Deltec MKB-100-200 shunt resistor with a resistance value of 0.5 milliohm was placed in series with the positive output terminal of the power supply and the sample so the exact current flow at any given time could be determined. To record the voltages across the sample as well as the shunt resistor the same Agilent 34970A switch unit and 20 channel multiplexer from the previous four probe experimental setup was used. This was done by connecting one channel of the multiplexer to the positive and negative terminals of the copper electrodes as connecting both ends of the shunt resistor to another channel. The Agilent 34970A switch unit was controlled via a program using the VEE Pro software that would receive the measured voltage readings and record them into an excel document for later examination by the experimenter. A diagram of Zantout's original setup can be seen in Figure 4.3. It can be seen in the figure that Zantout was also interested in recording temperature readings of the samples during testing which was not an objective of this experiment.

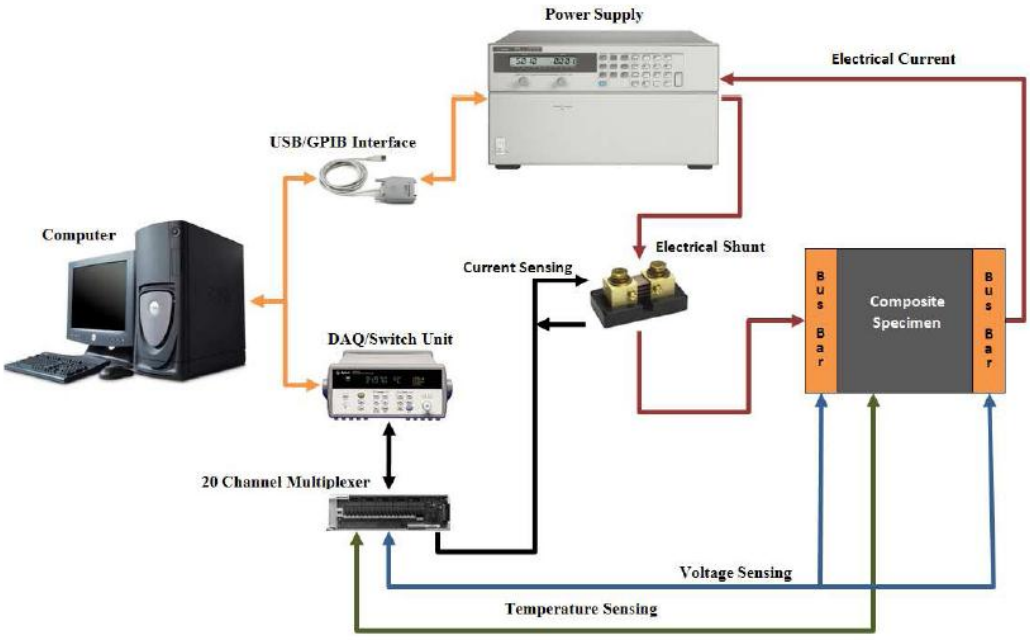

Figure 4.1: Original two probe test setup (Zantout, 2009, p.51)

In order to safely restrain the carbon fiber samples and copper electrodes in position during the two probe electrical resistance testing a fixture was created and is shown in Figure 4.2 (Zantout, 2009). The fixture was designed to sandwich the composite sample and electrodes through the use of a wooden bottom plate as well as wooden and aluminum plates on top. All three plates had five square inch holes cut into the center so that the sample could be exposed for impact as well as temperature testing. Also, each plate had slots cut out near every corner so that the plates could be slid over a wooden base that had four long bolts protruding upwards. To assemble the fixture first the wooden bottom plate was placed on the base. Next the composite was aligned in the middle of the bottom plate and the copper electrodes were lined up along the samples appropriate edges. The top wooden plate would then be lowered over the sample and

electrodes followed lastly by the aluminum plate. The plates were clamped down through the use of four cast steel nuts screwed onto the bolts attached to the wooden base which allowed for tightening by hand with no additional tools (Zantout, 2009). To prevent the copper electrodes from sliding out the sides of the fixture two 18 inch long Craftsman bar clamps.

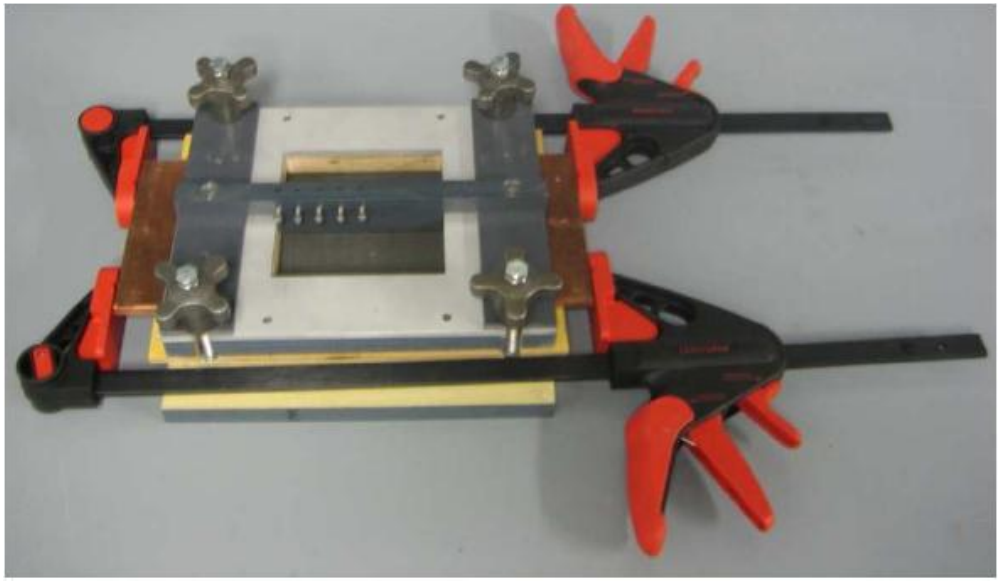

Figure 4.2: Test fixture developed by Zantout (2009, p.50)

4.3 New Experimental Set-up

The goals of the new experimental setup used in the present work included removing unneeded components of the previous setup, such as the temperature monitoring devices, as well as provide a means of testing the smaller sized samples than had previously been used. This first began with changing the hardware using in the recording of electrical current and voltage. Rather than using the 0.5 Ohm shunt resistor

as before to calculate the exact current produced by the Agilent 6692A power supply reading were taken directly from the power supply through the GPIB connection. Also changed was the means of measuring the voltage potential across the composite sample. Instead of the Agilent 34970A switching unit and multiplexer, an Agilent U2531A data acquisition unit was used. To control the entire system a new software program was written in VEE pro that allowed for the output of the power supply to be controlled via the desktop computer as well as the number of data recordings and time between recordings to be chosen. A diagram of the new hardware used is shown in Figure 4.3.

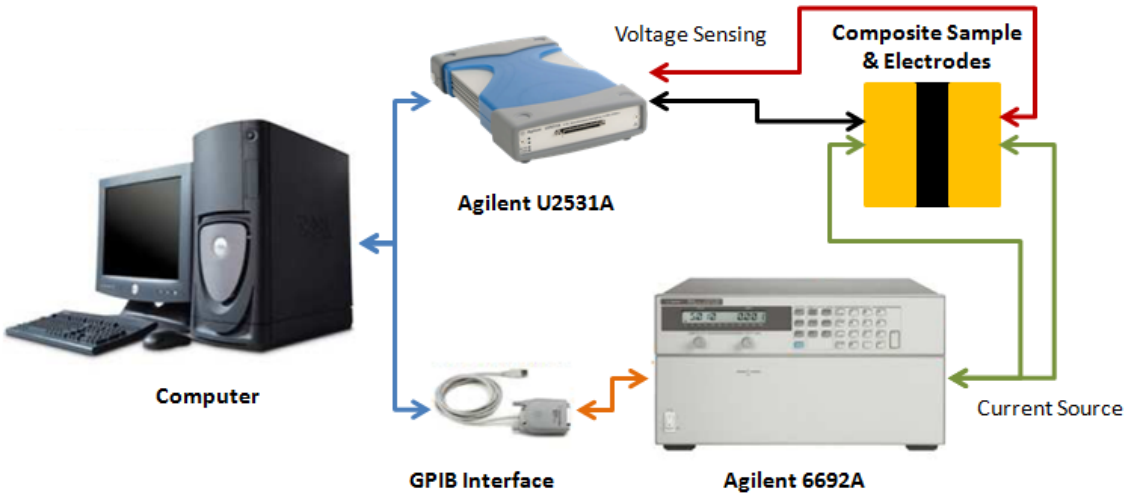

Figure 4.3: New two probe electrical resistance setup

Along with the new hardware setup a new fixture needed to be created for the smaller composite samples to be tested. For ease of assembly and cost reduction the new fixture was designed using the existing base plate with bolts, clamping hardware, and copper electrodes. Also reused was the aluminum plate which held the two wooden plates

down during testing. The two wooden plates were recreated so that the rectangular copper electrodes could slide all the way into the fixture and contact the narrower samples. This was done by rotating the locations of the samples so that the edges which were to be in contact with the copper electrodes were perpendicular to the shorter length of the wooden plate rather than the longer one as had been done previously. Also changed in the new wooden plate design was the removal of the center holes through the entire thickness of the plates. Unlike the previous experiment no impact or temperature testing was to be performed on the narrower samples so it was unneeded to be able to access them from the top of the fixture. A Pro/E drawing of the new top wooden plate is shown in Figure 4.4 and the completed new fixture can be seen in Figure 4.5.

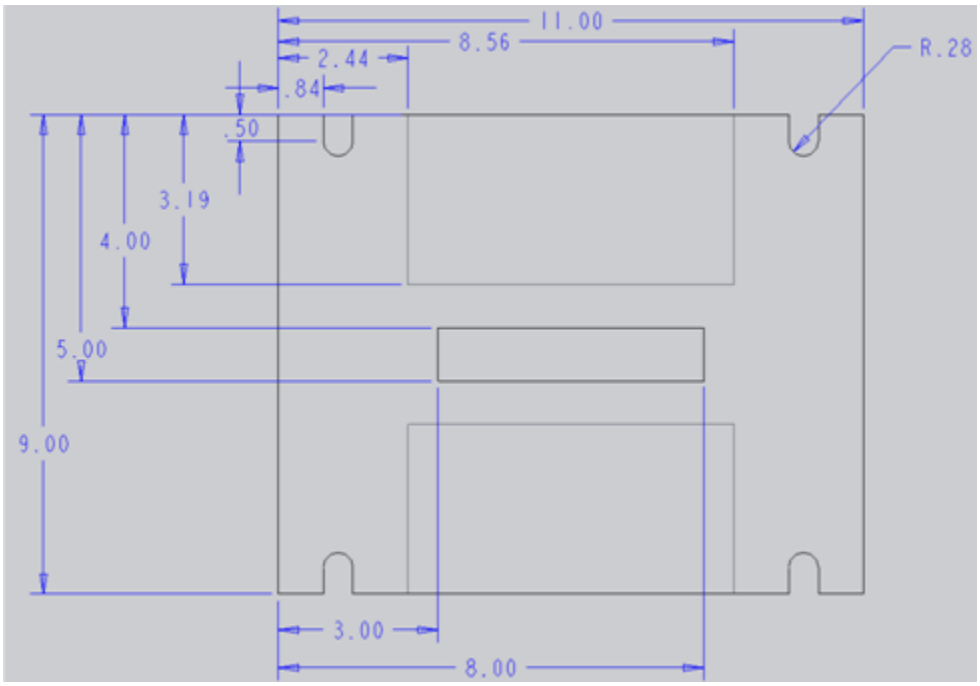

Figure 4.4: New wooden fixture used for two probe testing, units in inches

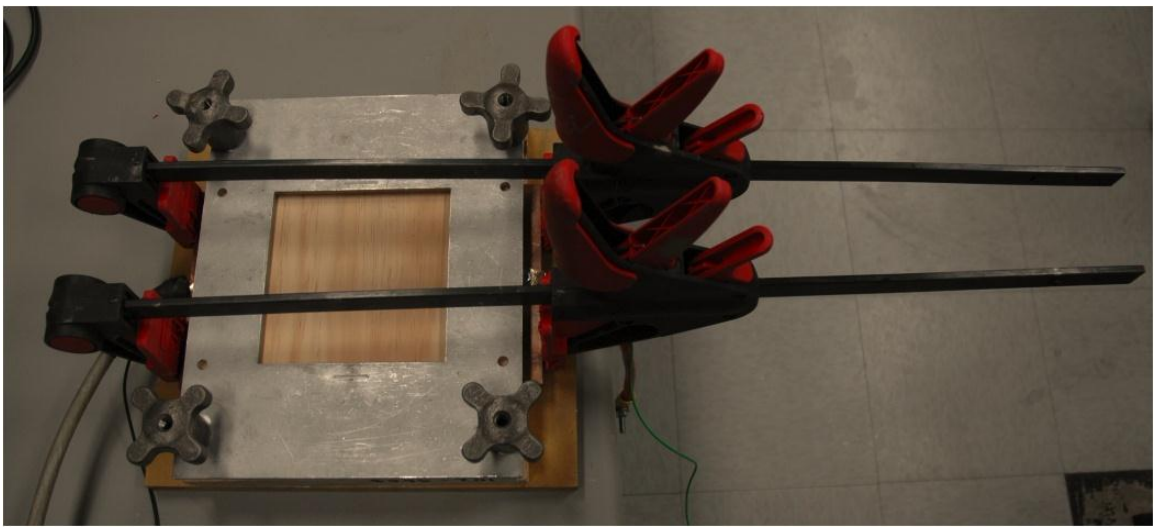

Figure 4.5: Complete fixture for narrow sample testing

4.4 Composite Sample Preparation

The samples were prepared in a similar fashion to those that had been previously tested in the works of Zantout, Deierling, and Hart (Zantout, 2009: Deierling, 2010: Hart, 2011). From the water jet cutting process there were two different sample types that were to be tested by the two probe electrical resistance method. These included samples that were approximately two inches wide by six inches long as well as ones that were six square inches. Though the samples consisted of two different sizes the process of preparing them for testing remained the same no matter if they were the smaller or larger widths. The exact physical characteristics for each sample are shown in Table 4.1 and Table 4.2 for the two inch and six inch wide samples respectively.

Table 4.1: Physical characteristics of narrow composite samples

Sample	Width (mm)	Length (mm)	Thickness (mm)
1-1-0	50.4	152	2.23
1-2-4	50.5	152	2.27
1-3-7	48.9	152	2.35
2-1-0	47.1	152	2.26
2-2-4	49.2	152	2.22
2-3-7	48.9	152	2.29
3-1-0	50.8	152	2.19
3-2-4	49.8	152	2.29
3-3-7	48.9	152	2.49

Table 4.2: Physical characteristics of wider composite samples

Sample	Width (mm)	Length (mm)	Thickness (mm)
1-1-0	152.4	152.4	2.32
1-2-4	152.4	152.4	2.30
1-3-7	152.4	152.4	2.33
2-1-0	153.2	152.4	2.13
2-2-4	151.6	152.4	2.30
2-3-7	152.4	152.4	2.34
3-1-0	152.4	151.6	2.27
3-2-4	151.6	153.2	2.54
3-3-7	152.4	152.4	2.56

4.4.1 Sanding of Composite Samples

The first step in the composite sample preparation was to ensure that the edges that would be in contact with the two copper electrodes would be smooth and straight. The more uniform the edges of the samples could be the less the contact resistance between the samples and electrodes would contribute to the resistance readings. As was

mentioned in Chapter 2, the water jet cutting did an excellent job of producing edges that were straight; this was not equally true for the edges of the samples which were the original edges of the eight inch square plates which were initially received. For these edges of the samples special care needed to be taken to make certain there were no uneven segments.

To straighten and smooth the composite edges a series of sequentially finer grit sand paper was used. First one 8.5 by 11 sheet of each 220, 400, and 600 grit sandpaper was laid with the abrasive upwards on a flat counter. The edges were secured to the counter using blue painters tape and were labeled such that there was no confusion as to which sheet corresponded to which grit. The samples were then taken one by one and placed with on edge which was to contact an electrode on the 220 grit sand paper. The sample was moved in a back and forth motion along the long length of the sandpaper ten times before being rotated so that the side of the sample which was initially facing away from the experimenter was then positioned towards him. The sanding motion was the repeated ten more times. By repeating the sanding process ten times for each position the risk of having uneven sanding along the edge of a sample was eliminated. After the sanding was completed on one edge the sample was flipped over and the process was repeated for the remaining edge. To validate that the edges were then straight a carpenters squared was placed along each one. If gaps between the square and sample were still seen the sanding process would be repeated for that edge. Once each edge on any given sample was straight the sanding process was repeated using the 400 grit and finally 600 grit sand paper.

4.4.2 Application of Conductive Epoxy

Once the edges of all of the samples had been sanded a layer of electrically conductive epoxy could be placed on them to further reduce the contact resistance during testing. This was done by first cleaning all of the edges with an acetone soaked paper towel to remove any composite particles left over from the sanding process. As discussed by Deierling (2010), the composite samples should only have very brief exposure to the acetone as it has the ability to degrade the polymer matrix when used. The epoxy selected was DURALCO 120 produced by the Cotronics Corporation. DURALCO 120 had been used in previous two probe electrical resistance experiments and was chosen because of high volume of over 70 percent silver as well as measured resistances of only 8e-5 ohm-cm (Cotronics Corporation, 2008). The epoxy was mixed thoroughly according to the manufacturers specifications with a resin to hardener ratio of 100:3.5 by weight (Cotronics Corporation, 2008). After being mixed, a thin layer of epoxy was spread across the previously sanded surfaces of the samples using a latex glove and index finger. All samples were allowed to cure for 24 hours to ensure the epoxy was fully cured. The last step in the sample preparation procedure was to smooth the cured epoxy surfaces to remove any excessive material and again minimize any contact resistances that could occur between the samples and copper electrodes. This was done in much the same manner as the composite material was sanded with the sand paper being placed on a smooth, flat surface. The difference between the two was that for the epoxy sanding only 600 grit sand paper was used so that too much of the epoxy layer could not be removed. After sanded the samples were ready for the two probe electrical resistance testing.

4.5 Two Probe Experimental Procedure

With the samples prepared, setup completed, and control mechanism finished the two probe electrical resistance testing has been performed. The first samples tested were the narrower two inch by six inch samples. Each sample was taken individually and a thin layer of Duralco 120 resin was applied along the edges of each sample on top of the cured epoxy which had previously been sanded which would be in contact with the copper electrodes. A layer of resin was also added to the contact surfaces of the electrodes themselves. The purpose of the additional resin was to better eliminate the contact resistance between the electrodes and sample, thus reducing the chance of the sample overheating and the polymer matrix degrading (Zantout, 2009). After the application of the additional silver resin the samples were then taken and inserted into the two probe test fixture.

The process of assembling the two probe test fixture is shown in Figure 4.6. This included first placing the wooden base with hardware attached as in step one. In step two the lower wooden plate was placed on the base and in step three the composite sample and electrodes were placed on that. In steps four and five the upper wooden and aluminum plates were put on top of the sample before being tightened down using the cast iron nuts. Lastly the electrodes were clamped into place with the craftsman bar clamps as shown in Figure 4.7. Once completed the sample could be tested for its electrical resistance in the fiber direction.

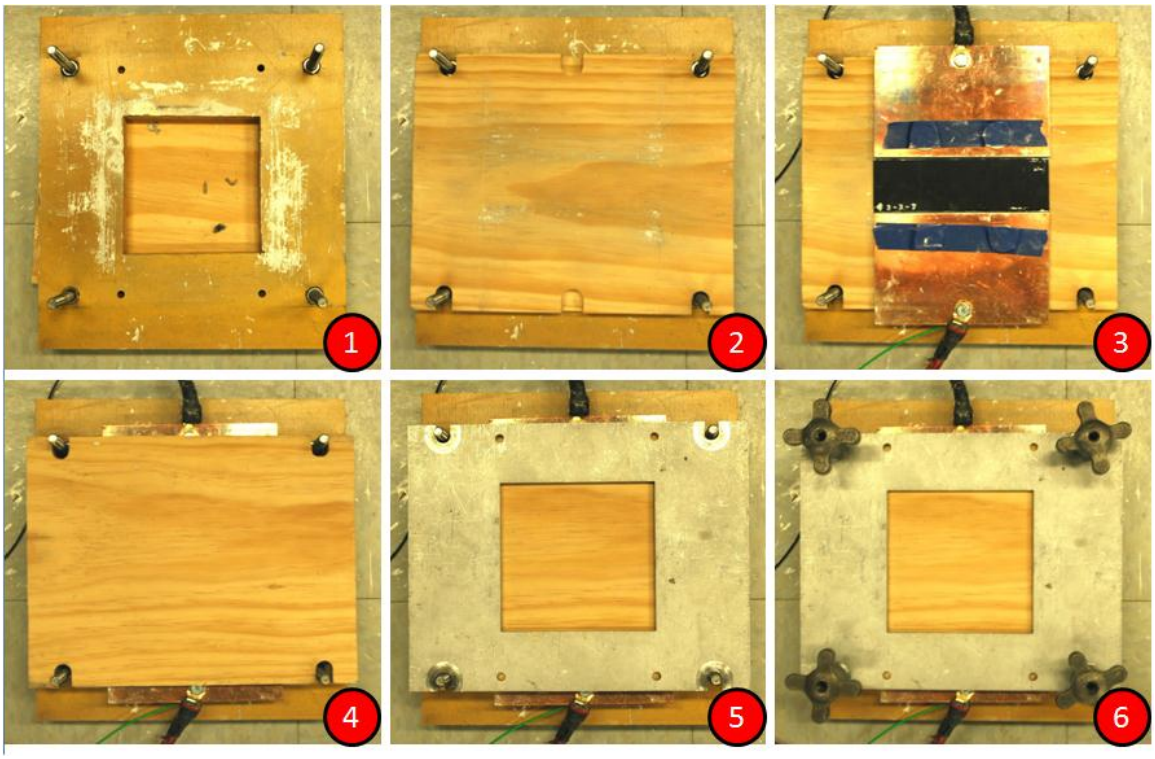

Figure 4.6: Steps for assembling two probe test fixture for narrow samples

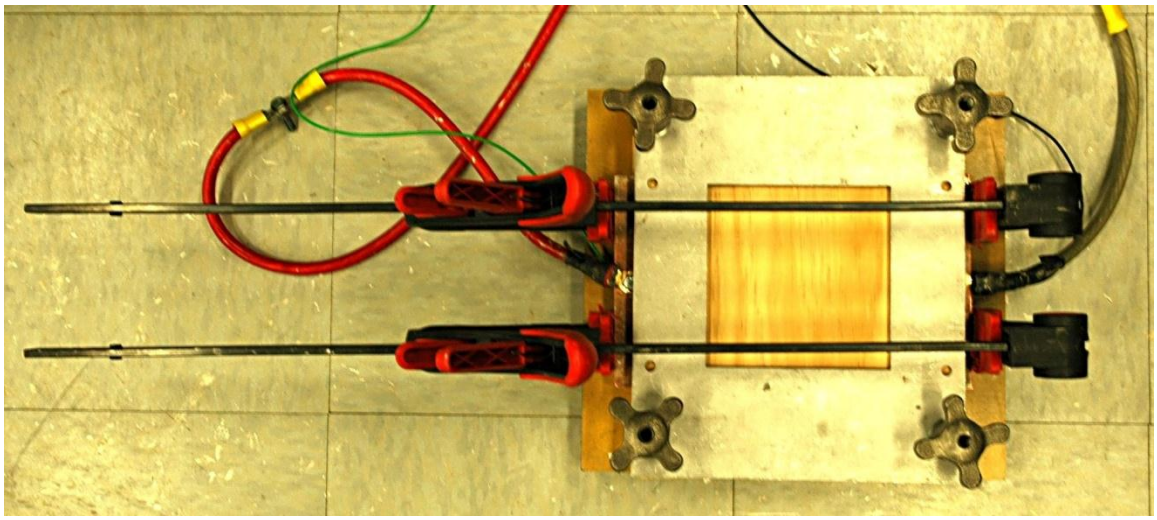

Figure 4.7: Completed narrow sample two probe test fixture

After being secured in the test fixture each sample was tested using the previously described experimental setup. The process included turning on the Agilent 6692A power supply and Agilent U2531A data acquisition unit as well as starting the VEE pro software on the desktop computer. Then the current settings were adjusted as well as the number of data points to be taken and time between readings. Once this was complete the start button was pressed and the program was allowed to run until all the data was recorded. For each of the two inch wide samples source currents of 0.1, 0.2, 0.4, 0.6, 0.8, and 1 A were used. Once a sample was measured at all of the desired current levels it was removed from the fixture and the next sample was inserted. Between each sample the resin on the electrodes was smoothed out prior to further testing.

The six inch square composite samples were tested in a very similar manner to the two inch wide ones. Figure 4.8 shows the steps followed for assembling the square sample test fixture. As can be seen from the figure the only major change between the narrow and wide (i.e. square) sample fixtures is that there is no need for a bottom wooden plate for the wider sample as they span across the hole in the wooden base. The completed fixture is shown in Figure 4.9. As with the narrow samples, once a sample was in the test fixture all equipment was turned on and the VEE pro software was used to control the hardware and collect data. The wider samples were only tested at the 1 A current level as it was found with the narrow samples that adjusting the current levels had no effect on the resistance differences between samples.

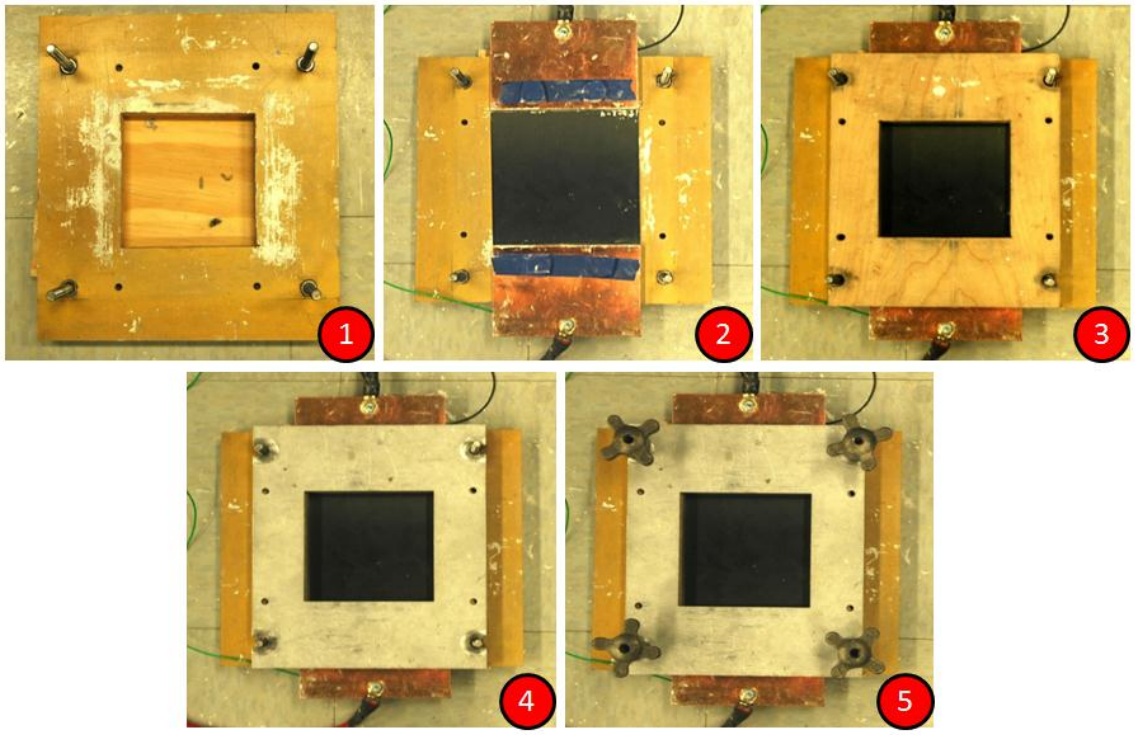

Figure 4.8: Steps for assembling two probe test fixture for wide samples

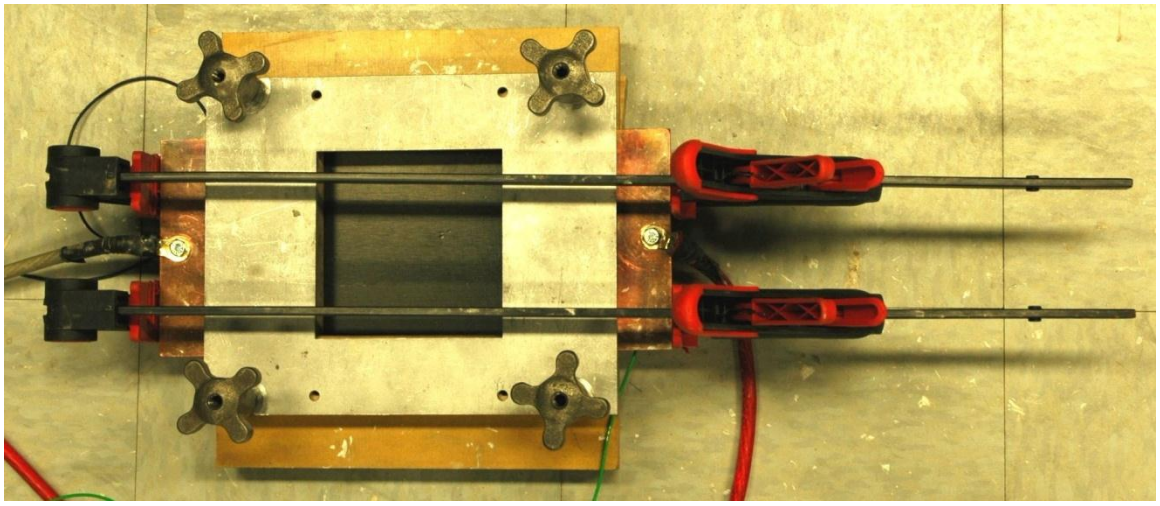

Figure 4.9: Completed wide sample two probe test fixture

4.6 Two Probe Experimental Results

When comparing the results of the electrical resistance testing the samples were organized much like they were for the four probe plane testing. This included comparing samples not only to others with the same number of buckypaper layers but also to samples of the same batch. Also it was determined that all of the samples only needed to be compared for one consistent source current rather than all of the currents used. This was because all samples exhibited similar trends of equal resistance decrease for source current increase.

4.6.1 Two Inch Wide Sample Results

The electrical resistance results for the narrow composite samples were grouped together first so that they could be analyzed and compared. Table 4.3 shows the results for all nine of the narrow samples.

Table 4.3: 1A resistance values found for two inch composite samples

Sample	Resistance (Ohms)
1-1-0	0.1952
1-2-4	0.0907
1-3-7	0.1162
2-1-0	0.1302
2-2-4	0.0615
2-3-7	0.0627
3-1-0	0.1283
3-2-4	0.0908
3-3-7	0.0406

By comparing samples of the same batch it is possible to investigate the changes in the electrical properties of the CFRP composites as buckypaper layers are added. The results of this comparison are shown in Figure 4.10, Figure 4.11, and Figure 4.12. From the figures it can be seen that for every batch the resistance decreased as buckypaper layers were added to the pure carbon fiber samples. It is also shown that for batches one and two this decrease in resistance as large between the pure carbon fiber sample and the four buckypaper layer sample whereas the four and seven layer buckypaper samples are much closer in resistance. In fact it can be seen that for the batch one samples the four buckypaper layer sample has a lower resistance than the seven layer sample. This trend did not continue in the batch three samples where a linear decrease in resistance was found with increased number of buckypaper layers showing a benefit to the additional layers in the seven buckypaper layer sample.

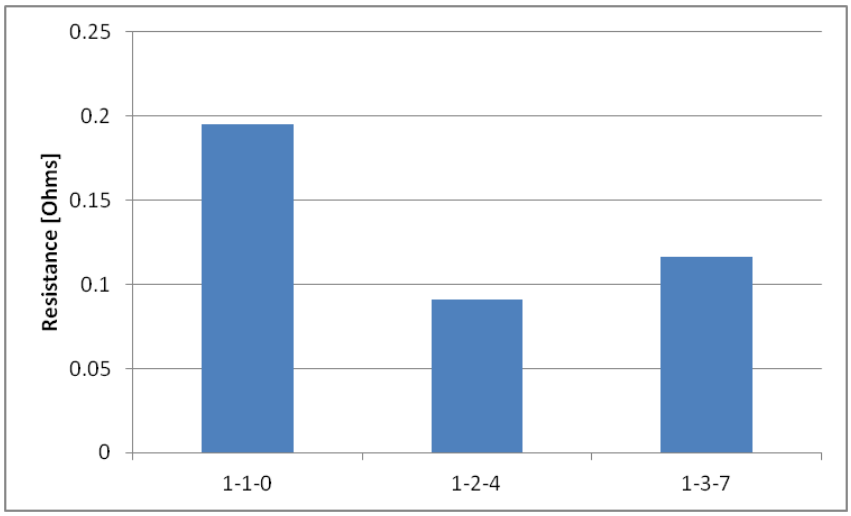

Figure 4.10: Electrical resistance at 1A source current for narrow batch one samples

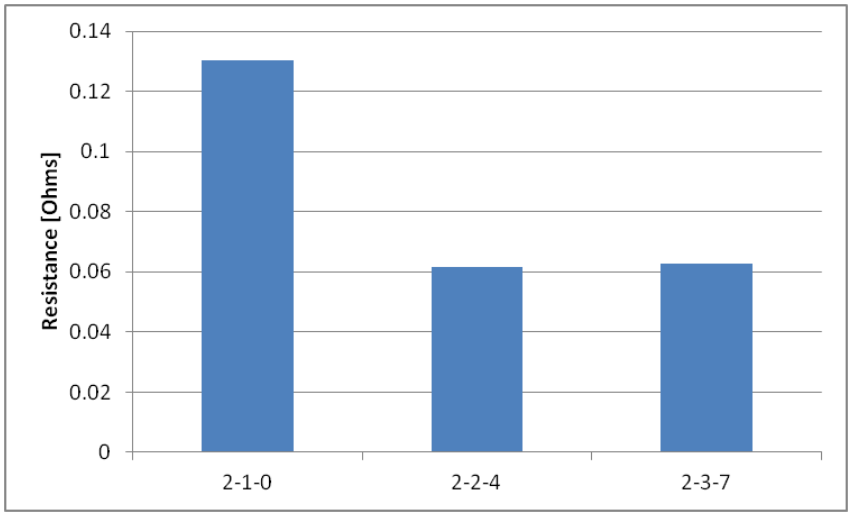

Figure 4.11: Electrical resistance at 1A source current for narrow batch two samples

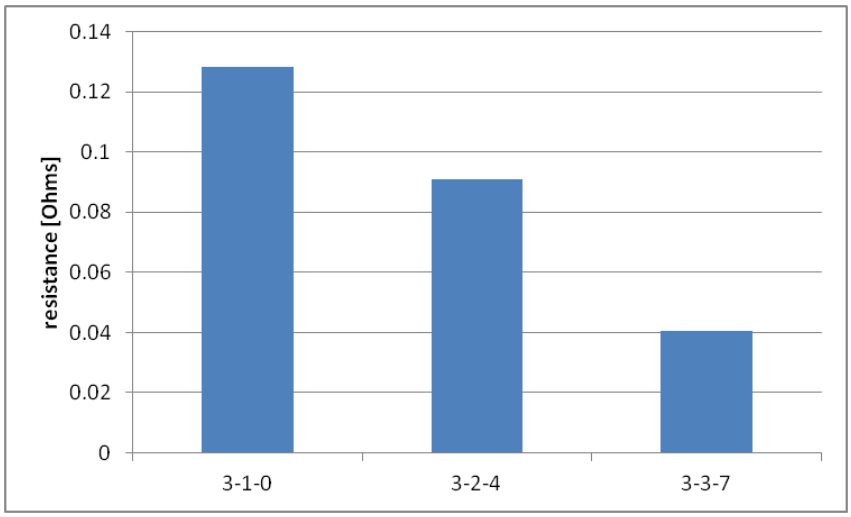

Figure 4.12: Electrical resistance at 1A source current for narrow batch three samples

Comparing the same samples not by batch but rather number of buckypaper layers allows the trends between the batches to be more apparent. This is shown in Figure 4.13, Figure 4.14, and Figure 4.15 with samples of pure carbon fiber, four layers of buckypaper, and seven layers of buckypaper respectively. The pure carbon fiber sample bar graph in Figure 4.13 shows the batch one sample having the greatest resistance with the batch two and three samples being close in magnitude. The four buckypaper layer samples did not continue this relationship trend and instead the batch one and three samples are shown to be similar and the batch two sample had a resistance that was much lower. The seven layer buckypaper graph shown in Figure 4.15 is much like the pure carbon fiber sample trend in that the batch one sample had a greater resistance than the batch two and three samples. The difference between the two graphs is that the electrical resistance of the batch two sample was higher than that of the batch three sample instead of being similar in magnitude.

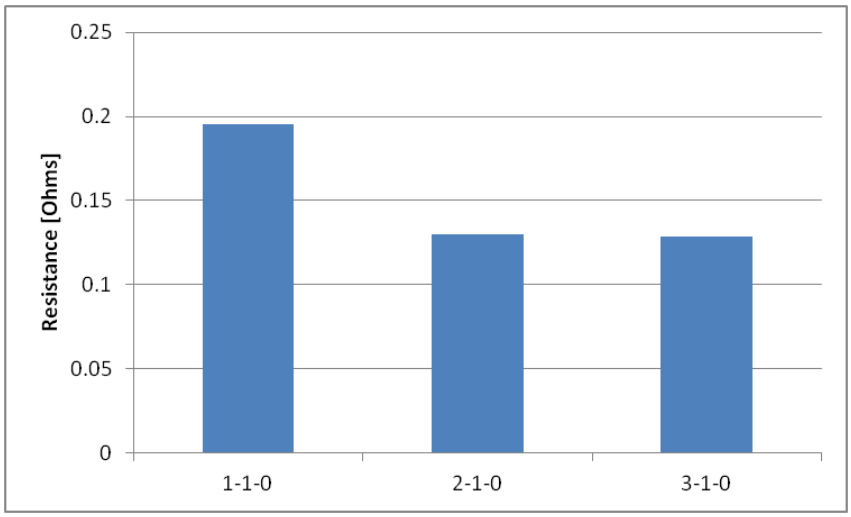

Figure 4.13: Electrical resistance at 1A source current for narrow samples with no buckypaper

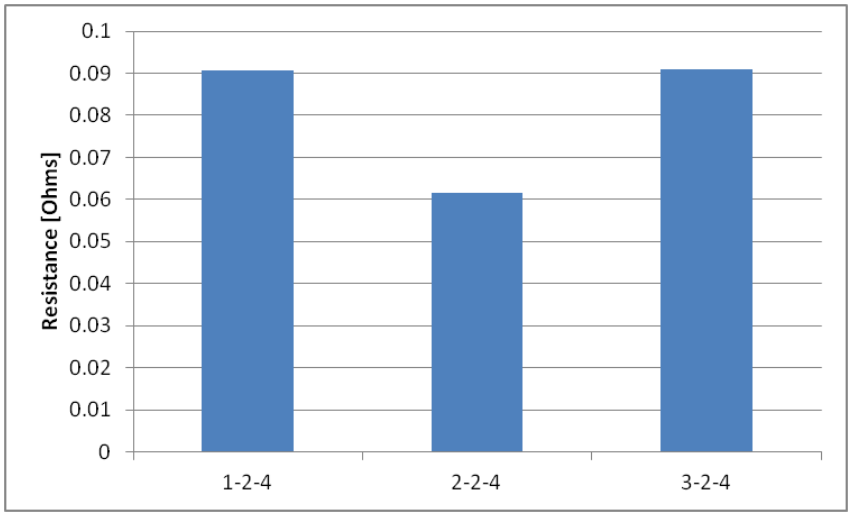

Figure 4.14: Electrical resistance at 1A source current for narrow samples with four layers of buckypaper

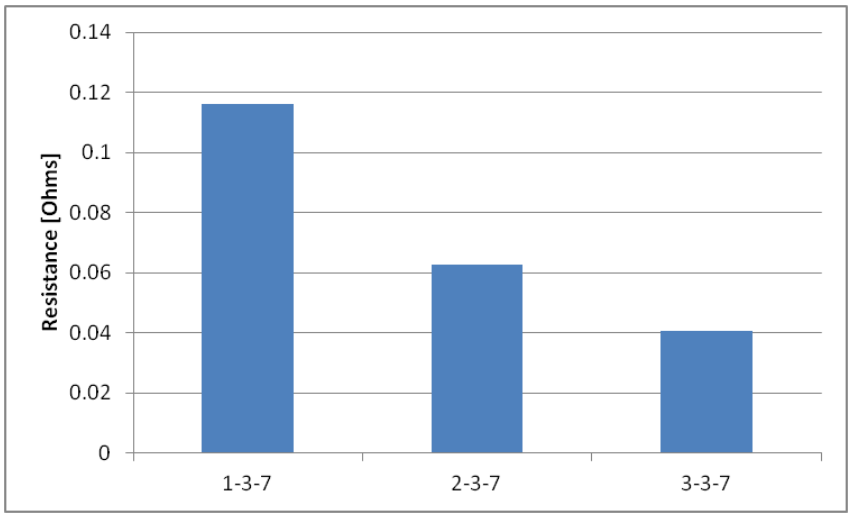

Figure 4.15: Electrical resistance at 1A source current for narrow samples with seven layers of buckypaper

Overall the two probe electrical resistance testing on the two inch wide samples provided some results which correlated well with the four probe plane testing discussed previously as well as some results that were completely different from what was expected. One trend that was the same for the two probe tests as was observed for the four probe testing was that the addition of buckypaper to a unidirectional carbon fiber sample does decrease its resistance. That being shown there was a difference in that the four probe testing had shown that the additional three layers of buckypaper between the four and seven buckypaper layer samples contributed to a small further decrease in resistance. This was only observed for the batch three samples in the two inch wide, two probe testing where the batch one and two results showed no reduced resistance benefits of the additional buckypaper layers.

Another interesting comparison between the two inch wide samples that were tested using the two probe method and those that were tested using the four probe method was the resistance trends between batches. The four probe method had found that the batch three samples were the most resistive followed by the batch one and lastly the batch two samples. For the two probe testing batch two was still always less resistive than batch one for all sample types but batch three varied from being the most resistive for the four buckypaper layer samples to the least resistive for the pure carbon fiber and seven buckypaper layer ones. This trend could have something to do with the two probe testing in the fiber direction having less dependency on the interlaminate resistances which were a major factor in the four probe testing.

4.6.2 Six Inch Wide Sample Results

To compare the changes in the electrical resistances as the sample width increases the six inch wide samples were also tabulated and compared. The electrical resistance results are shown in Table 4.4.

Table 4.4: Resistance values found for six inch wide composite samples

Sample	Resistance (Ohms)
1-1-0	0.1201
1-2-4	0.0568
1-3-7	0.0644
2-1-0	0.0922
2-2-4	0.1180
2-3-7	0.0699
3-1-0	0.0975
3-2-4	0.0529
3-3-7	0.0373

Much like the two inch wide samples, the six inch wide samples were first separated by batch number and represented graphically in bar graphs. Figure 4.16, Figure 4.17, and Figure 4.18 show the results for batches one, two, and three respectively. From investigation the plots it can be seen that there are some similarities as well as differences from the trends found in the results of the two inch wide samples as well as the four probe resistances discussed in Chapter 3. The similarities include the trends found in both the batch one and three samples. Both of these batches were found to have their pure carbon fiber samples to have the highest resistance. For batch one it was also found that the four buckypaper layer sample had the lowest resistance with the seven buckypaper sample being slightly higher. Also, the batch three samples showed a continually decreasing trend with resistance as the amount of buckypaper material was increased, with the seven buckypaper layer sample being the least resistive. Unlike the batch one and three samples, the samples from batch two did not continue the trends found in the

two inch wide samples. As can be seen in Figure 4.17 the four buckypaper layer sample was the most resistive at approximately 0.12 ohms after which was the pure carbon fiber sample and lastly the seven buckypaper layer sample. Of the combined 18 samples tested sample 2-2-4 for the six inch by six inch samples was the only one to have a greater resistance that the similar pure carbon fiber sample. This difference could be attributed to a higher contact resistance for sample 2-2-4 than the other two samples due to possibly a non uniform contact edge.

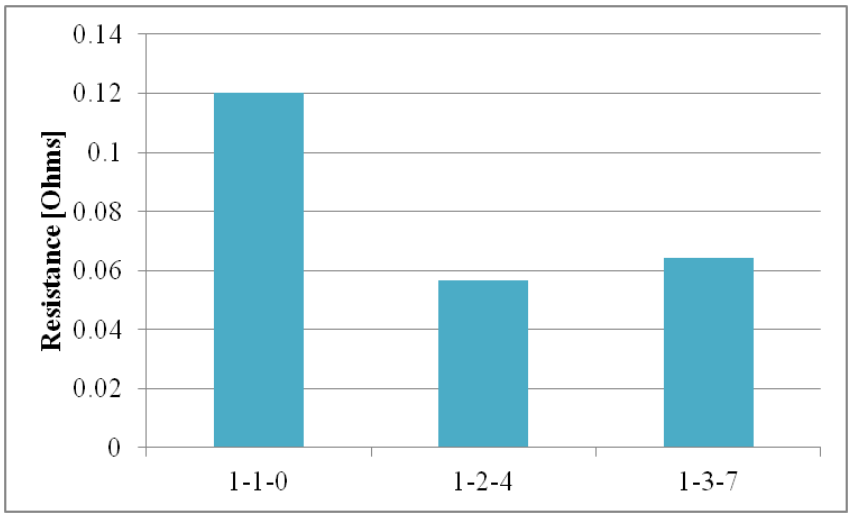

Figure 4.16: Electrical resistance at 1A source current for wider batch one samples

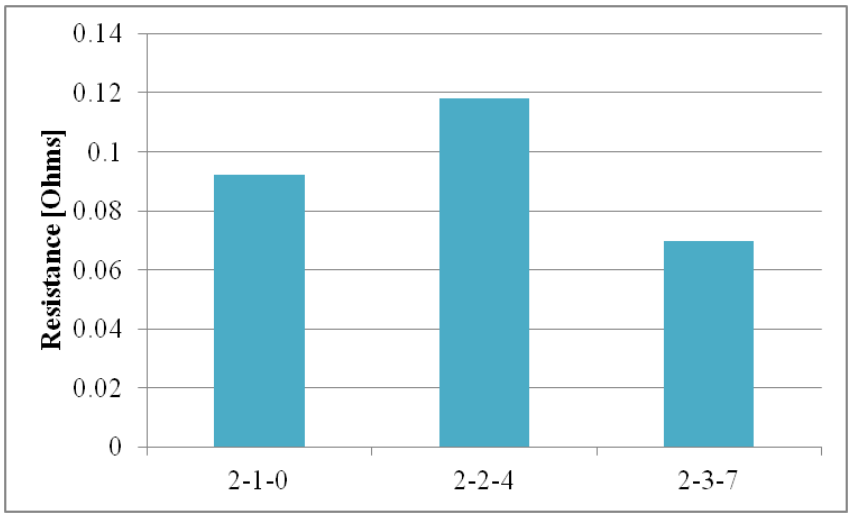

Figure 4.17: Electrical resistance at 1A source current for wider batch two samples

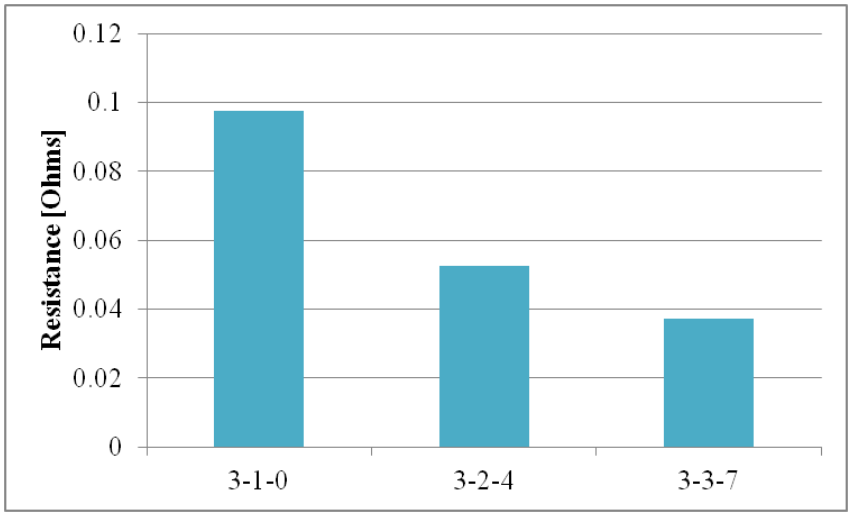

Figure 4.18: Electrical resistance at 1A source current for wider batch three samples

For a greater understanding of the electrical resistance trends samples with the same carbon fiber and buckypaper makeup were also compared. The results from the six inch wide two probe testing can be seen in Figure 4.19, Figure 4.20, and Figure 4.21 for pure carbon fiber, four buckypaper layer, and seven buckypaper layer samples

respectively. Of the pure carbon fiber samples shown in Figure 4.19 it can be seen that the batch one sample had the highest resistance followed by the batch three and batch two samples sequentially. This is the same trend that was found for the pure carbon fiber samples in the two inch wide two probe testing. The pattern of the batch one sample having the highest resistance did not continue for the four and seven buckypaper layer samples. In both of those plots it can be observed that the batch two samples were found to be the most resistive followed by the batch one and batch three samples. Also, sample 2-2-4 again compared poorly to the other samples with a much higher resistance than samples 1-2-4 and 3-2-4.

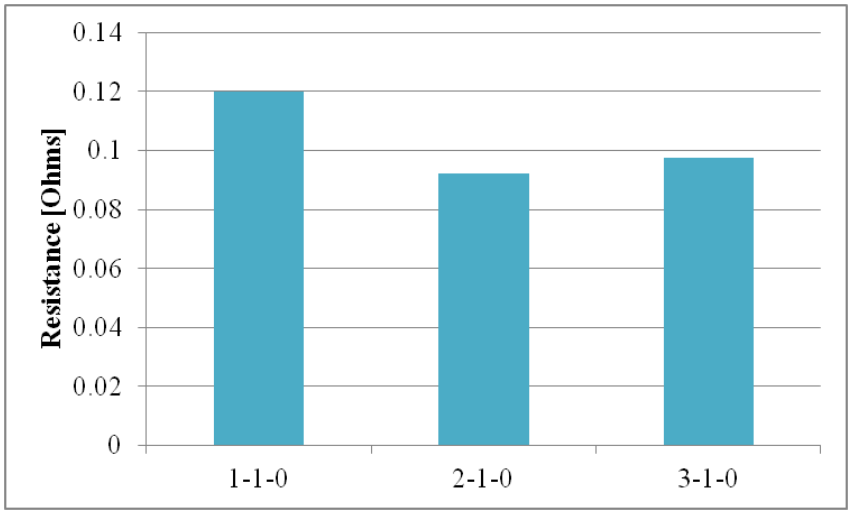

Figure 4.19: Electrical resistance at 1A source current for wider samples with no buckypaper

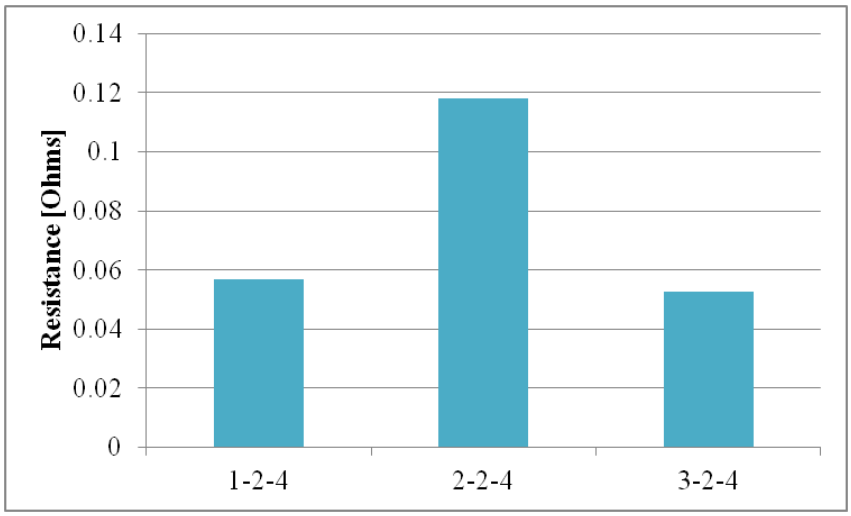

Figure 4.20: Electrical resistance at 1A source current for wider samples with four layers of buckypaper

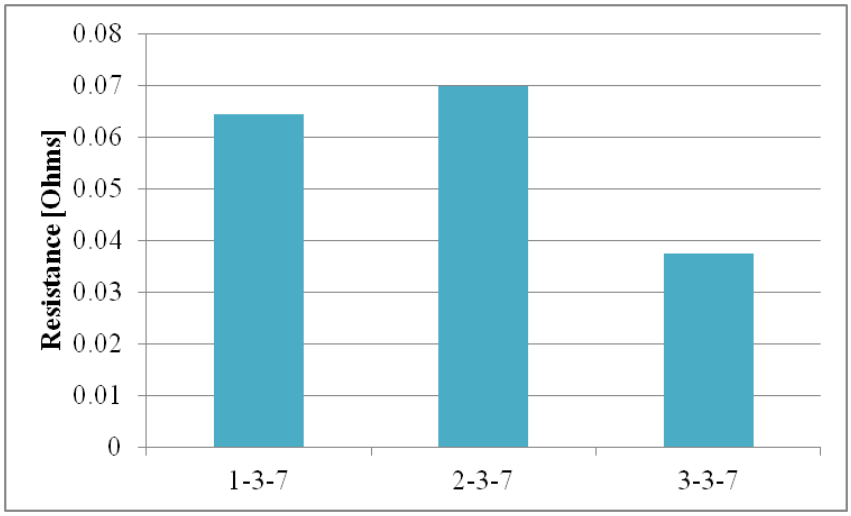

Figure 4.21: Electrical resistance at 1A source current for wider samples with seven layers of buckypaper

The 6 inch by 6 inch samples provided additional insight into the electrical properties of carbon fiber polymer composite when buckypaper material is added. The addition of four layers of buckypaper material did decrease the electrical resistance of two of the three batches of samples. Also the addition of three more layers of buckypaper proved to be beneficial in further reducing resistance in one of the batches. Anomalies also appeared in these samples with the batch two samples being the least resistive of the pure carbon fiber samples and most resistive of the four and seven layer buckypaper samples.

When comparing the 6 in by 6 in samples to those which were tested using the four probe method many of the same conclusions can be drawn that were found for the two inch wide samples which were tested by the two probe method. That is that unlike the four probe method, the two probe method found that the batch three samples tended to be the least resistive when compared to batch one and two. Also unique to the 6 in by 6 in samples was that the batch two samples that contained buckypaper were found to have the highest resistance rather than the lowest seen in the four probe samples. These differences can again be contributed to the two probe method measuring the resistances of the samples directly in the direction of the fibers and being sensitive to contact resistance which the four probe method was not.

4.7 Summary of the Electrical Characterization Results using the Two Probe Method

The greatest difference found between the four probe and two probe electrical resistance testing were the trends of the resistances of the three batches. The four probe testing showed consistently that the batch three samples were the most resistive followed

by the batch one samples and batch two samples in sequence. This was not true in the two probe electrical resistance tests for either the two inch wide or six inch wide samples where it was most often found that the batch one samples were the most resistive and the batch three samples were the least resistive. This shows that the interlaminate contact resistance and through thickness conductivity that were so controlling in the four probe testing did not contribute to the resistances in the two probe testing nearly as much. Instead the greatest contributing factor in the resistances of the samples tested using the two probe method was the contact resistances between the copper electrodes and the samples themselves. The greatest evidence of this is that the resistances found of the two inch wide samples were no less than those found for the six inch wide samples. If the electrical resistance of the materials were the largest contributing factor then greater resistances would have been found for the wider samples with mire resistive material than the narrow samples which was not the case.

While the contact resistance was found to be a large factor in the electrical resistance of the composites the material make up did still play a role. It was found for almost all samples from both the two inch wide and six inch wide testing that the addition of four layers of buckypaper did reduce the resistance of the composites. It was also found that the increase to seven layers of buckypaper did further decrease the electrical resistances for batch three samples but had little effect on the resistances of the batch one and batch two samples. This trend will be further investigated in the next chapter to determine if there is a limit to the number of buckypaper layers needing to be used in order to minimize the electrical resistance of a carbon fiber polymer composite.

CHAPTER 5

ELECTRICAL CURRENT PULSE EXPERIMENTS

5.1 Experimental Considerations

From the results of the four probe and two probe electrical resistance measurements and past experiences with Hart's research (Hart, 2011) the next step in experimentation was the introduction of the electric current of large magnitudes to the composite samples. Understanding the electrical resistances of the samples and trends of the reduction in resistances as the number of buckypaper layers increased was critical in determining safe levels of current that could be applied with no damage of the samples through either arcing or burning. The purpose of exposing the composite samples to large electric current was to characterize their behavior in an attempt to predict their response to a mechanical impact while electrified. It was also to gain the knowledge of the effects of the addition of carbon nanotube buckypaper layers to carbon fiber reinforced composites in higher pulsed current applications.

5.2 Current Pulse Experimental Setup

To produce the large current levels desired for the composite sample testing a specialized experimental setup had been devised in the past by Hart (2011). Prior to Hart's work the largest source of current that could be applied to composite samples at the UI Composites Laboratory was 110 A by the Agilent 6692A power supply which was described previously in the two probe electrical resistance experiment setup. The newer

experimental setup has utilized the most advanced equipment available in the lab as well as introduced a purposely built Current pulse generator.

5.2.1 Hardware Considerations

The main component used in the high current testing experimental setup is the electrical current pulse generator which was designed and manufactured by engineers at IIHR – Hydroscience & Engineering facility at The University of Iowa in 2010. The pulse generator main components include five capacitor modules capable of producing a total current magnitude of 2500 A. Each module is setup as an individual current pulse generator complete with two 6800 microfarad capacitors produced by Hitachi. They also contain an inductor and Powerex brand insulated gate bipolar transistor as well as the necessary electrical components to trigger the current discharge and protect from over charging. The modules as connected in parallel to a large bus bar which then can deliver the electrical current to the composite sample through a small gauge copper wire (Hart, 2011). The current pulse generator is housed in a large case which also includes a Tektronix TDS 2014B oscilloscope and a manual voltage setting knob. Many safety features are also incorporated into the system including a keyed on off switch, flashing strobe lights, and a delay system that prevents any operation for a period of time after a completed test allowing for the capacitors to fully discharge. A front view of the current pulse generator housing with the oscilloscope and safety equipment is shown in Figure 5.1.

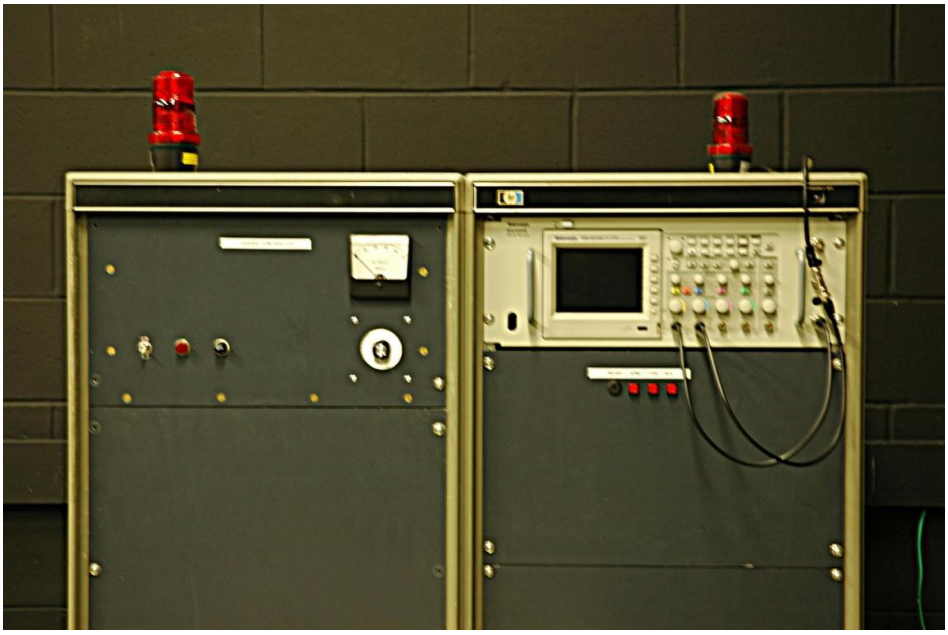

Figure 5.1: Front view of the current pulse generator

Two additional hardware components were used in the setup for the high current testing. These included the Agilent U2531A data acquisition unit, used in both the four and two probe electrical resistance measurements, as well as an Agilent U2356A multifunctional data acquisition unit. As it had been used before, the U2531A was set up to read to the voltages across the composite sample during testing. A change to this procedure from the previous testing was the need for a voltage divider to be in series between the composite sample and the U2531A data acquisition unit. This was because, unlike the electrical resistance testing, the high current pulse testing produced a voltage difference across the sample that was much greater than the 10 volt range of the U2531A. The voltage divider was made from two electrical resistors in series that combined reduced the voltage by a factor of 21. For this experiment the U2531A was also set to read a second channel that was connected to an amplifier attached to a shunt resistor in

the current pulse generator with a resistance of $1*10^{-4}$ ohms. This reading would allow the current magnitude through the sample to be determined through an entire pulse test. A view of the Agilent U2531A data acquisition unit is shown in Figure 3.5 in the setup section for the four probe electrical resistance tests.

The Agilent U2356A data acquisition unit was chosen for use as the triggering device for the capacitors in the current pulse generator as well as the U2531A DAQ recoding period. The current pulse generator was designed to be triggered when a voltage provided by an external source decreased five volts, which is within the 10 volt range of the two voltage output channels built into the U2356A (Agilent Technologies, 2011). Of these two output channels one was connected to the current pulse generator and one was connected to the DAQ. In previous experiments performed by Hart (2011) only one output channel in the U2356A was used for both of these functions but by separating them it was determined that more control could be given to the operator as to when thy would want the DAQ to begin recording. Much like the Agilent U2531 needs the Agilent U2901A terminal block in order to connect wires to the input port, the U2356A uses the Agilent U2802A 31 channel input terminal. This terminal has additional thermocouple capabilities that the U2901 does not but they were not utilized for this setup as no temperature readings were required. An image of the Agilent U2356A data acquisition unit is shown in Figure 5.2.

Figure 5.2: Agilent U2356A data acquisition unit (Agilent Technologies, 2011)

With the hardware selected the remaining step of the experimental setup was the attachment of all components. The Agilent data acquisition units were both connected to a desktop computer via USB cables and were also both connected to their required terminal blocks. One channel of the Agilent U2802A terminal block was then connected to the trigger input of current pulse generator using 22 gauge wires. The Agilent U2901A was connected by one channel to the two resistor voltage divider and by another channel to the internal amplifier in the current pulse generator via four additional 22 gauge wires. The voltage divider was also connected to the copper electrodes which were to be in contact with the composite samples during testing. Lastly the current pulse generator was connected to the electrodes using small gauge wires which could allow for large current magnitudes to pass through them with little resistivity. A schematic of the completed setup is shown in Figure 5.3.

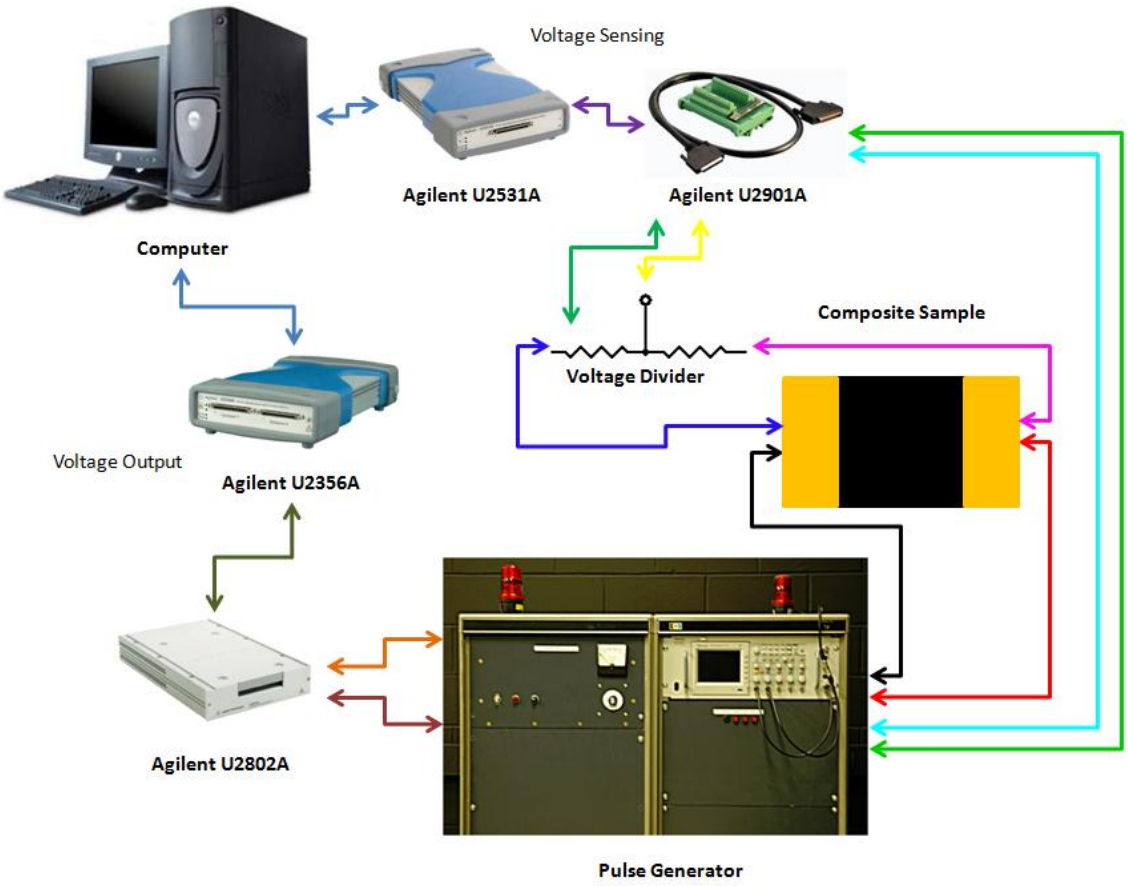

Figure 5.3: Complete setup of current pulse and data recording equipment

5.2.2 VEE Pro Software Program

Much like the experimental setups for both the two probe and four probe electrical resistance measurements the VEE Pro software program was used by Hart (Hart, 2011) to develop a means for controlling all hardware during the experiment. When the program is first started it sets the output voltage of both of the Agilent U2356A's output channels to five volts. After the current pulse generator is charged the user notifies the program through the click of a button and after a preset time delay to

allow all operators to move safely away from the equipment the U2356A's output voltages are changed to zero. One of the output channel triggers the pre-charged current pulse generator to release the energy stored in the banks of capacitors while the other is used to trigger the Agilent U2531A to begin recording data. Once the electrical charge has been fully sent to the composite sample the output voltages of the U2356A are returned to the original five volts.

While the VEE program does control the release of the current pulse it does not record any of the current or voltage data needed for analysis. For that a commercially available software program was chosen called Agilent Measurement Manager. The software program has its advantages because all controls are operated through a user interface rather than having to be programmed line by line such as in the VEE software. For this experiment the user can set how long they want to record as well as which channels to watch as well as the frequency that data is collected. Once set up, the Agilent software program will begin reading when the U2356A output signal drops to zero volts, the same trigger that tells the current pulse generator to fire. The software program will then take the voltage readings from two channels on the U2531A, one which measures voltage across the composite sample and one which measures the voltage across the shunt resistor for later determining the current magnitudes. Once the pulse is completed all data is recorded in a Microsoft Excel spreadsheet to later be analyzed and plotted.

5.3 Sample Preparation

The sample preparation was mostly completed for the composite samples when they were tested using the two probe electrical resistance measuring setup. This included

ensuring the sample edges were straight and smooth thorough sanding using successively finer grained sandpaper. Then the samples were cleaned and DURALCO 120 highly conductive epoxy was applied to the edges of the samples that would be in contact with the copper electrodes. The epoxy was allowed to cure before being lightly sanded again to remove any excess material that had been applied. Immediately prior to their use the samples received an additional light coat of DURALCO 120 resin with no hardener to help eliminate any potential contact resistance between the samples and the copper electrodes. It was especially important to minimize contact resistance during the experiments with high electrical current levels as high resistance will cause arcing and the burning of samples.

5.4 Current Pulse Experimental Procedure

Due to the high electrical energy used in the pulsed current experiments every precaution was taken during the experimental procedure to ensure safe and proper operation of the equipment. The first steps of the procedure were identical to those performed during the two probe electrical resistance testing. That included applying a thin coat of electrically conductive DURALCO 120 resin to the edges of the copper electrodes and composite sample that were to come in contact. Next the sample was inserted into the test fixture shown in Figure 4.8 and Figure 4.9 and the copper electrodes were clamped in using the same Craftsman bar clamps. The 1A electrical resistance test was then again performed on the sample in order to ensure that the electrodes were snugly fit against the composite and that the electrical resistance was not higher than

earlier found. If the resistance of the composite was greater than found previously it could cause damage when high current levels were applied to it.

Once the resistance of the composite sample was found to be the same as was previously determined the current pulse equipment could be setup for use. This included first detaching the Agilent 6692A power supply from copper electrodes and attaching the positive and negative leads from the current pulse generator to them. Instead of having to disconnect the power supply from the electrodes directly, which would have resulted in a change in the contact resistance between the electrode and DAQ wire connector between each sample, a quick disconnect feature was used. This consisted of having a one foot long lead wire always connected to the electrode while the power supply and current pulse generator leads attached to the end of that wire which is shown in Figure 5.4.

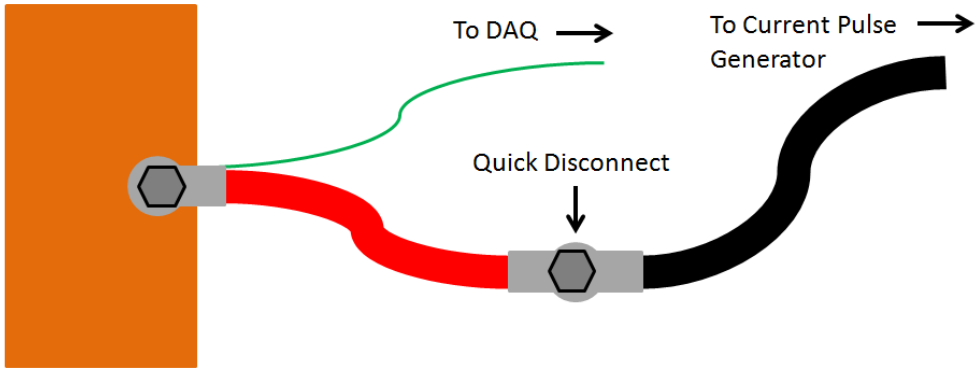

Figure 5.4: Quick disconnect mechanism for copper electrodes

Once the current pulse generator was connected the hardware could all be turned on. This included the Agilent U2531A and U2356A data acquisition units as well as the desktop computer with both the VEE and Agilent Measurement Manager programs

running. Once all hardware was powered on the Agilent measurement manager program could be set to the correct settings. This included selecting a single shot recording mechanism as well as choosing the correct two channels to record voltages during the experiment. Also set was the recording rates and sample size of each channel. The recording rate was set to 10000 times per second and the sample size was set at 500. This allowed for 50 milliseconds of data which is far larger than the 10 to 20 millisecond electric current pulses generated. Lastly the trigger source for the single shot recording was set for when the source voltage on the Agilent U2356A dropped below its standard five volt setting and the ready button was pressed to arm the software.

With the Agilent Measurement manager setup complete a start button was pressed in the VEE program. This set the output voltages of the Agilent U2356A to five volts in preparation to trigger the Measurement manager and current pulse. Next the Oscilloscope built into the current pulse generator was turned on. The settings on the Oscilloscope were set to single sequence and the channels were adjusted using the control panel knobs to a point that the entire pulse curve would be captured. The oscilloscope was not used as the main recording device for the experimentation but was relied upon as a backup in case the desktop computer failed to capture the pulse event.

The next step was to arm the current pulse generator. This was done by first flipping the on/off toggle switch and verifying the system was on by viewing the red indicator light. Next the inhibiting key was inserted into its keyway and turned to its enable position. Lastly the “ARM” button was pressed which engaged the charging system and red warning strobe lights. The knob under the voltmeter was then turned clockwise slowly until the desired voltage was observed. Each of these features on the

current pulse generator is shown in Figure 5.5 and Figure 5.6 for the left and right panels respectively. The last step at the current pulse generator controls was to again press the single sequence button on the oscilloscope in order to set it to ready. With this completed the pulse was initiated from the desktop computer using the start button in the VEE software program. After the current pulse discharge was complete the entire system was left alone for 12 minutes to ensure that the capacitors were completely discharged prior to starting the procedure again. Each sample was tested at multiple voltage levels and each test was analyzed prior to moving on to a higher voltage level to ensure there were no indications that the sample had arced or burned during the prior test.

Figure 5.5: Left panel of the current pulse generator (Hart, 2011)

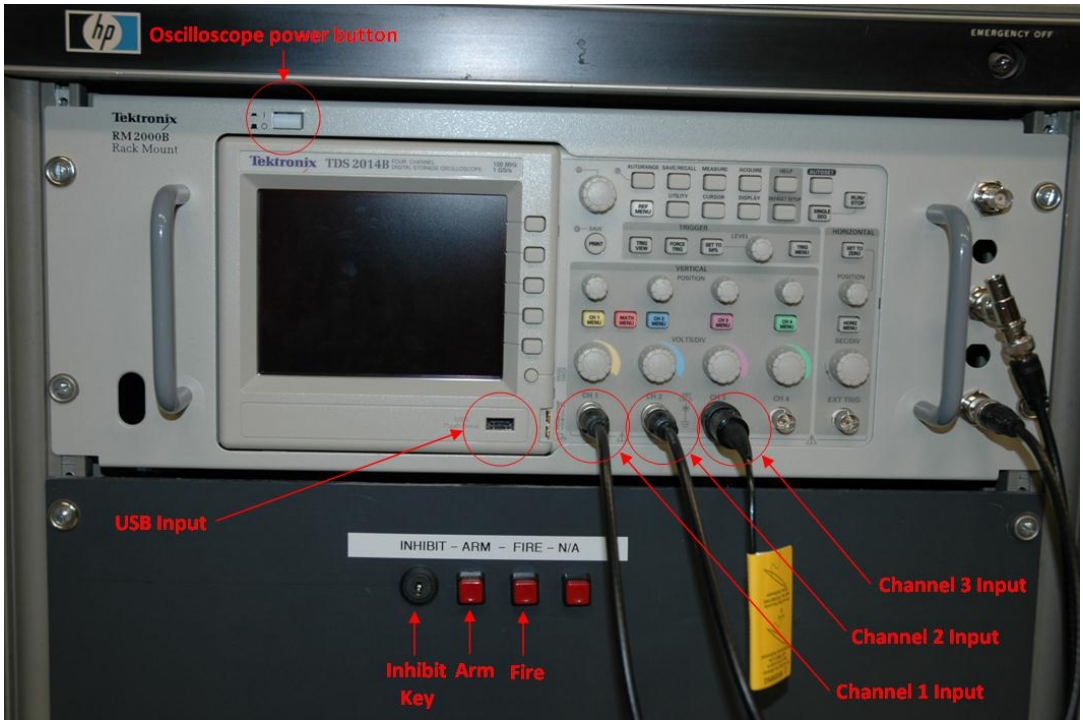

Figure 5.6: Right panel with oscilloscope of the current pulse generator (Hart, 2011)

5.5 Current Pulse Experimental Results

Current pulse experiments were performed on all nine of the samples and much like the previous experiments the results were compared by batch as well as by the number of buckypaper layers added to the carbon fiber reinforced polymer composites. Each sample underwent multiple current pulses with each successive pulse having a greater a greater current magnitude. Also recorded were the voltages across the samples during the testing which allowed for electrical resistances between samples to be compared. The results of these tests have allowed for a greater understanding of the effects of buckypaper material on high electrical current properties of composite materials.

5.5.1 Results of Samples with No Buckypaper

The first samples investigated were samples 1-1-0, 2-1-0, and 3-1-0 which contained no buckypaper and allowed for a comparison to previous experiments performed by Deierling (2010) and Hart (2011). Sample 1-1-0 was tested five times with an analog voltage setting ranging from 50 to 140 volts. The results of the current pulses versus time are shown in Figure 5.7. It can be seen from the figure that all analog voltage increases lead to increases in the current pulse magnitude and that all of the current pulses were smooth with no discontinuities or otherwise abnormal behavior. It should also be noted that thought the current magnitudes increased with each test the discharge time of the capacitors remained the same. This feature of the current pulse generator was very helpful in the coordination of the pulse-impact experimentation discussed later.

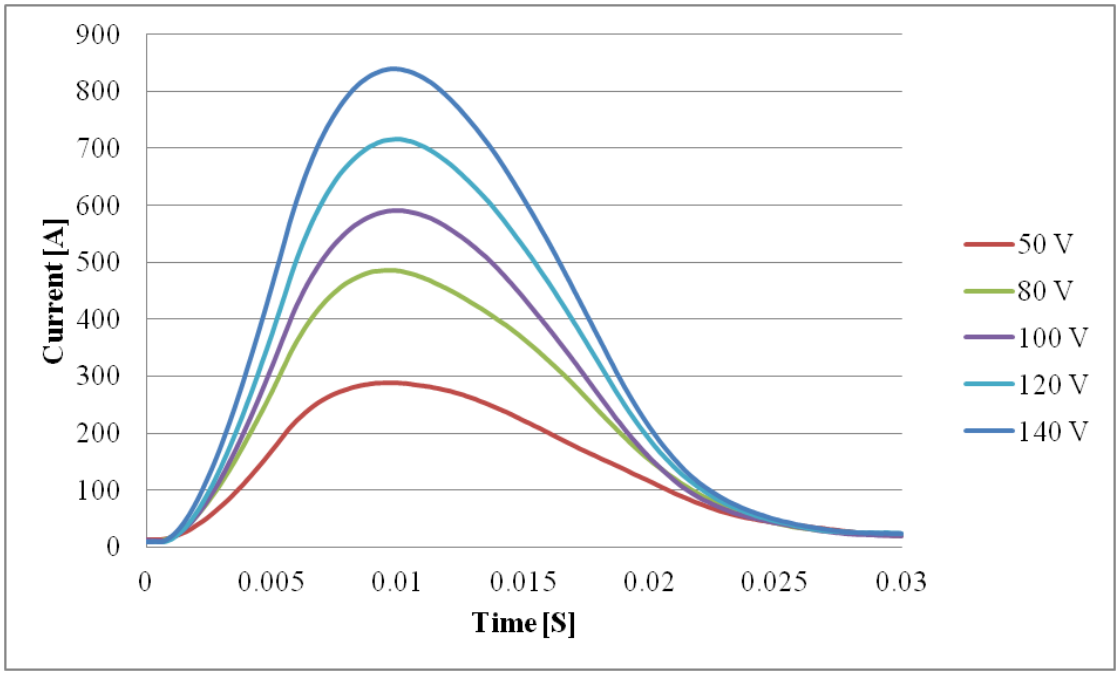

Figure 5.7: Current versus time for current pulse tests on sample 1-1-0

Sample 2-1-0 behaved slightly different from 1-1-0 which was previously discussed. The analog voltage pattern for 2-1-0 remained the same as 1-1-0 in that it started at 50 analog volts before being tested at 80 analog volts after which it was increased in 20 analog volt increments. The current pulse results of each test are shown in Figure 5.8. When sample 2-1-0 was tested at an analog voltage of 120 volts which correlates to current pulse maximum between 700 and 750 amps it did not behave as would be expected. As can be seen in Figure 5.8 the current versus time was not smooth and dropped more rapidly after the maximum current than occurred in sample 1-1-0. Also there is a discontinuous point at approximately 0.011 seconds which was not previously observed.

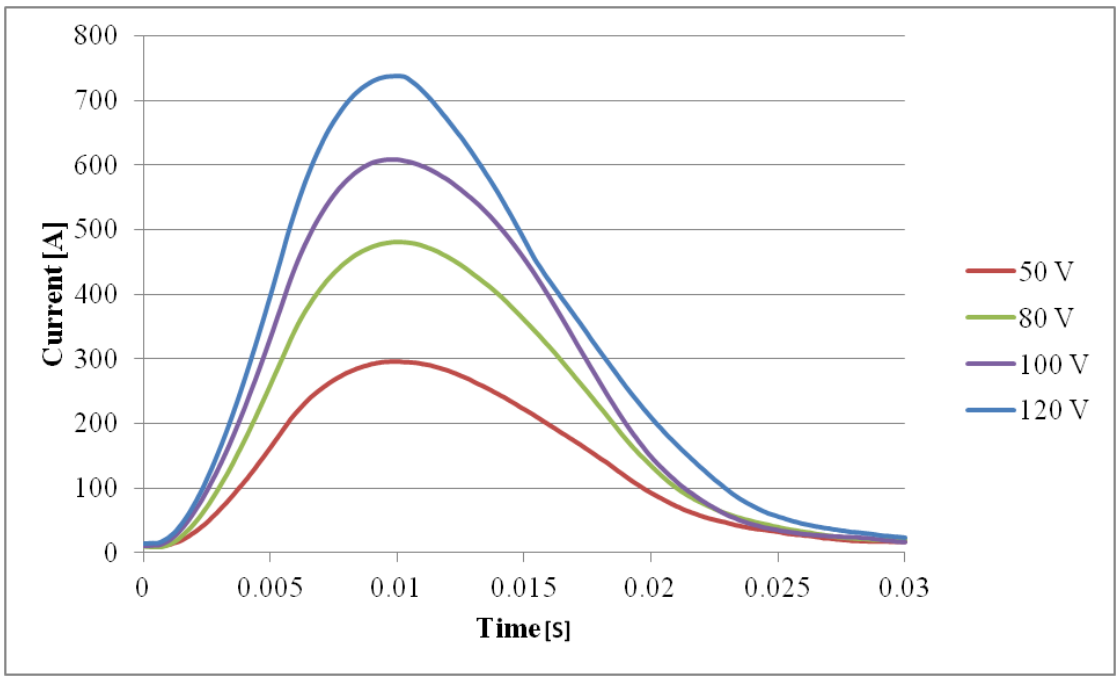

Figure 5.8: Current versus time for current pulse tests on sample 2-1-0

To further investigate the pattern change of sample 2-1-0 at the 120 analog voltage level the voltage across the plate was inspected. A plot of the voltages across the plate for all the tests for sample 2-1-0 is shown in Figure 5.9. A difference between the 120 volt test and the others is much more pronounced in this plot where instead of a smooth voltage curve with time there is a large voltage increase of 10 volts at 0.011 seconds. This is the same time that the discontinuity was observed on the current versus time plot. It can also be seen that the voltage increase occurred until 0.017 seconds before rapidly decreasing. This is the same time that there was a slope change on the current versus time plot to a slower rate of decreasing current. Though none of sound or odor signs of burning occurred for sample 2-1-0 at 120 volts it was determined that in order to preserve the sample for later impact testing the 140 analog volt test which was performed on sample 1-1-0 should not be repeated on 2-1-0. After removal of the sample from the test fixture it was confirmed that no visible damage had occurred during the testing.

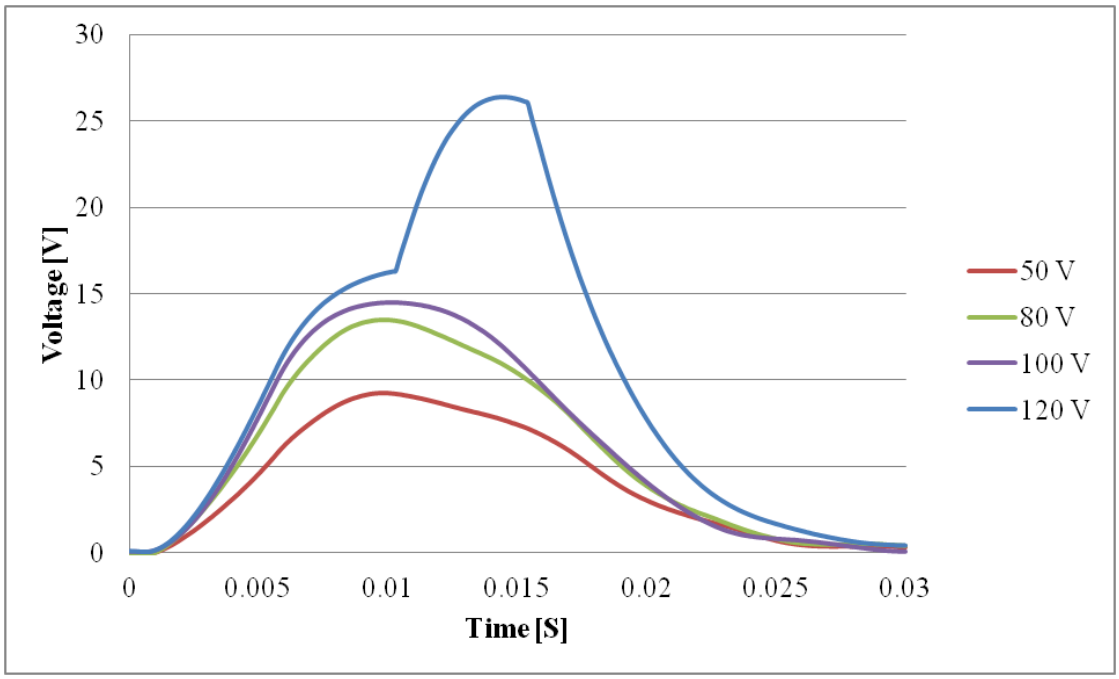

Figure 5.9: Voltage across sample 2-1-0 versus time during current pulse experiments

Sample 3-1-0 was also tested at all of the same analog voltage levels as 1-1-0 and 2-1-0 as well as the additional 140 volt level test performed on sample 1-1-0. The current magnitudes versus time for these tests are shown in Figure 5.10. It can be seen that for all test the current plots were smooth as were observed for sample 1-1-0 and there were no discontinuities. One difference between the tests of sample 3-1-0 and the other two samples was the current magnitude of the 80 volt test. Both samples 1-1-0 and 2-1-0 had maximum current magnitudes of approximately 480 amps while sample 3-1-0 only had a magnitude of approximately 420 amps. This variation is greater than observed for other tests but because the higher voltage testing for 3-1-0 returned to their expected values it was determined that the analog voltage on the current pulse generator must have been

slightly off for that test rather than there being an inherent difference in sample 3-1-0 compared to the other two.

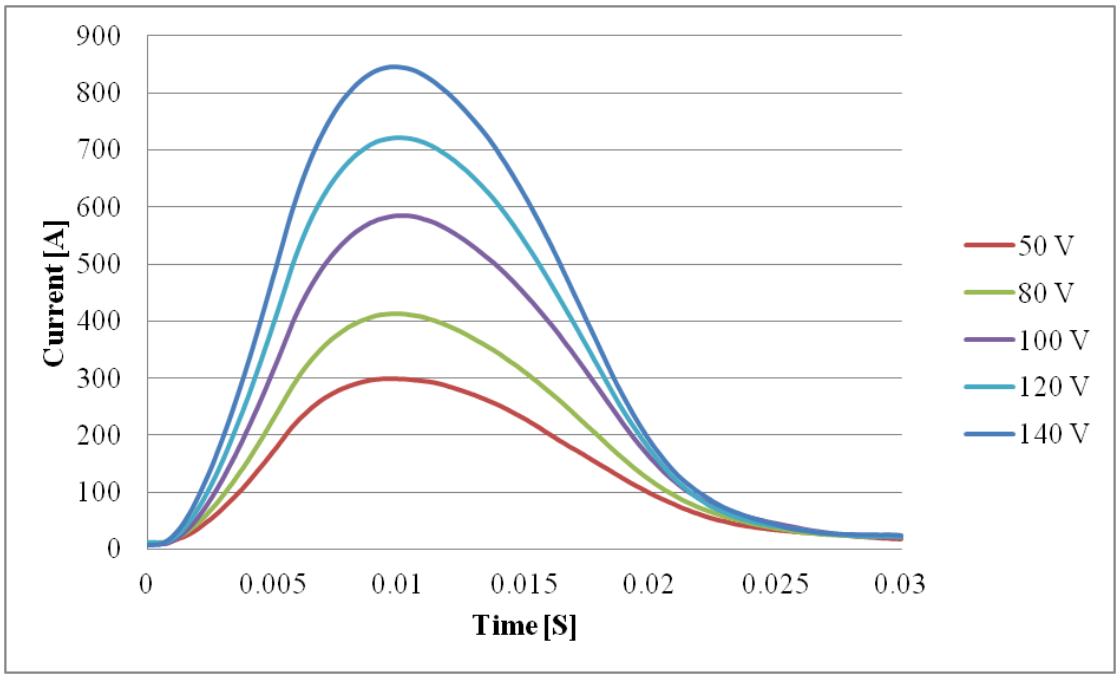

Figure 5.10: Current versus time for current pulse tests on sample 3-1-0

With all three purely carbon fiber samples tested their resistances versus current pulse magnitudes could be compared. The three samples were plotted with their resistances found at 1 A from Chapter 4 as well as the resistances found at each of the current pulse levels and the results are shown in Figure 5.11. The resistances for each analog voltage test were found when the current pulse was at its maximum amplitude. It can be seen that the greatest resistance drop for all three samples occurred between the 1 A test and the 50 analog voltage pulse test. At increased current levels the resistance decreases continued but at a diminishing rate with very little resistance decreases for

samples 1-1-0 and 3-1-0 between 120 and 140 volt levels. It should also be noted that the variations in resistance between each sample also decreased with the increased current with the exception of the 120 volt test for sample 2-1-0 where the abnormal voltage increase was found.

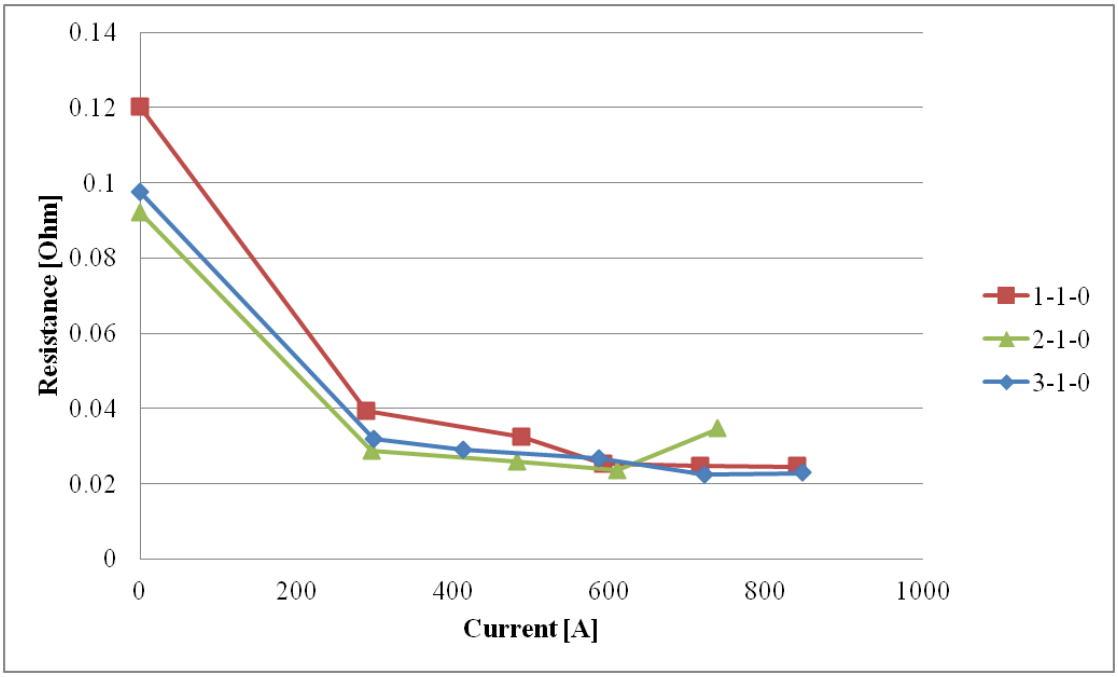

Figure 5.11: Resistance versus current magnitude for the pure carbon fiber samples

The results of all tests were quantified and are shown in Table 5.1 with the maximum current and resistance values for each analog voltage setting for each sample. The table shows the usually small variations between the maximum currents between samples at the same analog voltage levels as it is very difficult to be exact with the voltage controlled current pulse generator.

Table 5.1: Analog voltage, max current, and resistance for each test performed on the pure carbon fiber samples

Sample	Analog Voltage [V]	Max Current [A]	Resistance [Ω]
1-1-0	50	288.68	0.03935
	80	478.03	0.03248
	100	591.77	0.02537
	120	715.98	0.02468
	140	840.03	0.02460
2-1-0	50	295.19	0.02883
	80	481.56	0.02588
	100	609.20	0.02350
	120	737.14	0.03463
3-1-0	50	298.56	0.03198
	80	413.44	0.02908
	100	585.57	0.02677
	120	721.34	0.02250
	140	846.47	0.02286

5.5.2 Results of Samples with Four Layers of Buckypaper

Once the pure carbon fiber samples had all been tested with the current pulse generator the three samples with four layers of buckypaper were prepared and tested in a similar fashion. Sample 1-2-4 was tested starting at 50 analog volts followed by 80 and increased by 20 volt increments to 160 volts. The reasoning behind the additional testing at 160 volts for the four buckypaper layer samples was the lower resistances found at the 140 volt level than were observed for the purely carbon fiber samples. These lower

resistances reduced the risk of samples burning at the higher current levels. The current magnitude results for sample 1-2-4 are shown in Figure 5.12. One abnormality that can be observed is the small notch in the current curve for the sample during the 100 analog voltage test. Though this was concerning it did not occur at a current level that was any higher than the previously successful 80 volt test and did not seem to have an effect on the rate of decrease of resistance with the increased current so it was decided to continue the remaining tests.

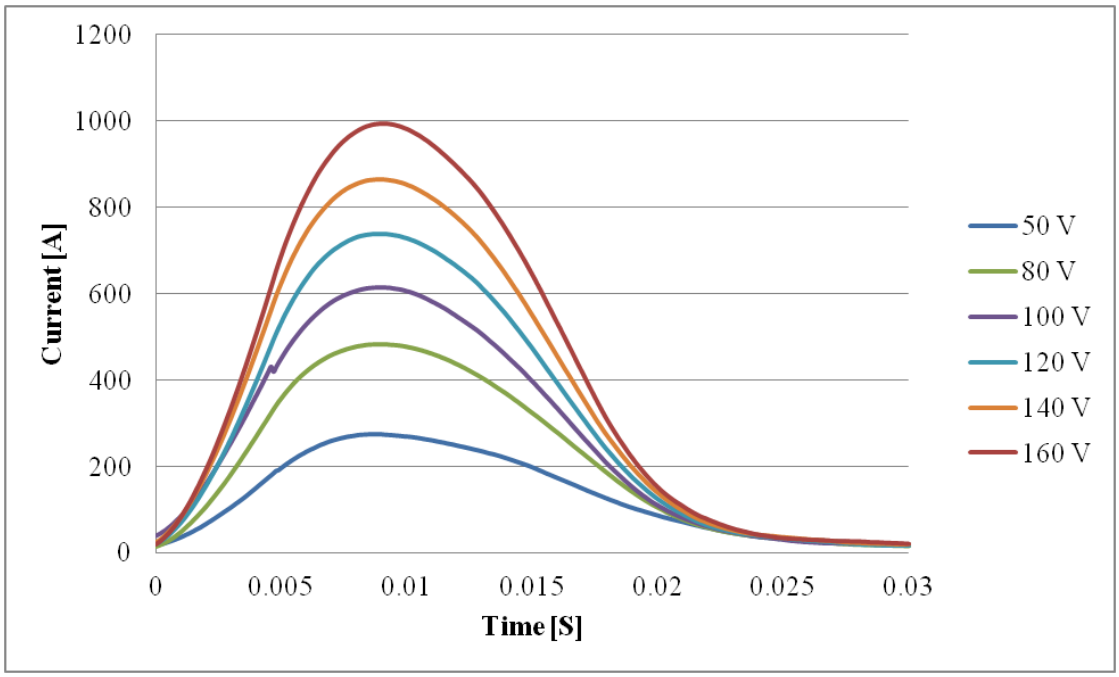

Figure 5.12: Current versus time for current pulse tests on sample 1-2-4

Sample 2-2-4 was tested at the exact same analog voltage levels as sample 1-2-4 with the largest test being 160 volts. The results of the sample 2-2-4 are shown in Figure 5.13 and like the results for 1-2-4 it can be seen that all tests went as would be predicted

except for the 100 analog volt test. For sample 2-2-4 the 100 volt test behaved differently than any seen before where the current pulse was delayed by approximately 0.01 seconds. Several factors could have resulted in this change including the DAQ starting to record slightly early or the current pulse generator being slightly late in recognizing the trigger signal. Besides the delay in the pulse though the magnitude and shape of the 100 volt test are what would be expected.

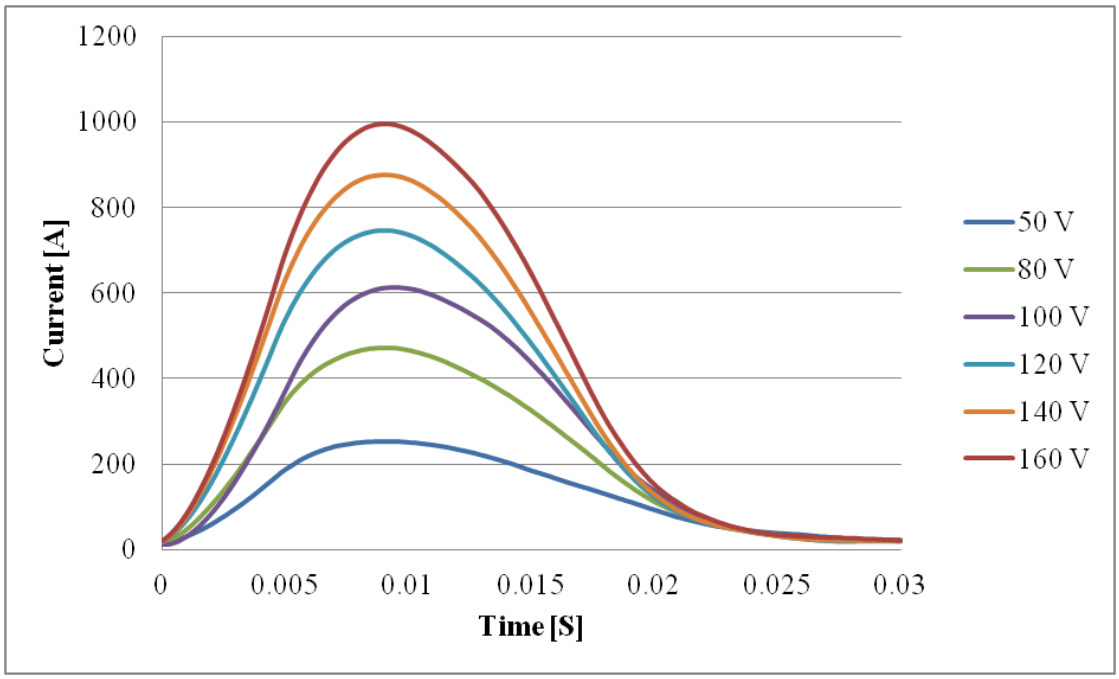

Figure 5.13: Current versus time for current pulse tests on sample 2-2-4

The remaining four buckypaper layer sample is sample 3-2-4 and the results from its current pulse testing are shown in Figure 5.14. All of the tests on sample 3-2-4 from 50 volts to 160 volts behaved exactly as would be expected. The current curves are smooth and the increases in maximum currents with increased analog voltages were the

same as what was observed for samples 1-2-4 and 2-2-4. Also there were no oddities in the 100 volt test as was seen in both of the previous samples. In addition to the standard tests chosen for all of the four buckypaper layer samples an additional test at 180 volts was performed. This was due to several factors including the curiosity of the maximum possible current that could be passed through the four buckypaper layer samples as well as the fact that the resistance of sample 3-2-4 had dropped to very low levels even at the 50 volt test. As can be seen from the current plot the sample was unable to withstand the high level of current which resulted in the sample burning.

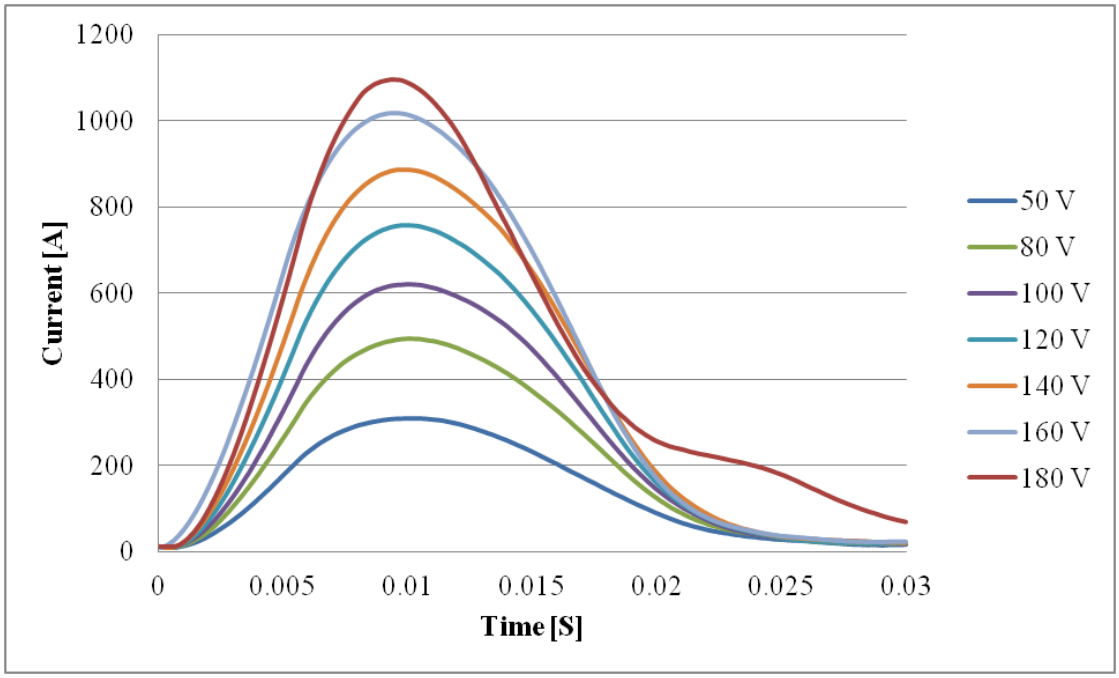

Figure 5.14: Current versus time for current pulse tests on sample 3-2-4

The voltage versus time plot for sample 3-2-4 gives greater insight into the change in the current pulse pattern for the 180 volt test. The plot is shown in Figure 5.15

and it can be seen that for the tests up to 140 volts the voltage curves are smooth and similar to the current curves. This trend changes with the 160 volt test where two small notches appear in the voltage curve, one at approximately 0.005 seconds and one near the maximum voltage at 0.01 seconds. These abnormalities were short in duration which at the time was rationalized as possible being due to the DAQ rather than the sample itself. After the burning it was more obvious that they were not due to the DAQ and were a warning to not increase the current levels on that sample.

For the 180 volt test that burned sample 3-2-4 several interesting observations can be made. Much like sample 2-1-0 during its 120 volt test, sample 3-2-4 encountered a large voltage spike. While the spike was only 10 volts for sample 2-1-0 and did not cause any visible damage the spike for sample 3-2-4 was much greater at approximately 35 volts. The increase in voltage for sample 3-2-4 occurred earlier than that of 2-1-0 at 0.008 seconds. The earlier spike could be attributed to the current pulse being greater than that needed to burn the sample where for sample 2-1-0 the current pulse may have been right on the burning threshold. Another interesting note is that though the current spike was much greater for sample 3-2-4 the duration of the increased current was approximately the same length of time. This much greater voltage increase over the same period of time is another indication of why sample 3-2-4 burned and sample 2-1-0 did not.

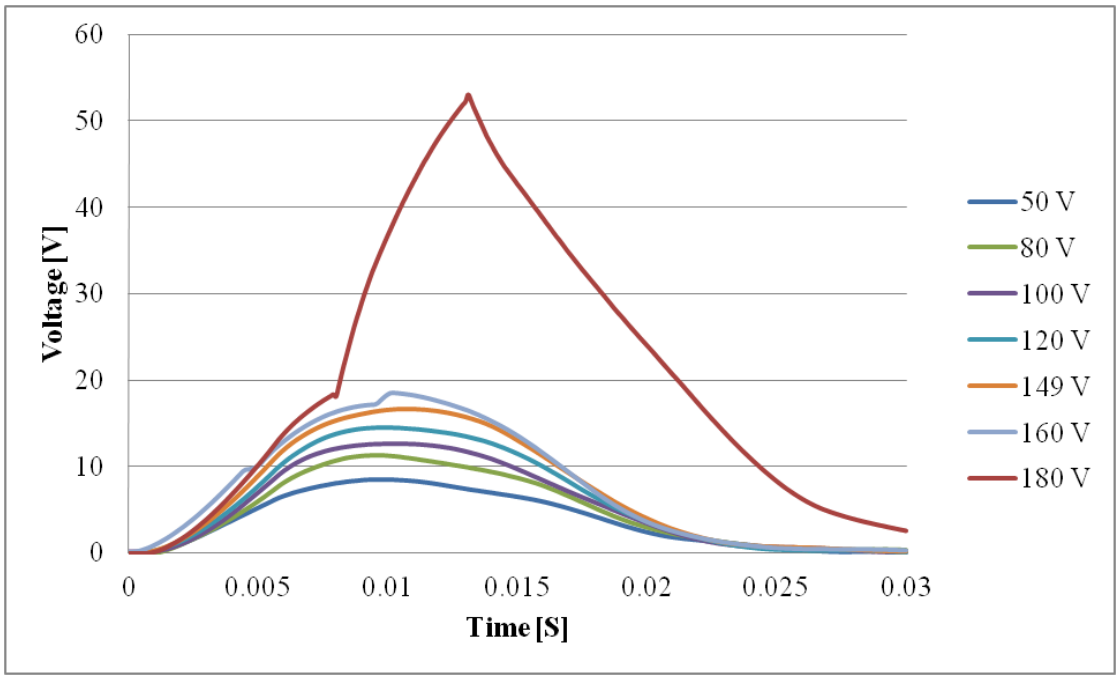

Figure 5.15: Voltage across sample 3-2-4 versus time during current pulse experiments

After disassembling the test fixture for sample 3-2-4 some burning was observed. All of the burning was found to be on the top surface of the sample and it was only visible on one side of the surface that was closest to the negative copper electrode. The other surfaces and edges of the sample appeared normal though internal or non-visible damage could have occurred. A close up of the burned surface is shown in Figure 5.16 where discoloring can be seen especially in the middle of the sample. Also, a line where the test fixture was in contact with the sample is shown and it appears that the burning did not extend beyond the contact region. This is understandable because the area of the sample in contact with the test fixture would have been much more confined allowing the amount of heat to increase much greater than for the portions of the sample open to the air.

Figure 5.16: Close up view of the burned surface on sample 3-2-4

Comparing the electrical resistances of each of the three samples with four layers of buckypaper also provided some interesting observations. A plot was created much like was done for the pure carbon fiber samples and can be seen in Figure 5.17. As with the pure carbon fiber samples the greatest resistance decreases for all three samples occurred between the 1A test performed in the previous chapter and the 50 analog voltage test. Also, the batch 2 sample (2-2-4) which had a much higher 1A resistance than the other two samples decreased much more allowing the three samples' resistances to be much closer. Another observation about the resistance decreases from the 1A test to the 50 volts test was that sample 3-2-4, which was very close in 1A resistance to sample 1-2-4, decreased a much greater amount than 1-2-4 but at higher analog voltages they returned to being very close in values. In fact with increasing analog voltage the resistance of all three of the three samples became more uniform with the results being approximately the same for the 120, 140, and 160 volt tests. Lastly, the burning of sample 3-2-4 can also be seen with the large increase in resistance from the 160 volt test to the 180 volt one.

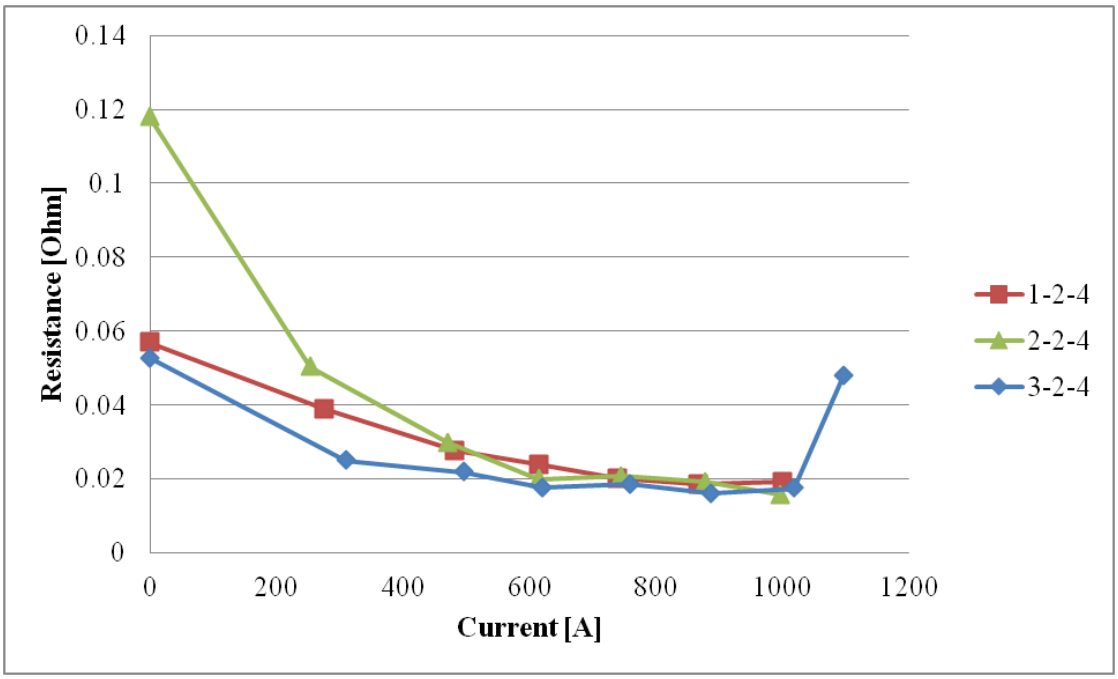

Figure 5.17: Resistance versus maximum current magnitude for samples with four layers of buckypaper

When comparing the resistances of the four buckypaper layer samples to those of the pure carbon fiber ones previously discussed another trend appears. That is for tests greater than 100 analog volts it can be seen that the resistances of the four buckypaper layer samples are lower than those of the pure carbon fiber samples. This trend is true for all three of the four buckypaper layer samples. Also the resistance difference between the two types of samples is increased between the 120 volt test and 140 volt test showing a trend that with increased current the buckypaper material is effective at decreasing electrical resistance. Table 5.2 shows all of tabulated results for the four buckypaper layer samples including the maximum current and electrical resistance at maximum current found for each test.

Table 5.2: Analog voltage, max current, and resistance for each test performed on the samples with four layers of buckypaper

Sample	Analog Voltage [V]	Max Current [A]	Resistance [Ω]
1-2-4	50	275.94	0.03895
	80	482.34	0.02758
	100	615.19	0.02381
	120	738.51	0.02011
	140	866.05	0.01857
	160	999.24	0.01917
2-2-4	50	252.62	0.05035
	80	470.83	0.02977
	100	614.02	0.01994
	120	745.04	0.02074
	140	876.62	0.01908
	160	995.37	0.01575
3-2-4	50	310.56	0.02493
	80	495.89	0.02180
	100	620.43	0.01761
	120	758.40	0.01858
	140	886.14	0.01600
	160	1017.52	0.01740
	180	1095.73	0.04788

5.5.3 Results of Samples with Seven Layers of Buckypaper

The last set of samples to be tested was those that contained seven layers of buckypaper. Sample 1-3-7 was completed with the same analog voltage levels that were used for the four buckypaper layer samples including 50, 80, 100, 120, 140, and 160

volts. The current versus time plots for these tests are shown in Figure 5.18. All of the tests behaved as would be expected with smooth current curve. The only exception to this was the 160 analog volt test where it can be seen that the current level decreased to approximately negative 40 A before increasing in a standard fashion. This negative current had never been seen with any of the previous pulse experiments and because the lower and higher analog voltage tests behaved smoothly it was regarded as a mistake by the current pulse generator. Another interesting observation about all of the pulse tests on sample 1-3-7 is the lower than expected current levels. For example the 160 analog voltage test on sample 1-3-7 had a maximum current of 813.8 A while all previous tests had current levels for the same analog voltage of approximately 1000 A. With the exception of the 80 analog voltage test for sample 3-1-0 all other tests produced consistent current levels for all tests.

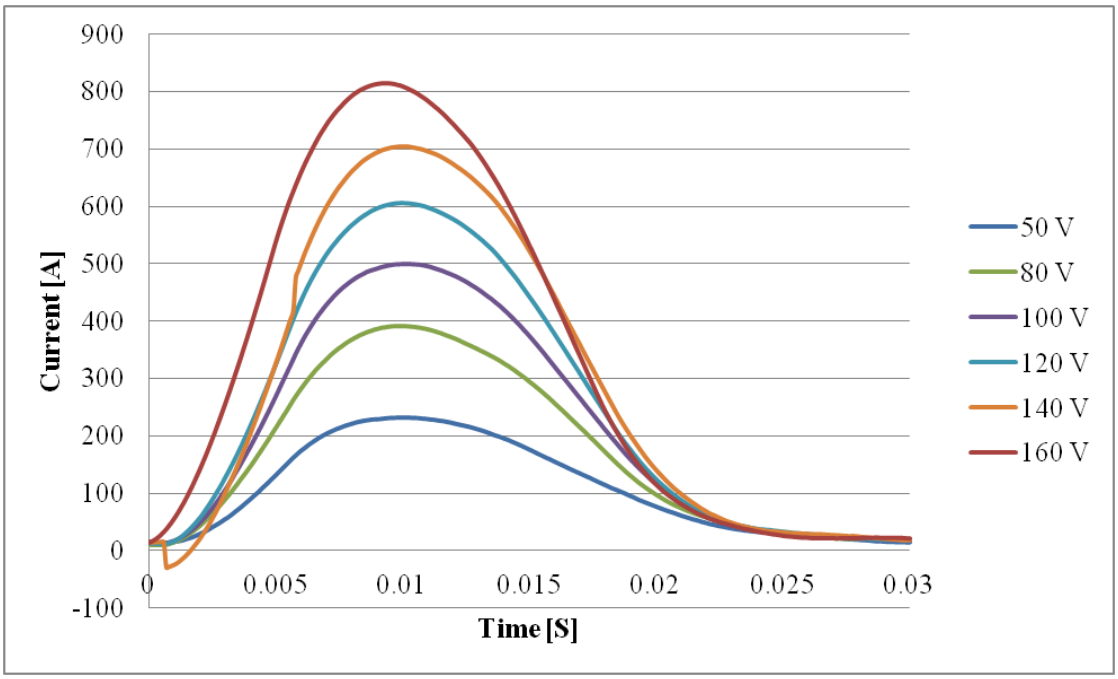

Figure 5.18: Current versus time for current pulse tests on sample 1-3-7

Sample 2-3-7 continued the testing trend with the same pattern of increasing analog voltages used. All current curves were smooth for this sample with the exception of a small discontinuity in the 80 analog voltage test with can be seen in Figure 5.19. This discontinuity occurred at roughly the same time that similar ones were seen for the 100 analog volt test for samples 1-2-4 and just previously shown in the 140 analog volt test for sample 1-3-7. Because the discontinuities occurred relatively far away from the maximum current levels they weren't as concerning for sample damage as if they had occurred at the peak. That being said the fact that all three occurrences happened at the same time could point to some functionality issues of the current pulse generator. A good trend that was observed for sample 2-3-7 was that the low maximum current levels found for sample 1-3-7 did not occur and all tests produced maximum current levels that were

similar to those of the pure carbon fiber samples as well as the samples with four layers of buckypaper.

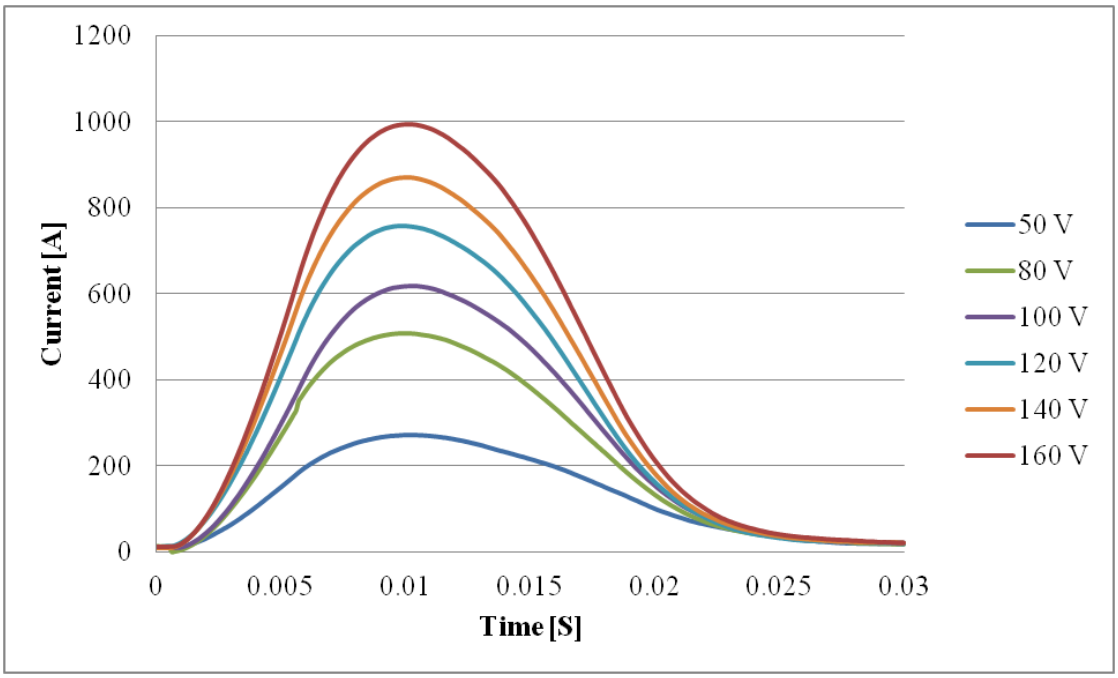

Figure 5.19: Current versus time for current pulse tests on sample 2-3-7

The last sample tested was sample 3-3-7. The results of its current versus time curves for all tests are shown in Figure 5.20 and it can be seen that all tests behaved exactly as was expected. All current curves are smooth and the maximum currents all were within the range that had been observed with all previous samples with the exception of 1-3-7. There were also no discontinuities, negative points, or oddities in the voltage curves which would lead to any concerns about damage in the specimen.

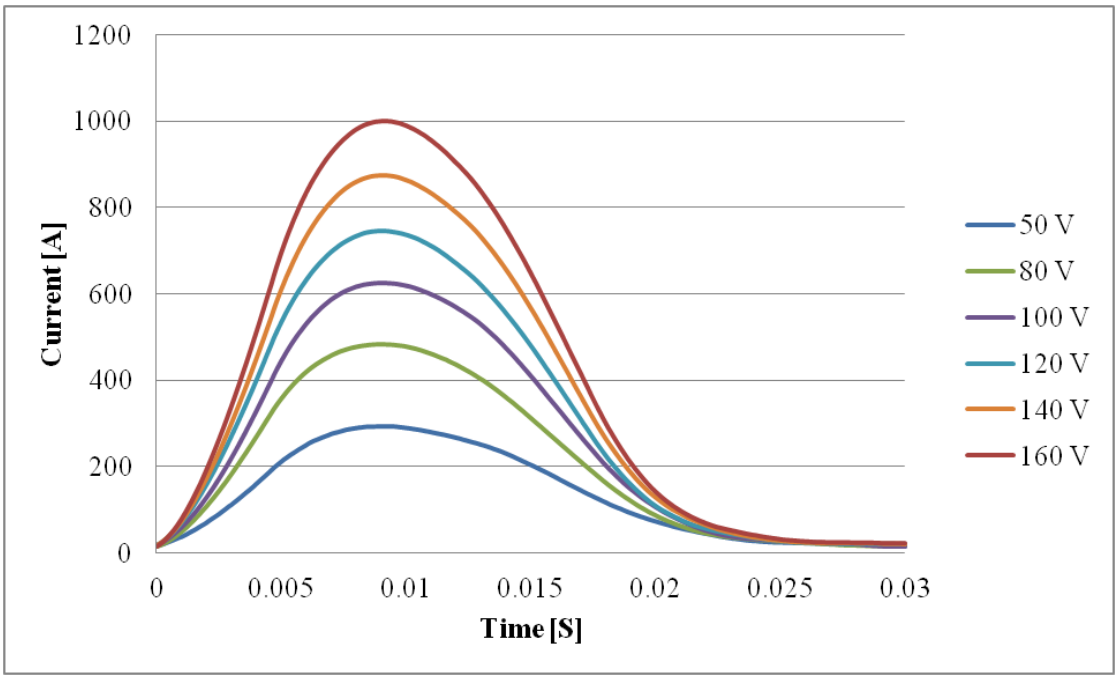

Figure 5.20: Current versus time for current pulse tests on sample 3-3-7

All three of the seven buckypaper layer samples exhibited the same trends as the pure carbon fiber and four buckypaper layer samples in that their resistances decreased with the increasing current of the current pulse tests. The results for these three samples are shown in Figure 5.21. As it can be seen the three samples became much closer in resistance as the current magnitude was increased and samples 1-3-7 and 2-3-7 which initially had much higher resistances deceased more greatly to their final levels than did sample 3-3-7. One interesting trend in the graph was the large decrease in resistance between the 50 and 80 analog voltage tests for sample 2-3-7. The decrease between these two tests had a very similar slope to that between the 1A and 50 analog volt test which is something that was not seen for any of the other eight samples. Comparing the final resistance values for the 160 analog voltage test to those of the four buckypaper layer samples it can be seen that there is not a great difference between the two. The

resistances between 0.02 and 0.017 Ohms for the three seven layer samples put them with very similar quantities to those of the four layer ones.

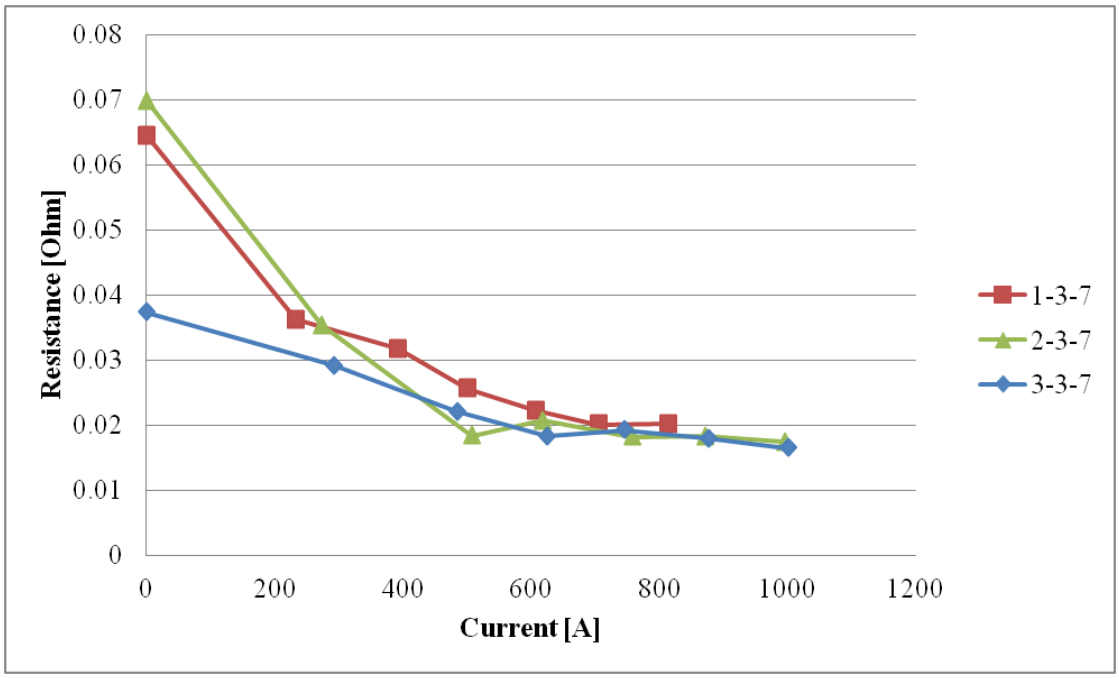

Figure 5.21: Resistance versus maximum current magnitude for samples with seven layers of buckypaper

The results of the maximum currents and resistances at maximum current were tallied and placed in a table much like those of the previous samples. The compilations of these results are shown in Table 5.3. From the table the lower maximum current levels for samples 1-3-7 can be seen when compared to 2-3-7 and 3-3-7 as well as the similarities in the resistances for higher analog voltage levels.

Table 5.3: Analog voltage, max current, and resistance for each test performed on the samples with seven layers of buckypaper

Sample	Analog Voltage [V]	Max Current [A]	Resistance [Ω]
1-3-7	50	232.4	0.03617
	80	392.2	0.03172
	100	500.4	0.02561
	120	606.1	0.02220
	140	704.4	0.02009
	160	813.8	0.02015
2-3-7	50	273.2	0.03530
	80	507.6	0.01836
	100	617.2	0.02070
	120	758.0	0.01821
	140	870.5	0.01830
	160	994.9	0.01740
3-3-7	50	292.5	0.02916
	80	483.9	0.02201
	100	624.5	0.01828
	120	745.1	0.01919
	140	875.8	0.01789
	160	1000.3	0.01646

5.6 Summary of the Electrical Current Pulse Experiments

When analyzing the current pulse experiments as a whole for all nine samples some interesting conclusions can be made. One of which is that there is no correlation between the rank of resistances measured at 1A for any group of samples and their electrical resistance ranks for high magnitude pulse tests. The 1A tests do give an indication of large contact resistances that must be addressed before testing but once a

sample has a safe resistance magnitude at 1A it was not possible to predict if this sample would fail (i.e. burn) at higher current levels. An example of this is sample 2-1-0 which had the lowest 1A resistance of the three pure carbon fiber samples. Sample 2-1-0 had a large resistance increase between its 100 and 120 analog voltage test and burned whereas samples 1-1-0 and 3-1-0 had larger 1A resistances but had no problems even during the 140 analog voltage test. Other examples exist with all eight other samples. In fact sample 2-2-4, which had the highest 1A resistance of any of the four buckypaper layer samples by far, decreased beyond samples 1-2-4 and 3-2-4 to have a slightly lower resistance than the other two for the 160 analog volt test.

Another trend observed for all three sample types was that the electrical resistances for any group of samples at high current levels were very similar in magnitude. For both the samples with four and seven layers of buckypaper the differences in resistances between similarly comprised samples all but vanished compared to the magnitude differences originally recorded in the 1A test. This convergence trend of resistance values was also true for the three pure carbon fiber samples but due to the burning of sample 2-1-0 higher analog voltage tests were not able to be performed to allow for very close resistance values.

The last trend observed was the effect of increased buckypaper on the electrical resistance of a sample. As decreased resistance at high analog voltage tests is directly correlated to decreased chances of burning, the addition of buckypaper layers to samples was done in the hope that their resistances would be lower than those of pure carbon fiber samples. Figure 5.22 shows the resistance versus current magnitude for all nine samples color coded by number of buckypaper layers. It can be seen that the addition of four

layers of buckypaper to the 16 layers of unidirectional carbon fibers did lead to a decrease in electrical resistance for the high analog voltage tests. That being so it can also be observed that the addition of three more layers of buckypaper to make the seven buckypaper layer samples did not further decrease this resistance. This pattern shows that for high current pulse experiments the additional cost of adding buckypaper layers greater than four to 16-ply unidirectional carbon fiber samples does not lead to decreased resistance.

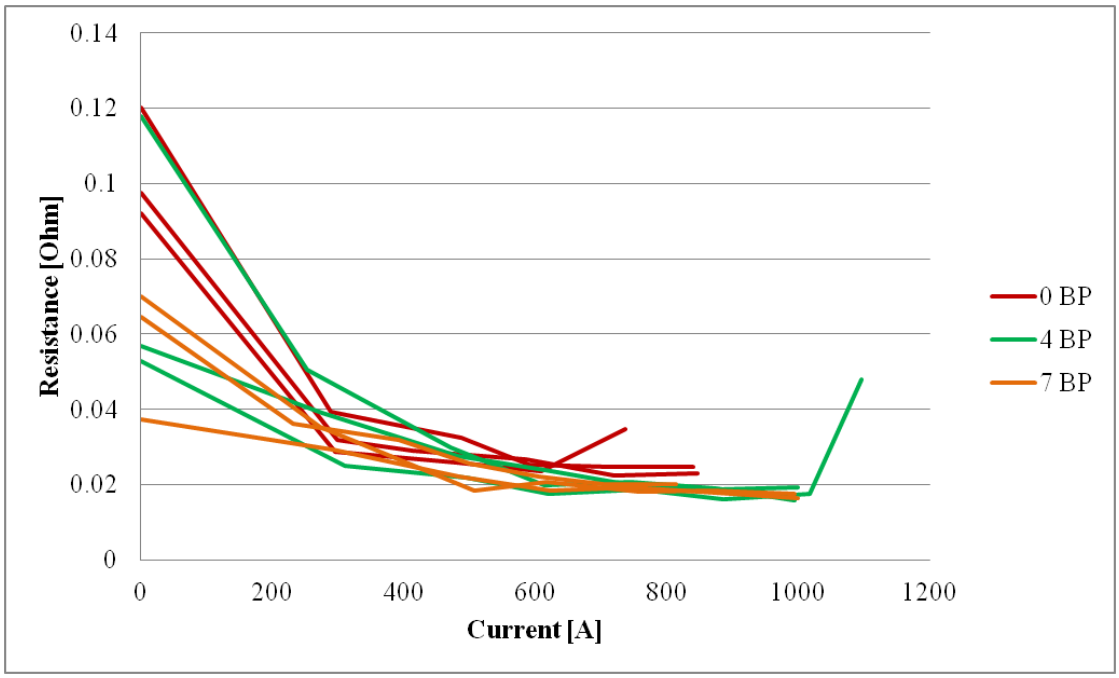

Figure 5.22: Comparisons of resistance versus current magnitude for the three types of composite samples with different layers of buckypaper

CHAPTER 6

COORDINATED IMPACT-CURRENT PULSE EXPERIMENTS

6.1 Experimental Considerations

The results of the current pulse experiments provided the necessary data in formatting the coordinated impact-current setup and procedure. From the previous current pulse experiments safe levels of current that could be used for coordinated impact events were determined. Also found were the resistance relationships between batches and types of samples which provided a means of further tailoring the experimentation. The strategies and theory used in this experiment to coordinate the impact with current pulse were developed in a large part by Hart who researched the effects of increasing current pulse magnitudes on carbon fiber reinforced composites impact characteristics using a very similar setup (Hart, 2011). Expanding on his knowledge allowed for the experimentation to occur and the relationships between number of buckypaper layers and electrification levels on the impact resistance of carbon fiber reinforced polymer composites to be investigated.

6.2 Impact-Current Pulse Experiment Setup

The coordinated impact-current pulse experimental setup was very much an extension of the current pulse experimental setup discussed in the previous chapter and shown in Figure 5.3. In addition to the current pulse generator and data acquisition systems used prior an Instron 8200 Dynatup Drop Weight Impact Machine, trigger

system, and impact data acquisition unit were incorporated in to provide a fully automated experimental setup.

The Instron 8200 Dynatup Drop Weight Impact machine is a very versatile piece of equipment and is widely used to study impact properties of carbon fiber reinforced polymer composites. The impactor allows the user to adjust the height from which a dead weight is dropped up to one meter above the specimen, as well as the quantity of that weight from 3 to 13.6 kilograms (Instron Corporation, 2004). By adjusting both the height and weight of the dropping carriage the user is able to control the amount of impact energy to apply for a specific test as well as the velocity of the tup when it makes contact with the material. To control when the drop weight is to be put in motion there is a releasing latch mechanism that is position at the desired height that the weight is to be dropped from. The impact test machine is fully instrumented with a velocity flag on the weight carriage and velocity detector positioned directly before the impact location. There is also a force gauge located inside the tup which allows for the load magnitude through entire impact events to be known. The last feature of the impactor equipment is a pneumatic braking system which allows for the tup to only impact the specimen the number of times desired by the experimenter. This prevents the tup from continuing to bounce on the tested material casing further damage after the desired load was applied. A diagram showing the front and side view of the Instron 8200 is shown in Figure 6.1. The optional pneumatic braking system that was incorporated takes the place of the stop blocks shown.

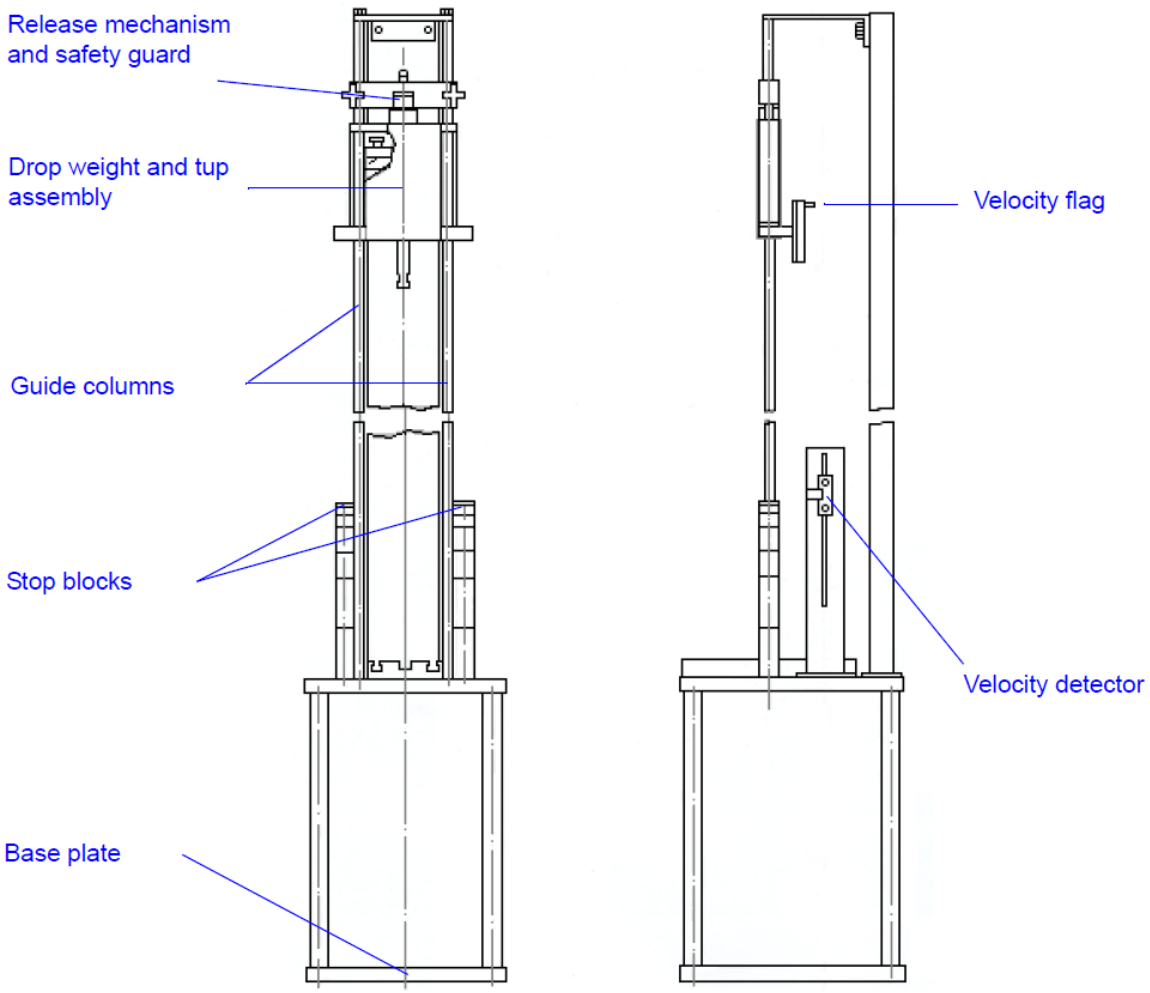

Figure 6.1: Instron 8200 Dynatup impact test instrument (Instron Corporation, 2004)

To control the dropping of the impact carriage and coordinate the impact event with a current pulse event an additional trigger mechanism had to be automated and incorporated into the setup. This was done using the same HP 6612C DC power supply that was used in the four probe electrical resistance testing and is shown previously in Figure 3.4. The output of the power supply was connected to an electric air solenoid valve which in turn was connected by pneumatic hose to an air actuated cylinder. The current pulse VEE program used in the experiments of the previous chapter was modified

to turn on the output channel of the power supply at a predetermined time which would then provide electric power to the solenoid valve. This would open the valve permitting air pressure to the actuated cylinder which would in turn allow its piston to extend. The piston was connected to the latch mechanism of the drop weight tested and its extension released the drop weight carriage allowing it to fall.

To record the data produced by the force gauge and velocity sensor on the Instron 8200 impact test machine an additional data acquisition system and desktop computer were used. The Instron Corporation included a purposely built data acquisition unit which easily mated to the sensors as well as plugged into a computer for control. Also included with the impactor was Instron's "Impulse Data Acquisition" software which allowed for the test parameters to be inputted for a specific experiment and provided raw data and graphs of the results. The required test parameters included weight of the drop carriage, shape and dimensions of the sample, the force sensor's calibration information, and estimated duration of the test. The computed results for the 8200 impactor included velocity at impact, force during impact, impact energy, absorbed energy, and deflection all of which are useful to understanding the impact strength of a material. A diagram of the entire coordinated impact-current pulse experimental setup with the current pulse generator as well as the Instron 8200 impactor and additional trigger and data acquisition equipment is shown in Figure 6.2. The greatest benefit of this setup was that all systems were controlled by the two desktop computers shown which allowed for very accurate easily usable results as well as the ability to remotely trigger experiments without the operator needing to be near the equipment during experimentation.

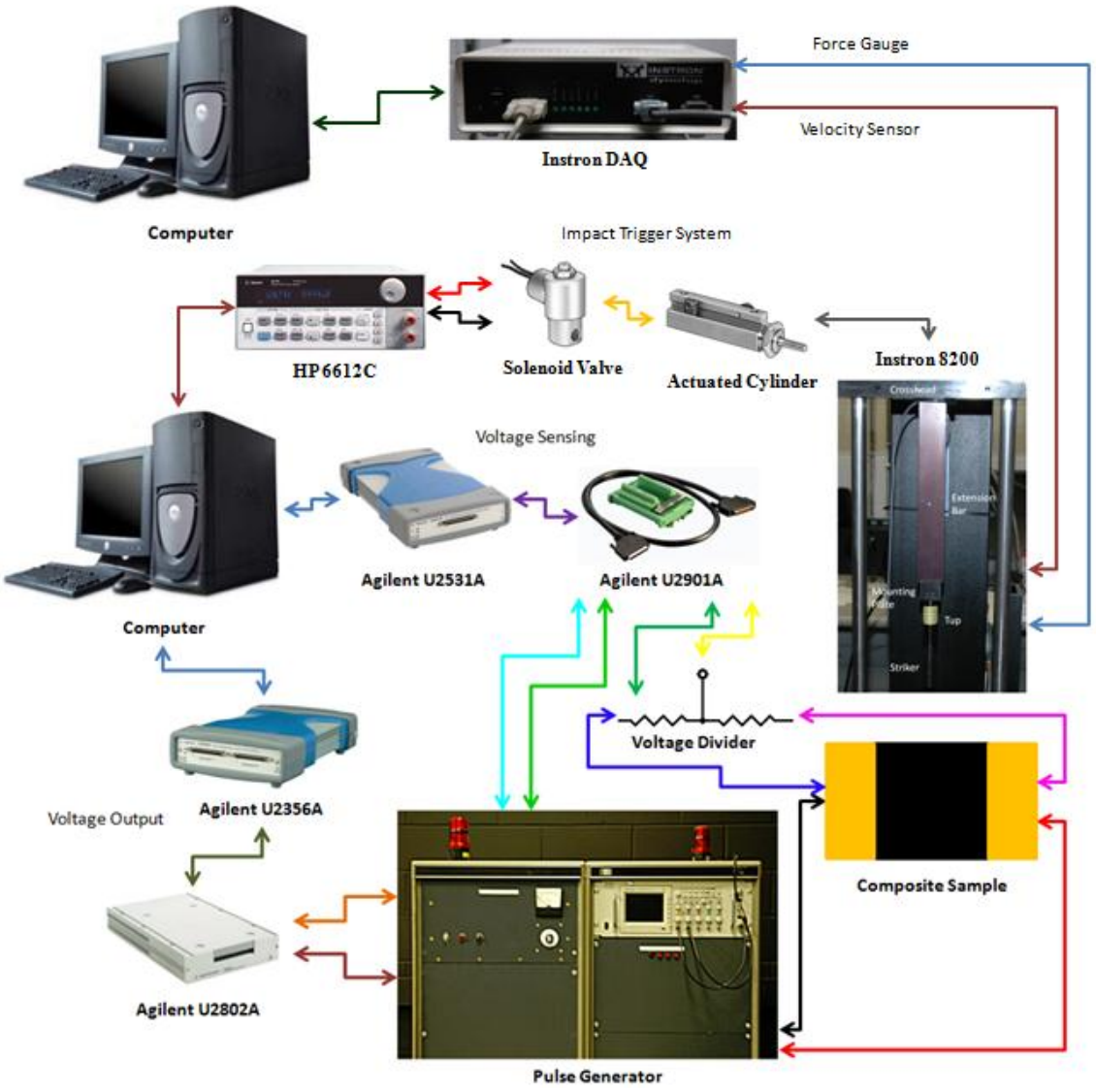

Figure 6.2: Coordinated Impact-current pulse experiment setup

6.3 Impact-Current Pulse Experiment Procedure

With the experimental setup complete the samples could be tested one by one following a detailed experimental procedure. Because two desktop computers, two data acquisition units, three software packages as well as two large pieces of equipment in the

current pulse generator and Instron 8200 impactor were all used in the coordinated impact-current pulse experiment it was important that a strict regimen was followed to prevent any necessary steps in the experimental setup to be forgotten. This included ensuring that the samples were properly prepared and the test fixture was correct as well as all equipment needed in the coordination of the two systems were correctly setup and ready before testing was attempted.

6.3.1 Composite sample and Test Fixture Procedure

All nine of the six inch by six inch composite sample that were used in the two probe electrical resistance and current pulse testing were also used in the coordinated impact experiment. Because of their previous uses the samples were already prepared with Duralco 120 silver epoxy on their edges which would be in contact with the copper electrodes. The only additional preparation needed to the samples was a wet application of Duralco 120 resin to ensure low contact resistances when the samples were inserted into the test fixture. The test fixture for the Instron 8200 impactor was very similar to the stand alone test fixture previously used including many of the same parts. The main difference between the two test fixtures was that the base plate on the impactor test fixture was permanently located in a position so that the tup would contact the samples in the middle of the base plate's unsupported region.

Once the sample had received the Duralco resin it was placed on the base plate of the new fixture. A carpenter's square was used to ensure that the sample was located exactly in the middle of the fixture. Once measured the copper electrodes were added and

the same wooden and aluminum top plated used in the previous test fixture were placed over the sample. Four bolts which were permanently attached to the test fixture were moved into position and the four hand tightened nuts were used to secure the top plates down. It was also important that all of the nuts were tightened to as close to the came torque as possible so that no uneven pressure was placed on the samples. The last step was to secure the copper electrodes using the craftsman bar clamps from the previous experiment. The complete setup test fixture is shown in Figure 6.3.

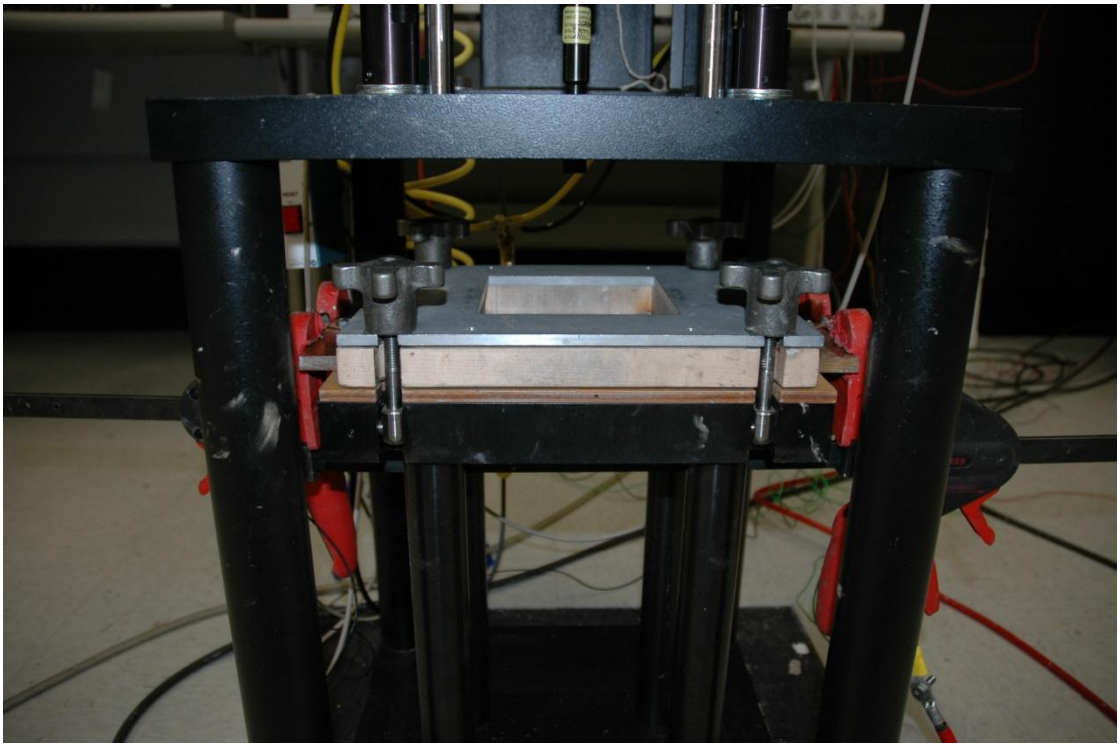

Figure 6.3: Composite sample test fixture in Instron 8200 impactor

6.3.2 Current pulse Generator Procedure

The current pulse generator was setup in an identical way to what was done for the current pulse experimental setup. This included plugging in the Agilent U2531A and U2356A data acquisition units as well as the pulser itself. It also included starting the Agilent data acquisition manager software and VEE program along with the built in oscilloscope on the current pulse generator. To test if all connections were still correct and that the trigger system was in working order the VEE program could be run without charging the pulser and it could be determined if all data collecting equipment went off as would be expected.

6.3.3 Instron 8200 Impactor Procedure

To prepare the Instron 8200 impactor once a composite sample had been placed in its test fixture several steps had to be completed. The first of which was determining the desired drop height and weight for the machines drop carriage that corresponded to the V_{50} impact velocity. The V_{50} impact velocity is the velocity at which 50 percent of the samples tested are perforated. For the impact tests performed in this study, all weights attached to the carriage were removed and only the 3.5 kilogram weight of the carriage itself was used as had been done in Zantout's research (Zantout, 2009). After many tests using old composite sample the height was adjusted to its final position of 11.1 centimeters above the samples surface which correlated to approximately a 3.5 Joule impact energy as was found using the potential energy equation. Once the weight and drop height were set the remaining setup steps were completed.

These included turning on the pneumatic braking mechanism as well as the HP 6612C power supply, Instron data acquisition unit, desktop computer, and Instron software. The current level on the power supply was then adjusted to it maximum two amp output so that when activated by the VEE program it would act in voltage control mode providing enough power to the pneumatic solenoid valve to open. In the software package a new experimental method was made that included entering the drop carriage mass of 3.5 kilograms, the square shape of the test sample and its thickness, and the estimated time of impact which was exaggerated to ensure that all data would be collected. With the method completed a new impact test could be selected via a screen icon and given a name describing the sample. This then popped up a notification asking if the sample was ready to be tested. It was not selected that it was ready until just before the experiment was set to start as it only allowed for a 30 second window for impact once it was selected.

6.3.4 Impact-Current Pulse Coordination Procedure

To coordinate the impact of the tup with the current pulse created by the current pulse generator the VEE program that was developed by Hart (2011) was used. This program allowed for the specific procedure to charge the current pulse generator to occur as well as the wait time between the start of impact and pulse events to be adjusted for different drop heights. In order to do this two wait functions were incorporated into the software. One of which was permanently set at 0.445 seconds which was found to be the time it took for the HP power supply, solenoid valve, and air actuator to release the drop

carriage after receiving the signal from the program. The other time was adjustable and was set to the time it took the tup to fall almost all the way to the surface of the sample. For these experiments that time was found to be 0.161 seconds. With the two times combined it was ensured that the maximum current from the current pulse generator would directly correlate with the maximum load of the tup on the composite sample. This timing adjustment was the last step completed prior to testing being able to take place.

6.3.5 Final Test Preparations and Initiation Procedure

In order to complete a successful coordinated impact-current pulse test several steps needed to be performed. The first step was to select the start button on the VEE program which turned on the two five volt output channels on the Agilent U2356A which were used for triggers. Next the software program waited for the users to charge the current pulse generator and set the oscilloscope to single sequence. As the current pulse generator was charging it was also ensured the impactor's drop carriage was in position and that the brake system was lowered to allow for contact between the sample and the tup. Once the current pulse generator was charged to the desired analog voltage the Instron software was told that an impact event was about to occur by selecting the start button in the previously discussed pop up window. Also the start button was selected on the Agilent Data Management software to prepare it for its trigger from the U2356A. Lastly the OK button was selected on the VEE program which began a countdown to the test. The countdown lasted ten seconds which allowed for the experimenters to leave the room in case the tup became damaged during impact causing sharp plastic pieces to be

shot across out of the impactor. Once the countdown was completed the test would start and the coordinated impact-current pulse test could take place with the tup striking the samples once before bouncing off and being caught by the pneumatic brakes. All nine samples were tested in a way identical to this.

6.4 Impact-Current Pulse Experiment Results

The coordinated impact-current pulse experiments were conducted in three phases. The batch one samples were impacted with no current pulse added to allow for benchmark impact properties to be known on the pure carbon fiber, four buckypaper layer, and seven buckypaper layer samples. The batch two samples followed and were tested with a coordinated pulse of 100 analog volts. Lastly the batch three samples were testing with an analog voltage of 160 volts. For both of the batches that were electrified a 1A test was performed prior to the coordinated test to ensure that resistances were low enough that no burning occurred. It was found for all samples that the 1A resistance decreased from the results discussed in Chapter 4 as would be expected after the current pulse tests. The results of the coordinated impact-current pulse tests for all three batches were compared by number of buckypaper layers as well as against each other in determining the effect of the addition of an electric current pulse.

6.4.1 Non-Electrified Impact Results

The first of the samples tested for the non-electrified impact experiments was sample 1-1-0. The result of this test was a line crack through the composite sample

parallel to the fiber direction which occurred at approximately 3.9 milliseconds with a force of 1490.6 N. The next sample tested in the Instron 8200 was sample 1-2-4. On its first test with the same drop weight and height as sample 1-1-0, sample 1-2-4 withstood the impact and showed no signs of physical damage. In fact the test was repeated at the same impact energy level until the sample broke which took a total of five impacts. When it did fracture the sample exhibited the sample line crack pattern as sample 1-1-0 through the entire 6 inch length of the sample. The last sample tested was sample 1-3-7 which when impacted fractured on its first test. This occurred at approximately 4.3 seconds with a force of 1664.9 N. The force versus time plot for the first test on all three samples is shown in Figure 6.4. It can be seen that sample 1-2-4 experienced a force load of 1974 N and did not fracture as is shown in the other two samples with the large drops in force loads at those specific times. Also shown is the relative uniformity in the loads applied for all three samples with time with sample 1-3-7 only experiencing a slightly higher force throughout than the other two samples.

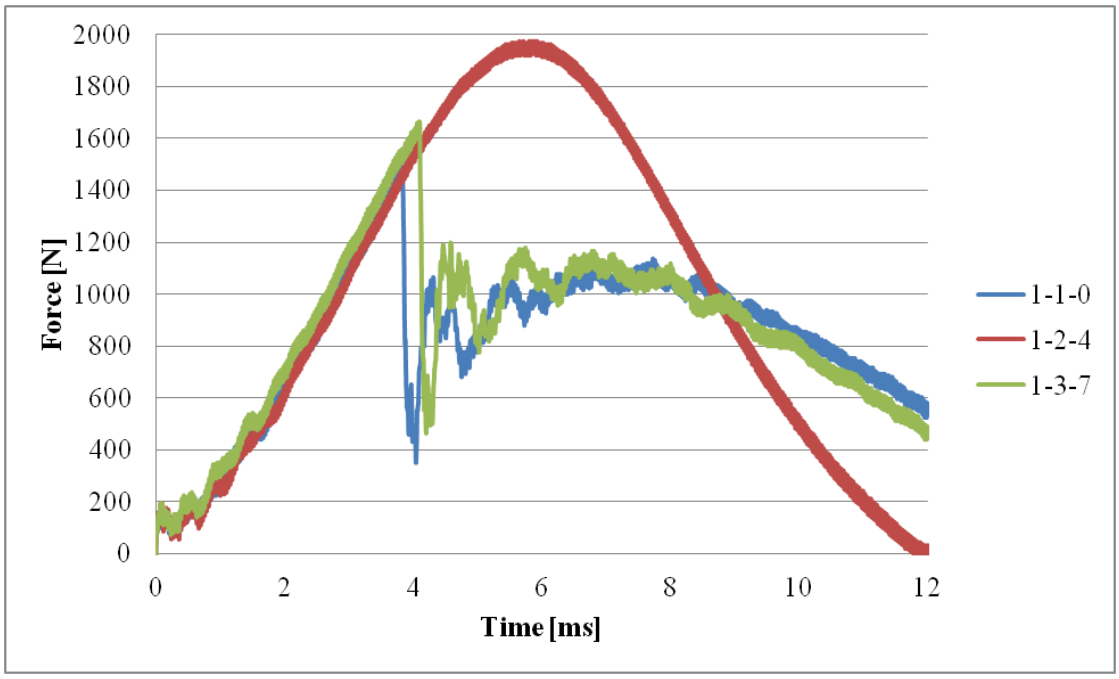

Figure 6.4: Force versus time for the batch one samples with no electrification

In addition to the force, the deflection of the samples was recorded during the impact events. The deflection versus time curved for all three samples are shown in Figure 6.5. Sample 1-2-4 which did not fracture was the stiffest among the three samples followed closely by sample 1-3-7.

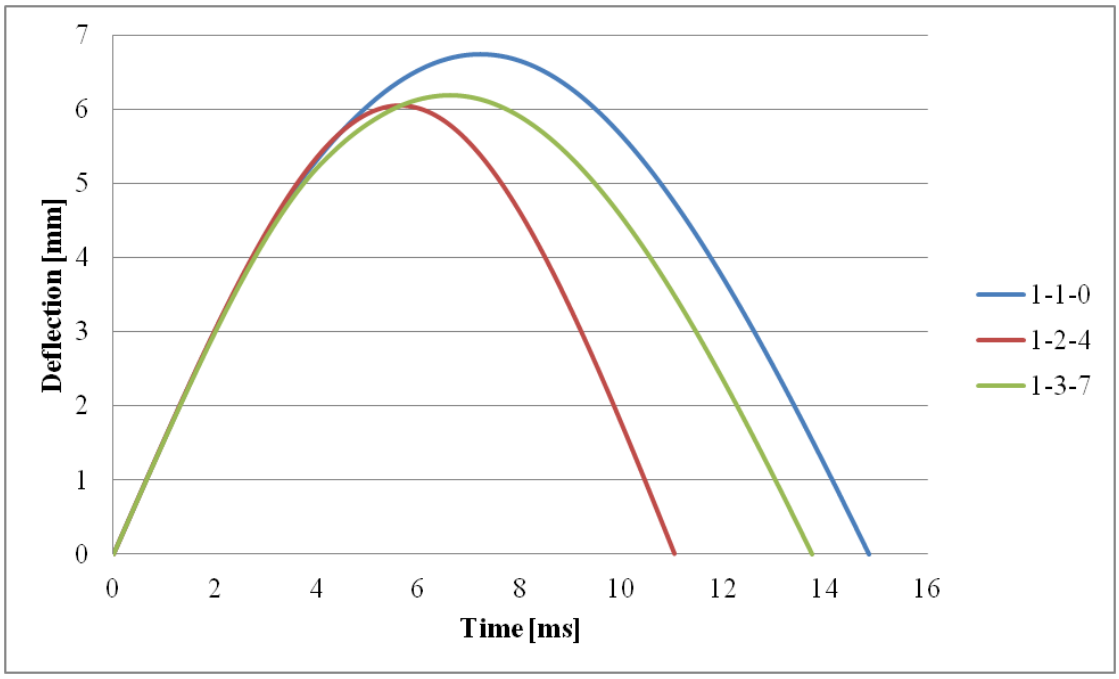

Figure 6.5: Deflection versus time for the batch one samples with no electrification

Figure 6.6 shows the corresponding force versus displacement curves for all three samples. The plot only shows the deflection as the force was increasing as the upward slope was the cause of the fracture in the two samples that did break.

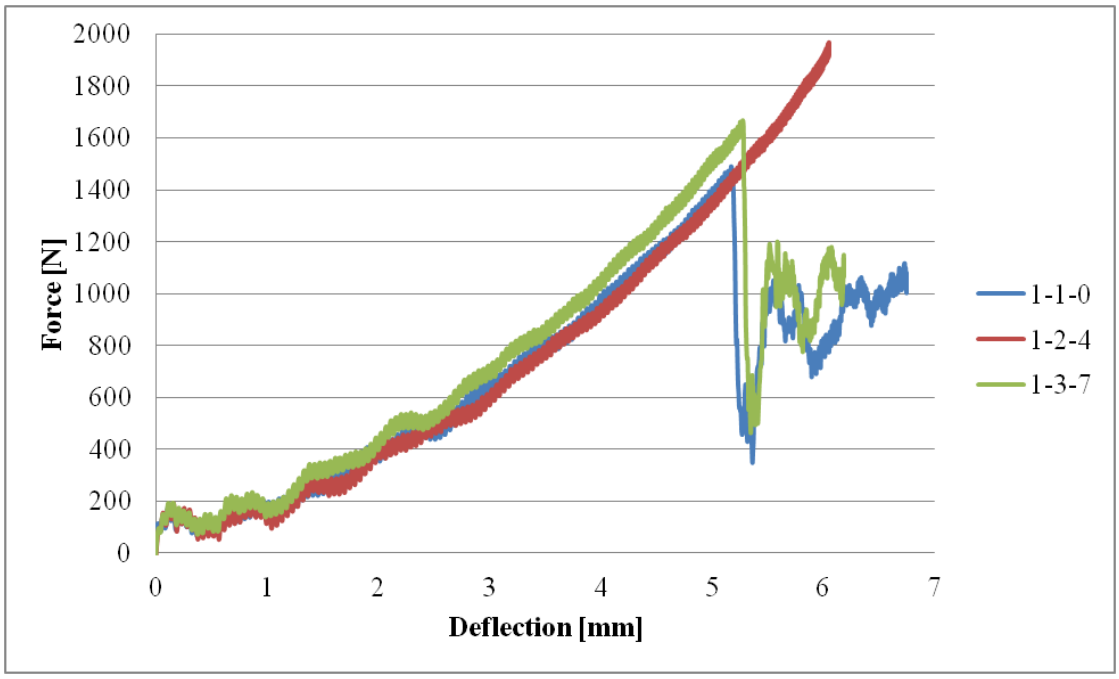

Figure 6.6: Force versus deflection for the batch one samples with no electrification

Though sample 1-2-4 did not fracture during its first impact test it did on its fifth. Figure 6.7 shows the force versus time graphs for all five impacts on sample 1-2-4. Note that the first four impact rests resulted in practically identical impact forces. Fracture of sample 1-2-4 occurred in the fifth test at a force of 1845.3 N which was larger than the fracture forces of both samples 1-1-0 and 1-3-7.

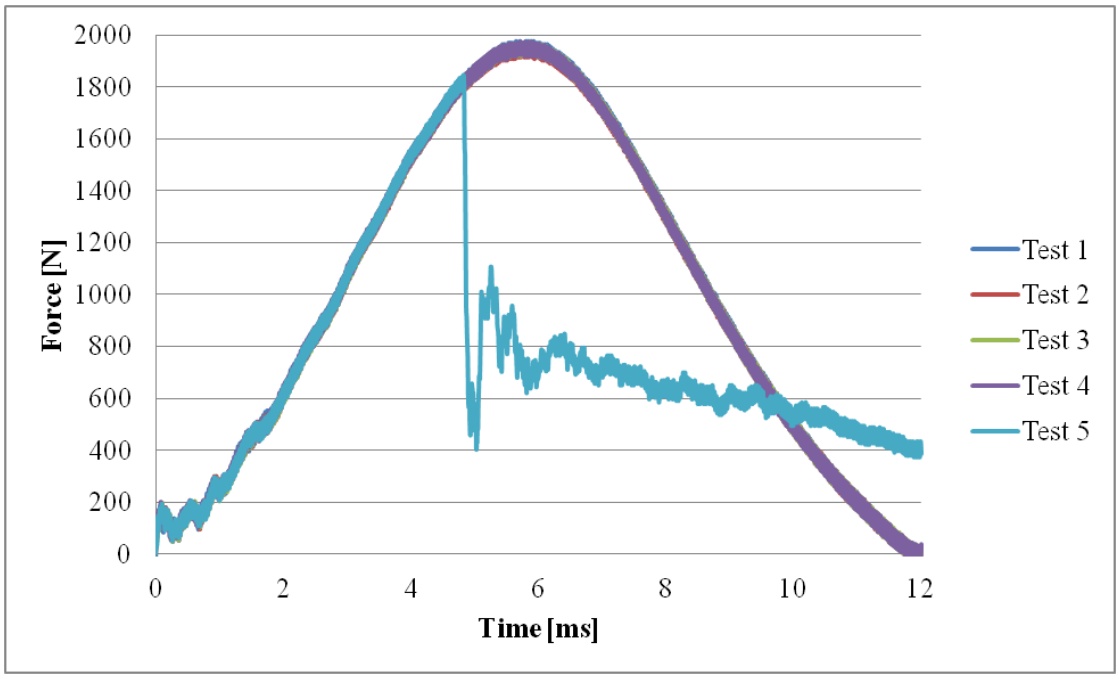

Figure 6.7: Force versus time for the five impacts on sample 1-2-4

The deflection versus time for the five impact tests on sample 1-2-4 was also plotted and is shown in Figure 6.8. Much like the previous force versus time plot it can be seen that the first four tests behaved identically.

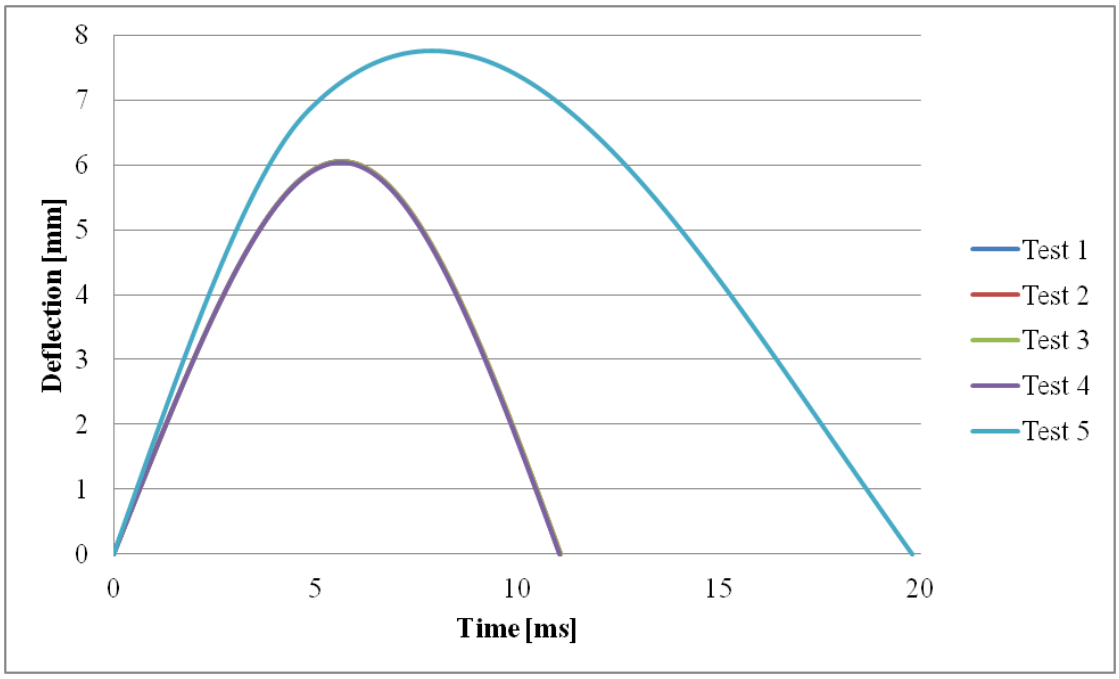

Figure 6.8: Deflection versus time for the five impacts on sample 1-2-4

Force versus deflection plots for sample 1-2-4 are shown in Figure 6.9. The fifth test is shown to have had a much lower force versus deflection than the previous four experiments as well as the larger overall defection.

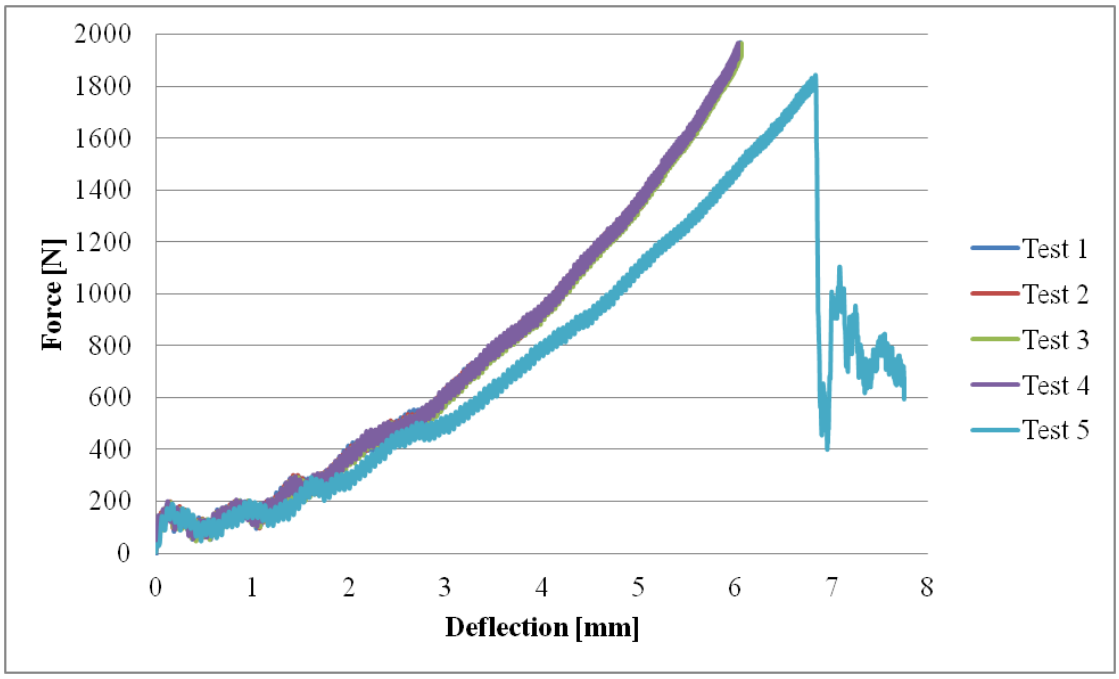

Figure 6.9: Force versus deflection for the five impact tests on sample 1-2-4

Table 6.1 contains the experimental data for all tests performed on the samples of batch one. As can be seen, the impact velocities for all tests were very close at approximately 1.48 m/s for all tests with the exception of the last test on sample 1-2-4 which had a velocity of 1.6114 m/s. This increased velocity was also show to increase the energy to max load to 4.964 J versus the 4.45 to 4.49 J seen in the previous four tests. This difference in properties for the fifth test could have been a contributing factor in the final fracture of the sample.

Table 6.1: Combined data on impacts of all batch one samples

Sample	Test #	Electrical	Drop Mass [kg]	Drop Height [cm]	Velocity [m/s]	Impact Energy [J]	Absorbed Energy [J]	Peak Load [N]	Peak Current [A]	Damage
1-1-0	1	No Pulse	3.5	11.1	1.4842	3.8548	3.1090	1490.6	N/A	Line Crack
1-2-4	1	No Pulse	3.5	11.1	1.4867	3.8680	4.4886	1974.0	N/A	No Damage
	2	No Pulse	3.5	11.1	1.4816	3.8416	4.4630	1964.3	N/A	No Damage
	3	No Pulse	3.5	11.1	1.4839	3.8533	4.4540	1972.7	N/A	No Damage
	4	No Pulse	3.5	11.1	1.4820	3.8438	4.4628	1971.5	N/A	No Damage
	5	No Pulse	3.5	11.1	1.6114	4.5441	4.9640	1845.3	N/A	Line Crack
1-3-7	1	No Pulse	3.5	11.1	1.4793	3.8294	3.5691	1664.9	N/A	Line Crack

The results of the impact tests on non-electrified samples were partly inconclusive due to the limited number of samples. It was not possible to determine whether or not the addition of the buckypaper layers had a noticeable effect on the impact resistance of the carbon fiber reinforced polymer matrix composites. This being true, it should be noted that the samples with buckypaper layers withstood higher impact forces before failure. For instance, sample 1-3-7 had about an 11.6% higher peak load than sample 1-1-0 with no buckypaper layers. The results of these impact tests provide a baseline for the study of the electrified samples, which is discussed next.

6.4.2 100 Analog Voltage Coordinated Impact Results

The objective of the study of electrified samples was three-fold: (1) to determine whether or not the application of a pulsed electric current changes the impact resistance of the composite samples; (2) to determine the effect of increasing the number of buckypaper layers on the impact resistance of electrified composites; and (3) to determine

the effect of increasing the electric pulse magnitude on the impact resistance of electrified composites.

Before testing electrified samples it was important that proper coordination needed to be ensured between the impactor and current pulse generator. As was discussed in the experimental setup and procedure of the coordinated impact-current pulse experiment the time delay between the dropping of the carriage in the impact tester and the releasing of the current pulse were required to be well synchronized in order to ensure that the maximum current was at approximately the same time as the maximum impact load. To test that this time delay was set accordingly a test was first performed on a previously used 16-ply cross-ply sample that was available in the lab. The current pulse magnitude and impact load are shown in the same plot in Figure 6.10 where they are well coordinated and have a time difference between peaks of approximately 0.002 seconds. Because of the small variations in drop time between tests it was found that this was the best coordination possible between the two events.

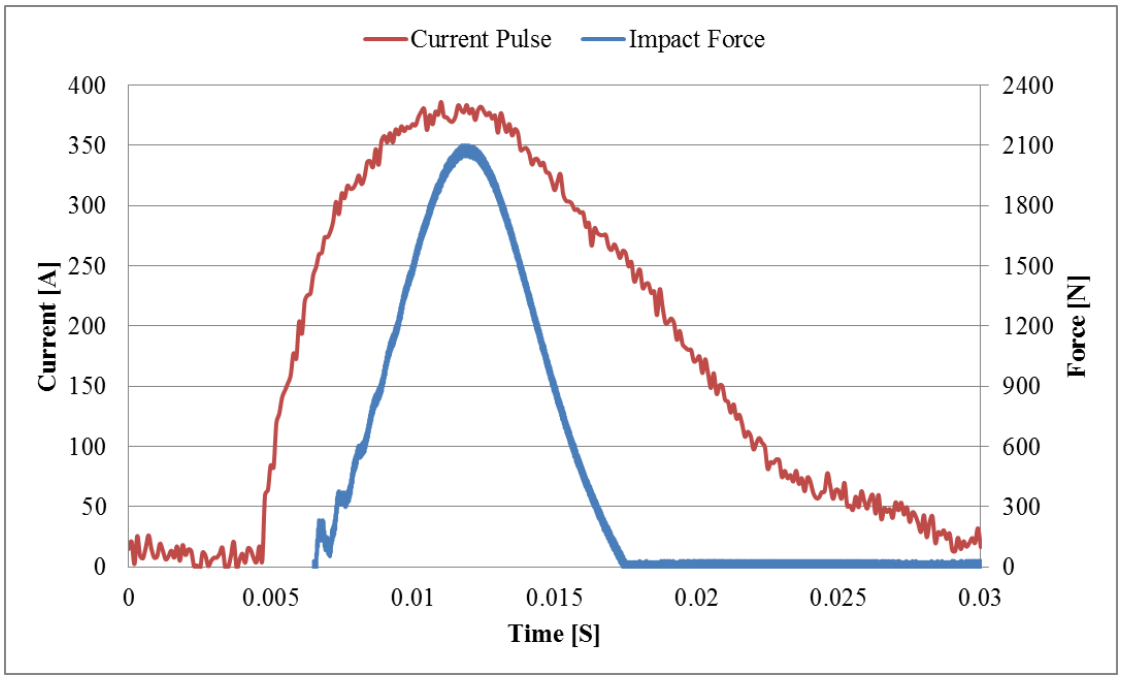

Figure 6.10: Impact-electrical current coordination test

Once coordination was ensured the three batch two samples were tested in order of the number of buckypaper layers they contained. The current pulse level chosen was 100 analog volts which correlated in the current pulse experiments of the previous chapter to a maximum current level of approximately 600 A. The first sample tested was sample 2-1-0 with no buckypaper layers. This sample did not show signs of physical damage after its first coordinated test but both fractured via a line crack and burned during its subsequent test. Sample 2-2-4 with four layers of buckypaper was tested next and it experienced substantial damage on its first coordinated impact fracturing at an impact load just above 1900 N. Sample 2-2-4 also showed signs of some burning occurring with portions of the edges which had been in contact with the copper electrodes being dark. The last sample tested was sample 2-3-7 that contained seven layers of buckypaper. This sample did not break when impacted with a coordinated current load

applied at the same time. In fact sample 2-3-7 withstood three coordinated tests with no substantial damage before being broken in half on its fourth test. The force versus time plot for the first tests of all three samples is shown in Figure 6.11 where it is seen that sample 2-2-4 was damaged at approximately five milliseconds. It can also be observed that both samples 2-2-4 and 2-3-7 experienced higher loads than did 2-1-0 which could be attributed to a slower drop velocity of the carriage on the 2-2-4 test.

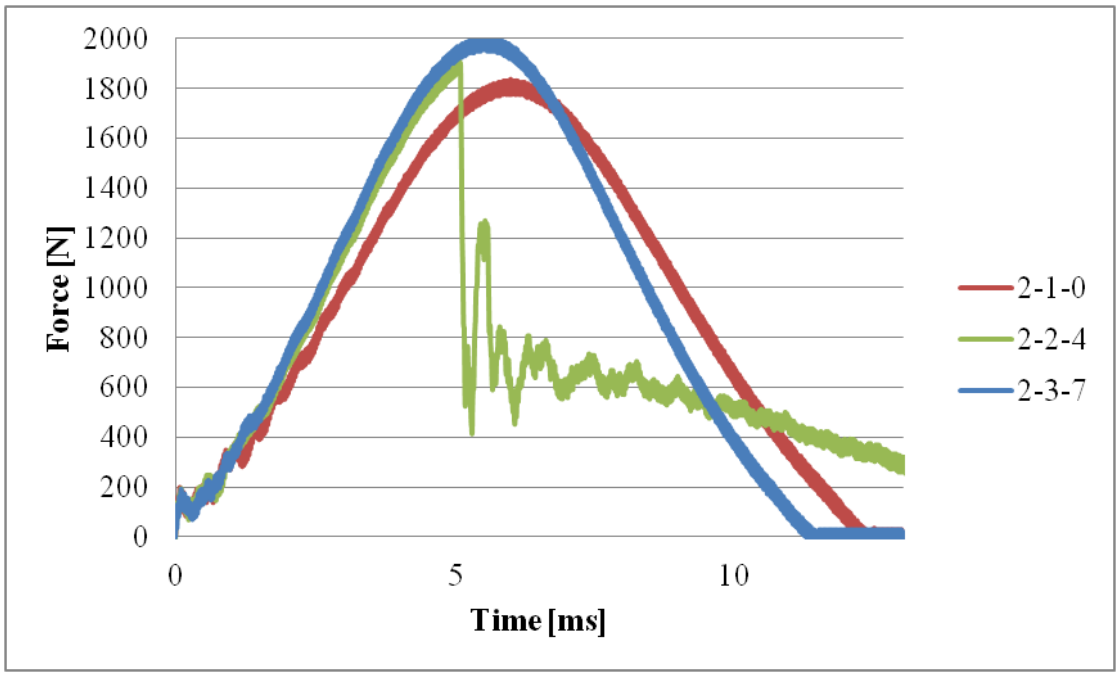

Figure 6.11: Force versus time for the batch two samples with 100 V current pulse

The deflection versus time plot for the three samples is shown in Figure 6.12 and it tells a similar story to the plots of the batch one tests. The similarities in the deflection patterns shown of the samples that contained buckypaper, as well as the fact that they

both deflected less than the pure carbon fiber sample, shows the stiffening benefits of using the nanotube material.

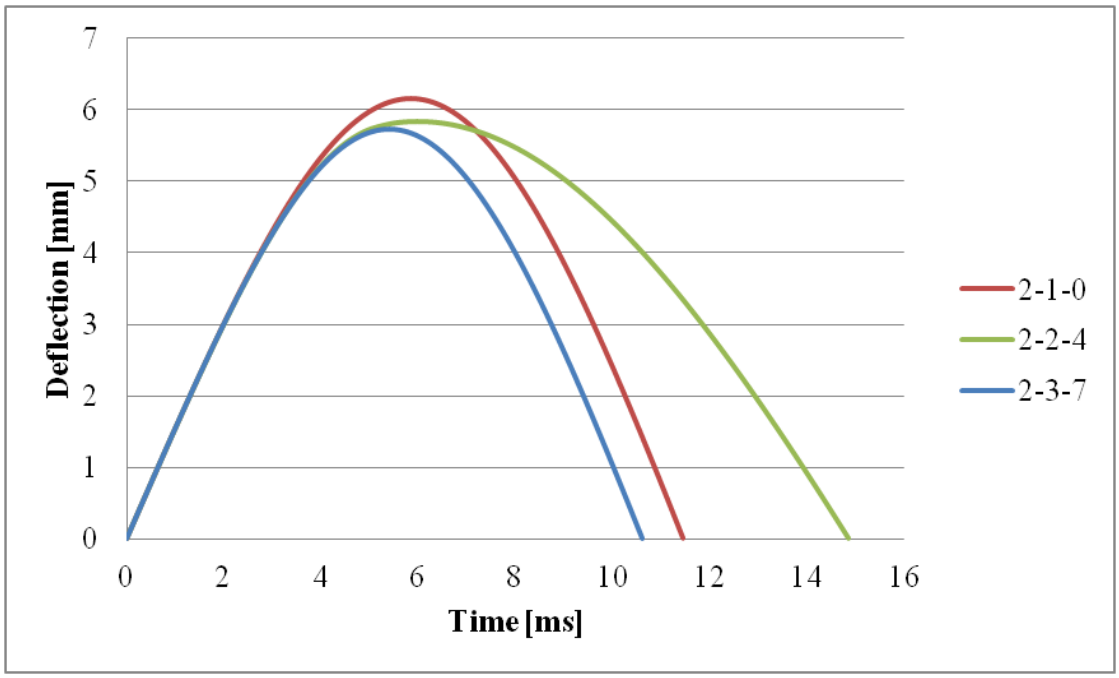

Figure 6.12: Deflection versus time for the batch two samples with 100 V current pulse

Plotting the force versus deflection of the first coordinated impact-current pulse tests on the batch two samples verifies the trends already discussed and is shown in Figure 6.13. What's most apparent from the graph is the difference between sample 2-1-0 and the two samples with buckypaper material. The lower the force far any given deflection on the sample shows that behaved less stiff than samples 2-2-4 and 2-3-7.

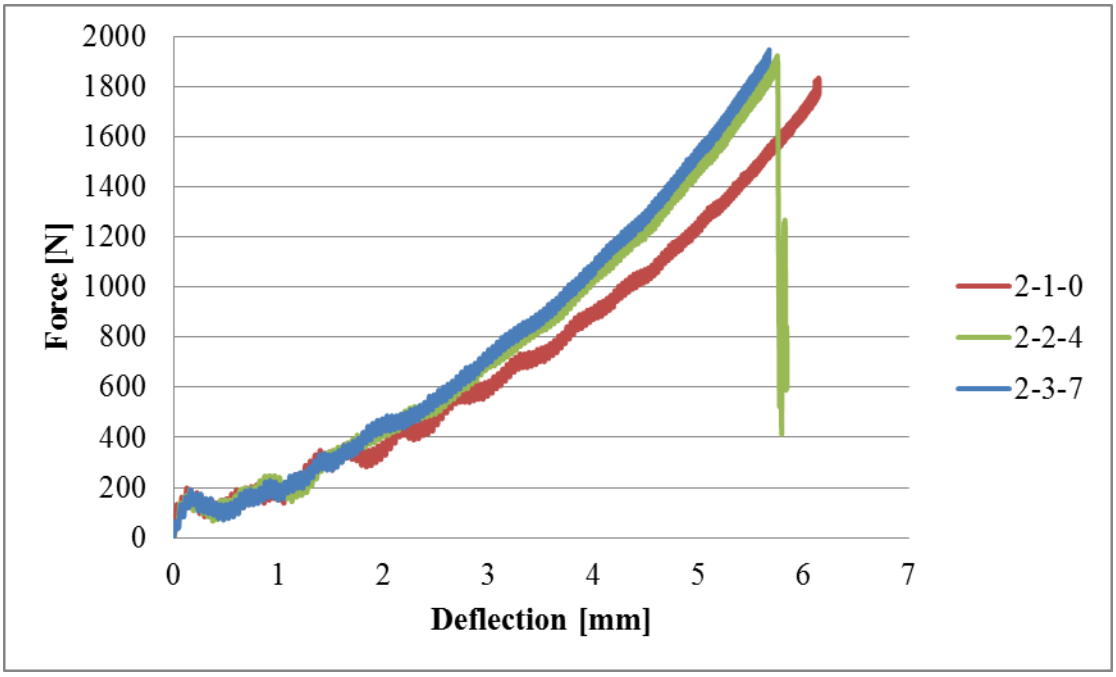

Figure 6.13: Force versus deflection for the batch two samples with 100 V current pulse

Sample 2-1-0 underwent two coordinated tests and experienced visible damage on the second one. The same three plots shown previously for all samples on their first tests were again used in comparing these two impact events. The force versus time, deflection versus time, and force versus deflection plots are shown in Figure 6.14, Figure 6.15, and Figure 6.16 respectively. It can be seen that in the second test the sample fractured at approximately 4.2 milliseconds with a load just above 1500 N. When comparing the two tests on the force versus deflection plot it is interesting exactly how close the relationship remained the same prior to fracture which is probably a good indication that very little internal damage occurred during that first test.

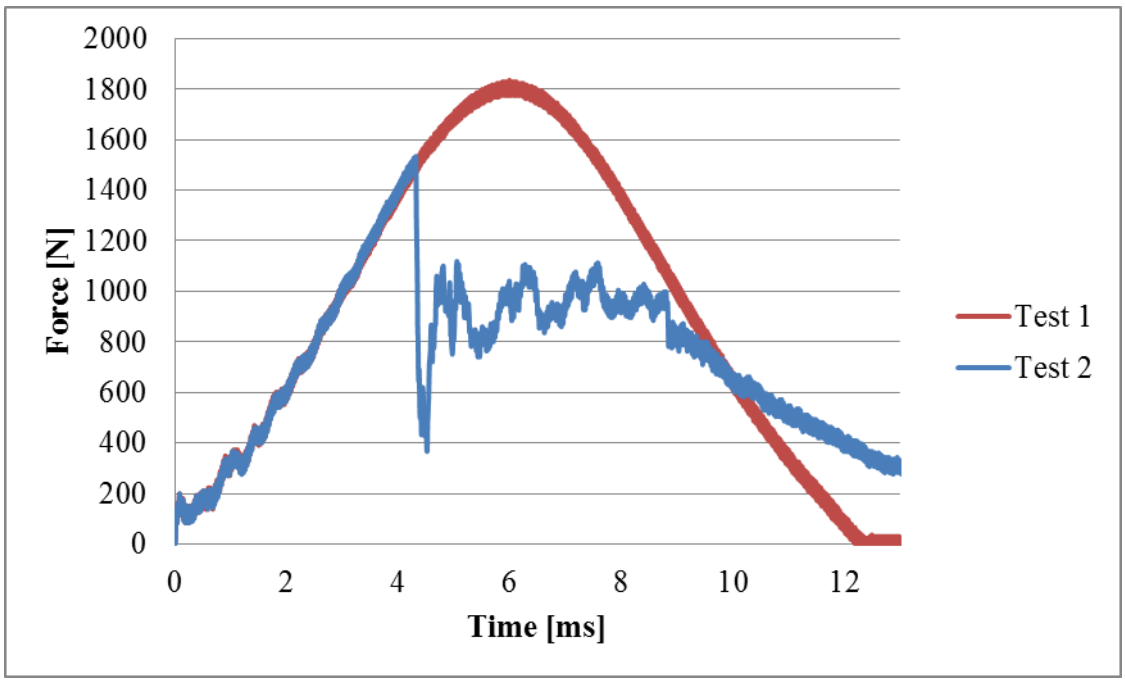

Figure 6.14: Force versus time for the two tests of sample 2-1-0

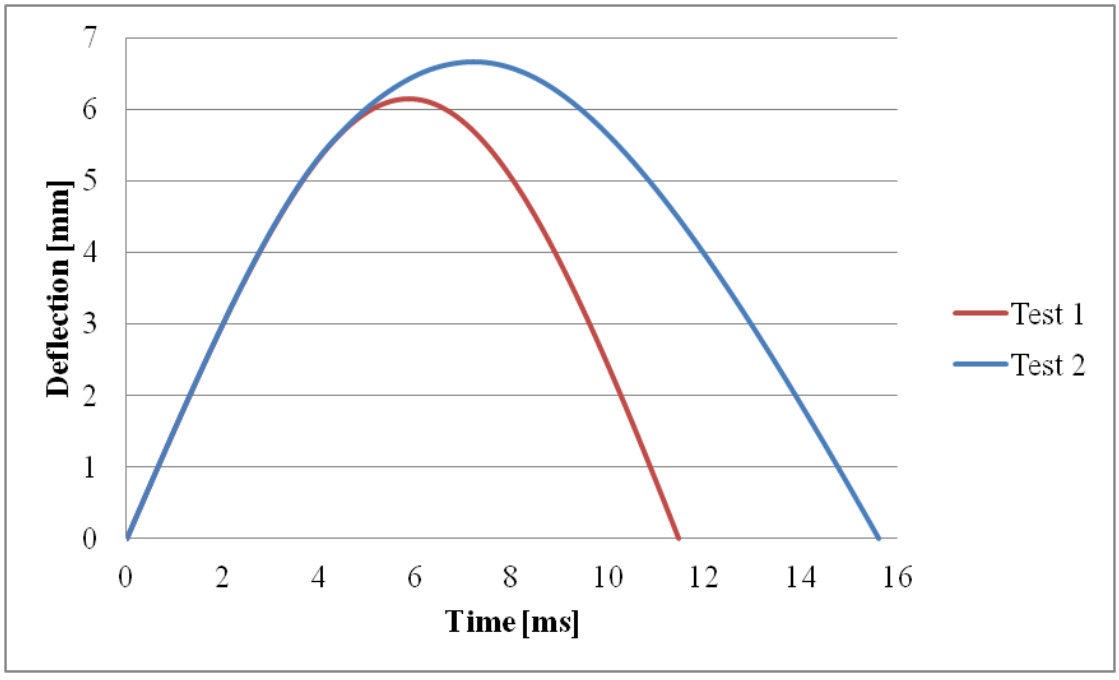

Figure 6.15: Force versus time for the two tests of sample 2-1-0

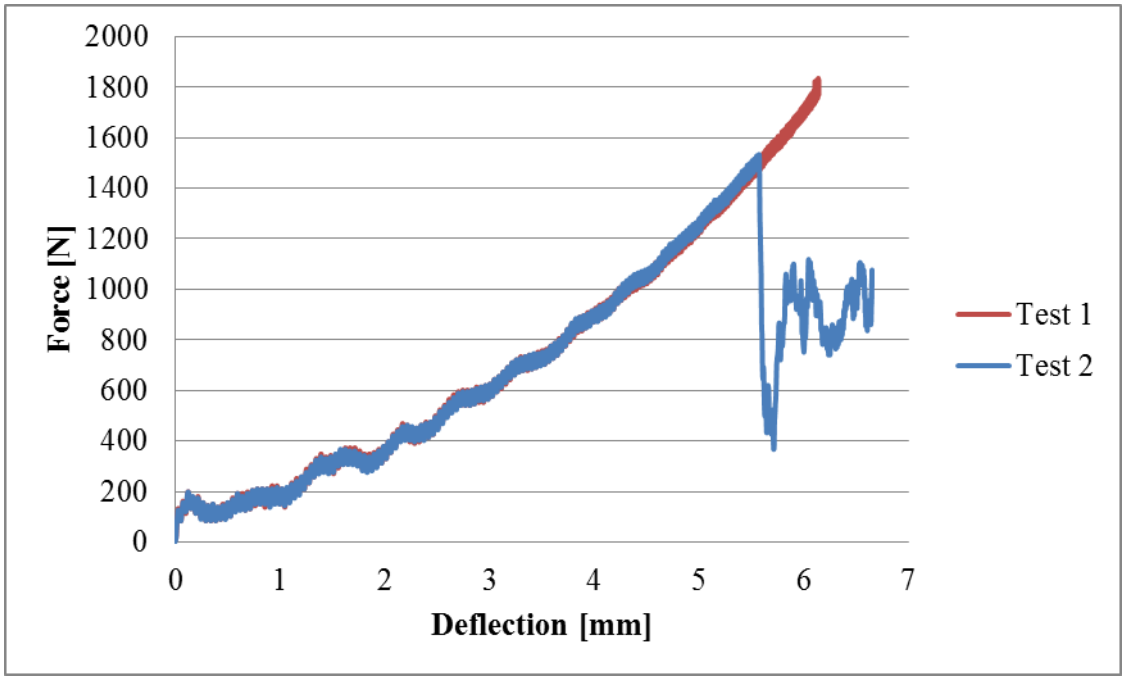

Figure 6.16: Force versus deflection for the two tests of sample 2-1-0

Much like sample 2-1-0, sample 2-3-7 experienced multiple coordinated impact-current pulse tests before visible damage appeared. The force versus time, deflection versus time, and force versus deflection plots for the four tests on sample 2-3-7 are shown in Figure 6.17, Figure 6.18, and Figure 6.19 respectively. From these plots a trend of how the sample reacted to each test can be seen. All three graphs show that for the first three tests sample 2-3-7 behaved nearly identically to the previous test. This includes force and deflection magnitudes as well timing and the relationship between the two. In the fourth test the sample fractured in a similar fashion to what has been shown for all damaged samples. This includes a sharp force decease at the time of the damage as well as prolonged deflection duration. The force versus deflection plot also show that the fourth test was very similar to the three previous ones and that the load experienced before damage was approximately 1800 N which was close to the maximum loads of 2000 N on

the other three tests. Both of these trends show that, like sample 2-1-0, sample 2-3-7 most likely did not experience much internal damage during the first three coordinated tests and fractured in a large part due to the damage done in the fourth test.

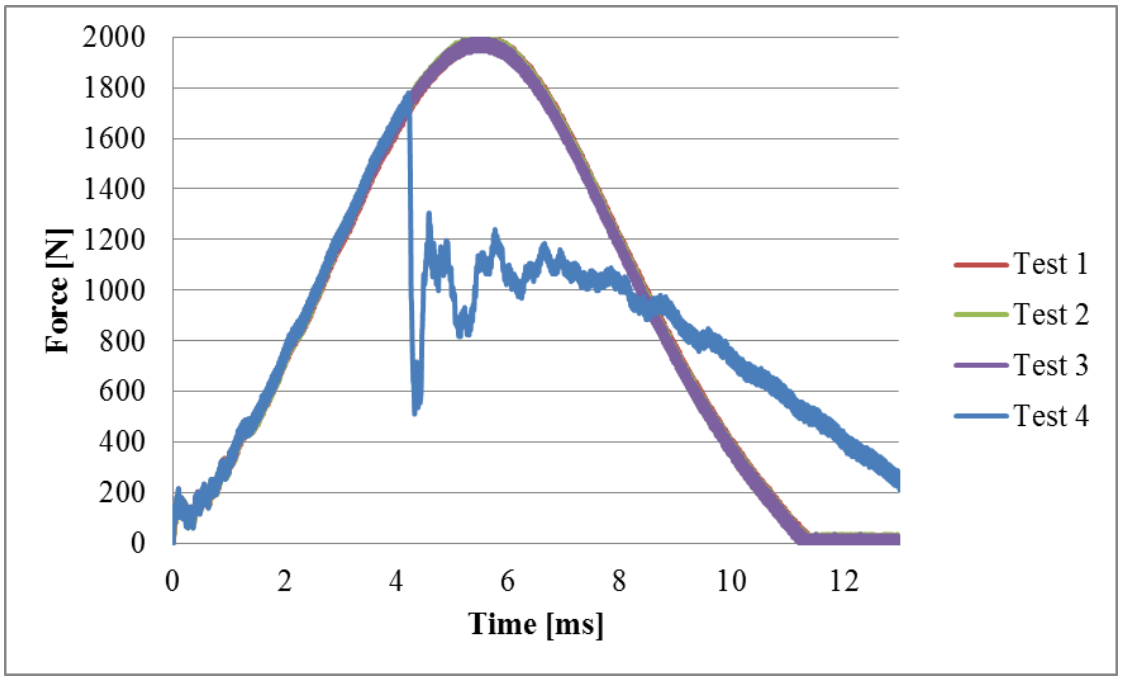

Figure 6.17: Force versus deflection for the four tests of sample 2-3-7

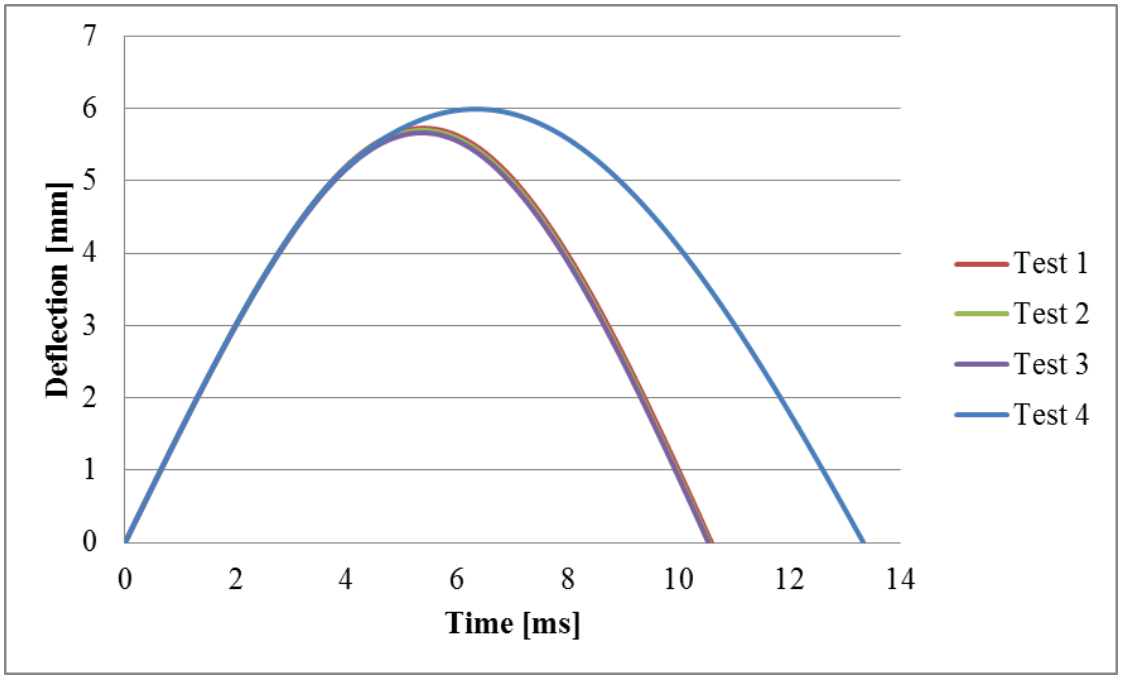

Figure 6.18: Deflection versus time for the four tests of sample 2-3-7

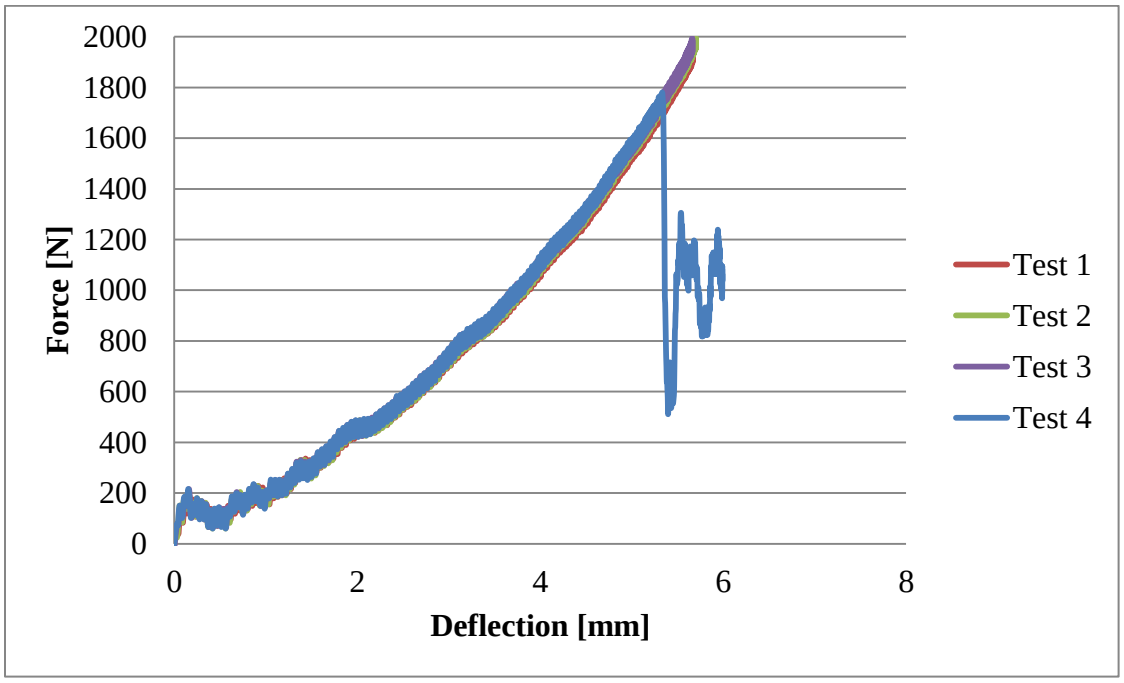

Figure 6.19: Force versus deflection for the four tests of sample 2-3-7

Tabulating and comparing the data on all the tests performed on the batch two samples allows for some conclusions to be drawn. Table 6.2 consists of all of the impact data including the maximum load and impact velocity. Table 6.3 includes the current pulse data for all the tests including the maximum current and current at peak load. Both tables show the damage that occurred during the tests with Table 6.2 having impact damage and Table 6.3 containing any burning that existed. It can be seen that the addition of the buckypaper layers increased the maximum impact load that went from 1834.4 N for sample 2-1-0 with no buckypaper to 2007.6 N (on first impact) for sample 2-3-7 with seven buckypaper layers. This is approximately a 9.4% increase in the peak load.

Table 6.2: Combined data on impacts of all batch two samples

Sample	Test #	Electrical	Drop Mass [kg]	Drop Height [cm]	Velocity [m/s]	Impact Energy [J]	Absorbed Energy [J]	Peak Load [N]	Peak Current [A]	Damage
2-1-0	1	100 V	3.5	11.1	1.4826	3.8469	4.4490	1834.4	476.7	No Damage
	2	100 V	3.5	11.1	1.4823	3.8453	3.5265	1533.7	294.9	Line Crack
2-2-4	1	100 V	3.5	11.1	1.4799	3.8327	4.3607	1923.4	291.5	Line Crack
2-3-7	1	100 V	3.5	11.1	1.4833	3.8504	4.4533	2007.6	497.4	No Damage
	2	100 V	3.5	11.1	1.4818	3.8425	4.4516	2002.8	502.5	No Damage
	3	100 V	3.5	11.1	1.4773	3.8190	4.4220	1999.0	515.1	No Damage
	4	100 V	3.5	11.1	1.4876	3.8728	3.8329	1780.3	423.0	Line Crack

Table 6.3: Current pulse data for the batch two 100 V coordinated tests

Sample	Test #	Maximum Current [A]	Current at Peak Load [A]	Voltage at Peak Load [V]	Resistance at peak load [Ω]	Electrical Damage
2-1-0	1	476.7	472.4	20.39	0.0432	No Burning
	2	294.9	293.1	62.42	0.2130	Heavily Burnt
2-2-4	1	291.5	231.8	66.73	0.2879	Lightly Burnt
2-3-7	1	497.4	472.3	10.45	0.0221	No Burning
	2	502.5	475.1	10.23	0.0215	No Burning
	3	515.1	487.0	10.57	0.0217	No Burning
	4	423.0	392.9	30.49	0.0776	Lightly Burnt

Moreover, the batch two samples which underwent coordinated impact-current pulse testing at a voltage level of 100 V showed some increased impact characteristics from the non-electrified batch one samples. Electrified samples 2-1-0 and 2-3-7 withstood their first impacts with peak load that were considerably higher than those at which non-electrified samples 1-1-0 and 1-3-7 sailed. Sample 2-1-0 exhibited a 23% increase in the peak load as compared to sample 1-1-0 and sample 2-3-7 exhibited a 20.6% increase in its peak load compared to the non-electrified sample 1-3-7. At the same time, electrified sample 2-2-4 which broke on the first impact, had a higher peak load than any of the broken samples in batch one. In the repeated impact tests non-electrified sample 1-2-4 was still able to withstand more impacts at five than any of the batch two samples, with electrified sample 2-3-7 coming the closest with four impacts.

From Table 6.2 and Table 6.3 it can also be seen that both the electrical and impact properties of samples 2-1-0 and 2-3-7 that were not damaged during their first impacts were fairly consistent. These included impact velocities, energy to maximum load, maximum current, and current at peak load. For the tests during which substantial damage to the sample occurred several trends stood out. These included a large voltage at

the peak load and for all three of the batch two samples, burning in the edges which had been in contact with the copper electrodes.

6.4.3 160 Analog Voltage Coordinated Impact Results

To further understand the elecro-mechanical coupling behavior of the carbon fiber/buckypaper composite materials the batch three samples were tested with a coordinated current pulse of 160 analog volts. The same impact energy and carriage drop height were used as well as the delay time a coordination shown in the previous two sections. The force versus time diagram for the three batch three samples is shown in Figure 6.20. The first sample tested was sample 3-1-0 with no buckypaper layers Due to a trigger issue with the current pulse generator it was impacted with no current load applied. As can be seen from the figure the sample was damaged at approximately two milliseconds with a force of 600 N unlike all of the previous samples though, sample 3-1-0 did not completely fracture and continued to resist larger forces after the damage. When the sample was removed from the fixture it was found that the damage showed on the back surface with a crack along the whole length of the sample but the front surface remained undamaged. A picture of both the front and back of samples 3-1-0 is shown in Figure 6.21.

After sample 3-1-0 was tested the current pulse generator was checked to ensure that the trigger function would properly work for the remaining two samples. Once assured that it would, sample 3-2-4 with four buckypaper layers was tested. As is shown in Figure 6.20 the same partial damage scenario that occurred for sample 3-1-0 repeated

itself for 3-2-4 even though 3-2-4 was under a current load and 3-1-0 was not. A small difference in the behavior is shown in the figure with sample 3-2-4 holding a slightly higher load before fracture. The last sample tested was sample 3-3-7 with seven layers of buckypaper and much like samples 3-1-0 and 3-2-4, sample 3-3-7 was damaged on the first test and it only exhibited damage on its upper surface.

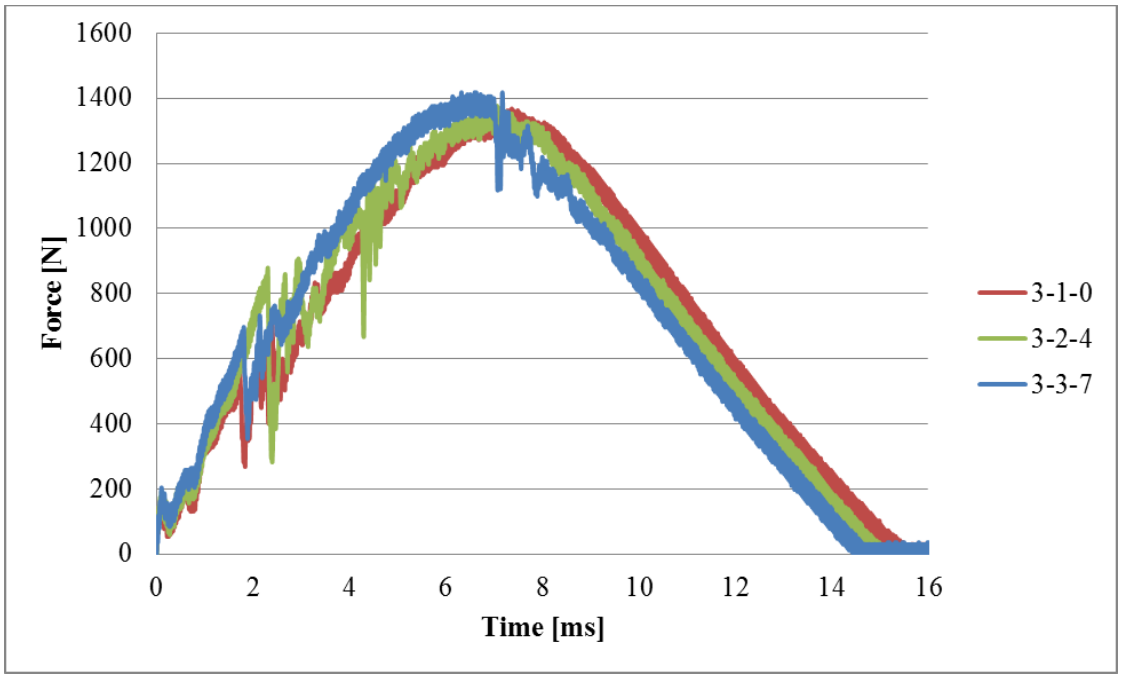

Figure 6.20: Force versus time for the batch three samples

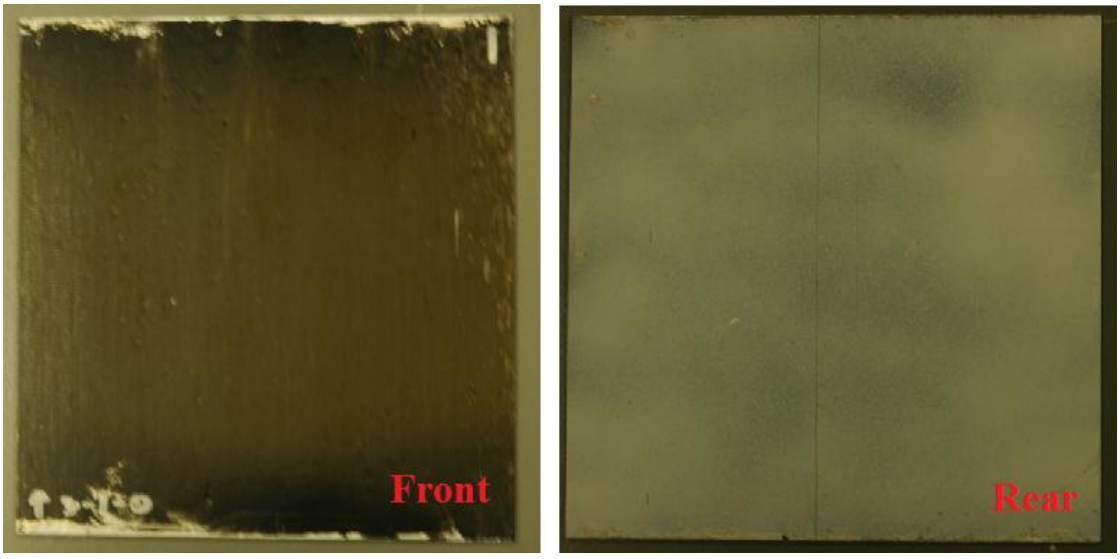

Figure 6.21: Sample 3-1-0 after impact event with damage showing on the back surface

Comparing the deflection versus time plot of the three batch three samples, which is shown in Figure 6.22, highlights one interesting trend. That is that though all three samples exhibited the same damage type with a crack on the back surface and no apparent damage on the front surface their impact durations and deflection magnitudes were different. The results show that the greater the number of buckypaper layers the less deflection and shorter impact time correlating to a stiffer material. This was also seen in the comparisons of the other two batches but not as clearly because both had samples that were completely fractured.

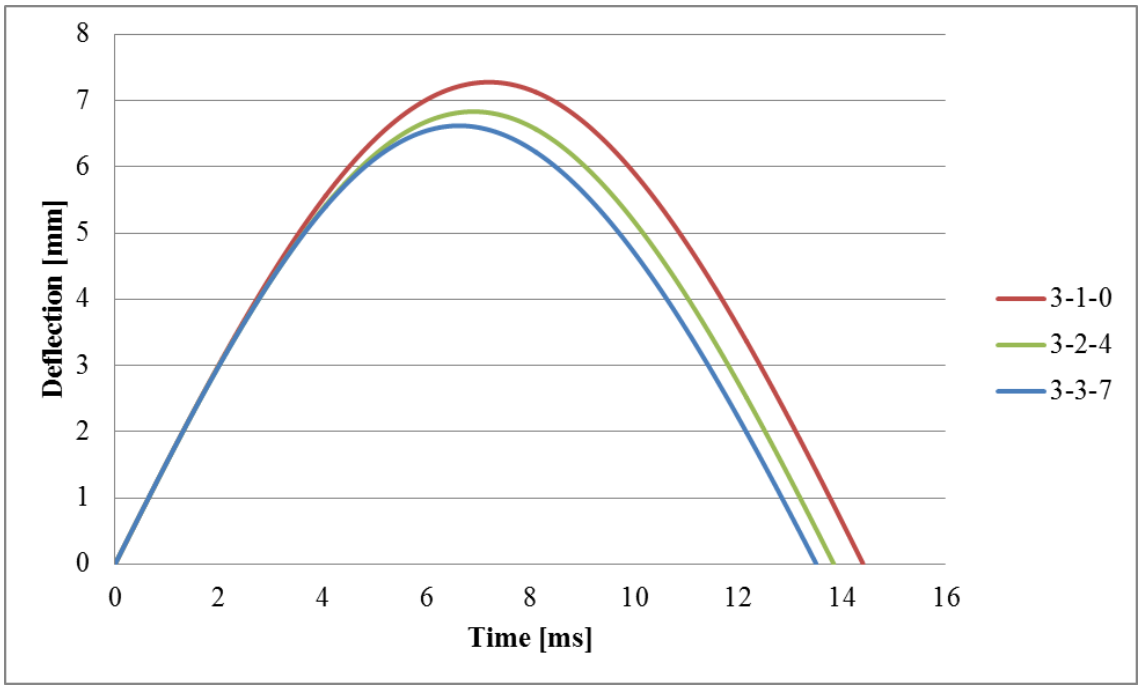

Figure 6.22: Deflection versus time for the batch three samples

The force versus deflection trend for the three samples shows more of the same trend seen in the above figure. As can be seen in Figure 6.23, sample 3-1-0 experienced the lowest force per deflection with sample 3-2-4 being in the middle and 3-3-7 having the greatest slope. It is also more apparent in this graph than the force versus time one that sample 3-3-7 withheld a slightly larger force than 3-1-0 did.

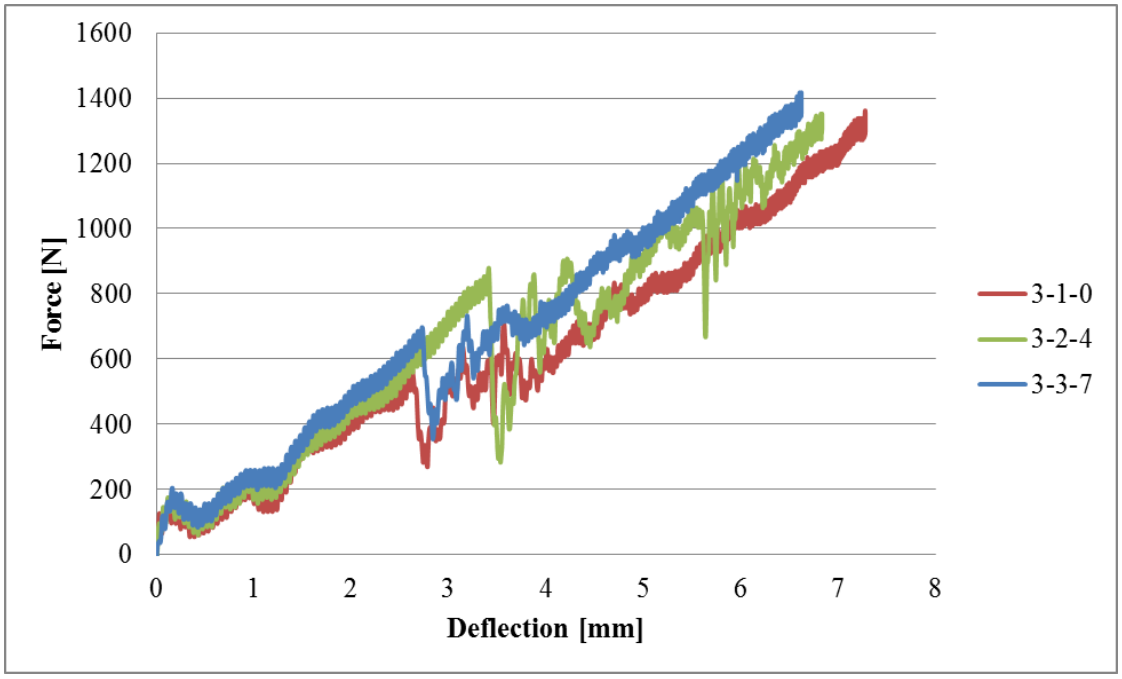

Figure 6.23: Force versus deflection for the batch three samples

The impact and electrical properties for the three samples are shown in Table 6.4 and Table 6.5 respectively. Due to the fact that sample 3-1-0 did not experience a current pulse during impact its results remain zero but from the other two samples it can be seen that sample 3-3-7 burnt and had a much larger voltage at the peak load when compared to sample 3-2-4. From this burning it is shown that the maximum current is much lower than was found for sample 3-2-4 and would be expected. The impact load data shows that the impact events on all three samples were uniform and there were no abnormalities with energies or impact velocities. Moreover, it can be seen that the addition of buckypaper layers increased the peak load. This trend was observed for all three batches. It is also worth noting that the peak impact loads in the batch three samples were lower than in the batch one and batch two samples. This could be due to manufacturing issues.

Table 6.4: Combined data on impacts of all batch three samples

Sample	Test #	Electrical	Drop Mass [kg]	Drop Height [cm]	Velocity [m/s]	Impact Energy [J]	Absorbed Energy [J]	Peak Load [N]	Peak Current [A]	Damage
3-1-0	1	No Pulse	3.5	11.1	1.4796	3.8312	4.4934	1367.9	N/A	Line Crack
3-2-4	1	160 V	3.5	11.1	1.4808	3.8375	4.4784	1376.4	1002.9	Line Crack
3-3-7	1	160 V	3.5	11.1	1.4862	3.8652	4.4679	1417.6	754.9	Line Crack

Table 6.5: Current pulse data for batch three coordinated tests

Sample	Test #	Maximum Current [A]	Current at Peak Load [A]	Voltage at Peak Load [V]	Resistance at peak load [Ω]	Electrical Damage
3-1-0	1	0	0	0	0	No Burning
3-2-4	1	1002.9	561.6	11.88	0.0212	No Burning
3-3-7	1	754.9	491.0	42.43	0.0864	Heavily Burnt

6.5 Summary of the Impact-Current Pulse Experiments

The results of the coordinated impact-current pulse experiments led to some conclusions about the impact response of non-electrified and electrified carbon fiber/buckypaper composite materials. The impact energy and velocity chosen for the impact setup portions of the test proved to be close to the V_{50} mark discussed earlier as some samples fractured on their first test and other took as many as five impacts to break. When comparing pure carbon fiber samples to those with buckypaper it was shown that for all samples, with the exception of sample 2-2-4, the addition of buckypaper did lead to an increase in impact resistance. This trend was not sensitive to the coordinated current level and was shown in the batch one samples which had no electrification as well as batch three which had a current load of up to 1000 A.

While the addition of buckypaper layers did increase impact resistance of the composite samples the results of the impact tests on the electrified samples are partially inconclusive. While batch two samples showed considerable increases in the impact resistance (up to 23%) compared to the non-electrified samples of batch one, there was no such trend observed for the samples from batch three, which all failed at much lower peak loads compared to the batch one and batch two samples.

CHAPTER 7

SUMMARY AND RECOMMENDATIONS

7.1 Summary

In this work the electrical and impact properties of carbon fiber reinforced composite materials with varying amount of carbon nanotube buckypaper layers were analyzed and compared. These assessments included the investigation of electrical resistances through different planes as well as in the fiber directions. They also included the study of the different materials responses to large magnitude, short duration current pulses. Lastly, coordinated impact-current pulse experiments were performed in order to understand the potential electro-mechanical coupling effects in carbon fiber polymer matrix composites with embedded layers of carbon nanotube buckypaper layers.

From the electrical resistance testing experiments several important results were found. These include the recognition of the variations in electrical properties that can occur in identically oriented carbon fiber materials with the same number of buckypaper layers as was shown in the four probe electrical resistance experiments. This variation was attribute to the manufacturing process. Also from these tests it was found that electrical resistance in all planes decreases with the addition of four layers of buckypaper to pure carbon fiber samples. An additional but less substantial resistance decrease was found with the addition of three more layers of buckypaper to make seven buckypaper layer samples. This conclusion can be beneficial in optimizing the number of buckypaper layers used for composite materials with the intent of reducing their electrical resistance.

The current pulse experiments further reinforced the results of the four probe multi-plane electrical resistance tests. The increased current pulses on the pure carbon fiber, four buckypaper layer, and seven buckypaper layer samples showed a comparative relationship in the decrease of electrical resistance by sample type. The result of this was a higher resistance at maximum current amplitude for the pure carbon fibers and lower resistances in the four and seven buckypaper layer samples with little resistance difference between them. Also found from the current pulse experiments was the trend that the electrical resistance variations between batches was all but eliminated at high current amplitudes. This sensitivity reduction in manufacturing variations at higher current levels could mean that no additional cost would need to be entered into quality control of the production of carbon fiber/buckypaper materials which are to be used for those purposes.

Subjecting composite samples to electric current pulses during impact testing led to an increase in the impact resistance with an increase in the peak impact loads up to 23% in the batch two samples, but electrified batch three samples exhibited much lower peak loads compared to the non-electrified samples of batch one, thus, leaving the results inconclusive. At the same time, it was found though that the number of buckypaper layers in a sample did lead to an increased impact resistance. From the coordinated tests it was also observed that the presence of buckypaper layers increased the stiffness of the samples which in turn reduced their deflection magnitudes and time as well as increased their load carrying capabilities.

7.2 Recommendations

To further investigate the electrical and impact properties of carbon fiber reinforced polymer composites with the addition of carbon nanotube buckypaper layers several recommendations can be made. In terms of expanding upon the resistivity results of the carbon fiber samples with the addition of buckypaper it would be beneficial to determine resistance trends of the materials as different number of buckypaper layers are added beyond the four and seven layer samples tested in this work. Also, to improve upon the two probe electrical experimental results a means of further reducing contact resistance between the copper electrodes should be investigated with the hopes that the decreased resistance would also lead to a decreased chance of burning the composite samples. Another recommendation is to create an automated means of coordinating the impact-current pulse experiment in order to eliminate the variations found between drop tests. Moreover, additional testing with an increased number of samples is required to determine the effect of the pulsed electric current on the impact resistance. Furthermore, batch to batch variability in the composite samples has to be minimized to enable proper interpretation of the experimental results.

APPENDIX: FOUR PROBE RESULTS

A.1 Narrow Sensing Electrode Results

Table A1: Sample 1-1-0 resistance values for narrow sensing electrodes

Sample 1-1-0						
Voltage (mA)	**Top [Ω]**		**Bottom [Ω]**		**Oblique [Ω]**	
	Resistance	**Std dev**	**Resistance**	**Std dev**	**Resistance**	**Std dev**
10	0.93021	0.00092	0.77959	0.00188	6.75832	0.00902
30	0.88589	0.00137	0.74071	0.00128	6.32743	0.00692
50	0.87736	0.00170	0.72870	0.00192	6.15131	0.01183
70	0.86472	0.00112	0.72339	0.00532	6.10631	0.05298
90	0.85721	0.00107	0.72327	0.00536	6.01797	0.02970
110	0.84990	0.00107	0.67830	0.00665	5.83042	0.02137

Table A2: Sample 1-2-4 resistance values for narrow sensing electrodes

Sample 1-2-4						
Voltage (mA)	**Top [Ω]**		**Bottom [Ω]**		**Oblique [Ω]**	
	Resistance	**Std dev**	**Resistance**	**Std dev**	**Resistance**	**Std dev**
10	0.10045	0.00079	0.09866	0.00049	0.45080	0.00070
30	0.09796	0.00018	0.09560	0.00013	0.43560	0.00051
50	0.09767	0.00011	0.09507	0.00010	0.43455	0.00040
70	0.09640	0.00004	0.09342	0.00013	0.43409	0.00071
90	0.09606	0.00008	0.09269	0.00004	0.43645	0.00089
110	0.09583	0.00003	0.09234	0.00011	0.43515	0.00039

Table A3: Sample 1-3-7 resistance values for narrow sensing electrodes

Sample 1-3-7						
Voltage (mA)	**Top [Ω]**		**Bottom [Ω]**		**Oblique [Ω]**	
	Resistance	**Std dev**	**Resistance**	**Std dev**	**Resistance**	**Std dev**
10	0.01498	0.00046	0.04821	0.00050	0.04033	0.00054
30	0.01390	0.00019	0.04560	0.00018	0.03740	0.00016
50	0.01341	0.00009	0.04490	0.00010	0.03715	0.00011
70	0.01330	0.00007	0.04549	0.00007	0.03748	0.00006
90	0.01316	0.00004	0.04528	0.00006	0.03744	0.00005
110	0.01316	0.00006	0.04537	0.00003	0.03749	0.00027

Table A4: Sample 2-1-0 resistance values for narrow sensing electrodes

Sample 2-1-0						
Voltage (mA)	**Top [Ω]**		**Bottom [Ω]**		**Oblique [Ω]**	
	Resistance	**Std dev**	**Resistance**	**Std dev**	**Resistance**	**Std dev**
10	0.19749	0.00046	0.47883	0.00065	0.69476	0.00064
30	0.19191	0.00035	0.44957	0.00029	0.66782	0.00024
50	0.19142	0.00016	0.44435	0.00027	0.66590	0.00020
70	0.19117	0.00016	0.43857	0.00026	0.66285	0.00015
90	0.19110	0.00012	0.43513	0.00023	0.66130	0.00011
110	0.19068	0.00016	0.43128	0.00018	0.65983	0.00018

Table A5: Sample 2-2-4 resistance values for narrow sensing electrodes

Sample 2-2-4						
Voltage (mA)	**Top [Ω]**		**Bottom [Ω]**		**Oblique [Ω]**	
	Resistance	**Std dev**	**Resistance**	**Std dev**	**Resistance**	**Std dev**
10	0.04420	0.00047	0.07124	0.00039	0.10290	0.00065
30	0.04090	0.00023	0.06728	0.00023	0.09986	0.00021
50	0.04067	0.00006	0.06769	0.00011	0.09919	0.00012
70	0.04121	0.00005	0.06744	0.00012	0.09817	0.00012
90	0.04099	0.00005	0.06704	0.00007	0.09770	0.00008
110	0.04078	0.00004	0.06652	0.00003	0.09753	0.00005

Table A6: Sample 2-3-7 resistance values for narrow sensing electrodes

Sample 2-3-7						
Voltage (mA)	**Top [Ω]**		**Bottom [Ω]**		**Oblique [Ω]**	
	Resistance	**Std dev**	**Resistance**	**Std dev**	**Resistance**	**Std dev**
10	0.02413	0.00042	0.02978	0.00064	0.03979	0.00059
30	0.02202	0.00016	0.02724	0.00018	0.03657	0.00016
50	0.02153	0.00007	0.02678	0.00010	0.03646	0.00009
70	0.02150	0.00005	0.02657	0.00008	0.03663	0.00007
90	0.02133	0.00003	0.02643	0.00007	0.03665	0.00003
110	0.02124	0.00006	0.02678	0.00004	0.03651	0.00003

Table A7: Sample 3-1-0 resistance values for narrow sensing electrodes

Sample 3-1-0						
Voltage (mA)	**Top [Ω]**		**Bottom [Ω]**		**Oblique [Ω]**	
	Resistance	**Std dev**	**Resistance**	**Std dev**	**Resistance**	**Std dev**
10	0.98850	0.00106	1.07377	0.00133	18.07252	0.01182
30	0.94907	0.00038	1.02624	0.00045	17.45557	0.00390
50	0.94121	0.00088	1.01359	0.00068	17.44092	0.00354
70	0.93265	0.00035	1.01164	0.00431	17.38336	0.00138
90	0.92586	0.00020	1.01459	0.00386	17.32696	0.00251
110	0.91803	0.00028	1.01560	0.00314	17.27502	0.00404

Table A8: Sample 3-2-4 resistance values for narrow sensing electrodes

Sample 3-2-4						
Voltage (mA)	**Top [Ω]**		**Bottom [Ω]**		**Oblique [Ω]**	
	Resistance	**Std dev**	**Resistance**	**Std dev**	**Resistance**	**Std dev**
10	0.10881	0.00048	0.15374	0.00043	1.08110	0.00086
30	0.10523	0.00023	0.14900	0.00023	1.04912	0.00031
50	0.10352	0.00017	0.14800	0.00009	1.04844	0.00016
70	0.10253	0.00015	0.14718	0.00007	1.04687	0.00017
90	0.10155	0.00019	0.14709	0.00008	1.04615	0.00015
110	0.10116	0.00015	0.14666	0.00005	1.04529	0.00010

Table A9: Sample 3-3-7 resistance values for narrow sensing electrodes

Sample 3-3-7						
Voltage (mA)	Top [Ω]		Bottom [Ω]		Oblique [Ω]	
	Resistance	Std dev	Resistance	Std dev	Resistance	Std dev
10	0.12445	0.00045	0.11095	0.00039	0.41322	0.00055
30	0.12069	0.00016	0.10801	0.00013	0.39822	0.00017
50	0.11995	0.00007	0.10722	0.00009	0.39736	0.00008
70	0.11911	0.00005	0.10658	0.00009	0.39683	0.00009
90	0.11888	0.00005	0.10646	0.00007	0.39716	0.00005
110	0.11895	0.00004	0.10600	0.00005	0.39671	0.00003

A.2 Wide Sensing Electrode Results

Table A10: Sample 1-1-0 resistance values for wide sensing electrodes

Sample 1-1-0						
Voltage (mA)	Top [Ω]		Bottom [Ω]		Oblique [Ω]	
	Resistance	Std dev	Resistance	Std dev	Resistance	Std dev
10	0.79709	0.00321	1.55335	0.00510	4.12516	0.00685
30	0.77415	0.00152	1.34666	0.00672	3.85818	0.00639
50	0.75955	0.00627	1.27631	0.00349	3.76745	0.00906
70	0.74527	0.00112	1.24210	0.01297	3.75745	0.03331
90	0.74165	0.00146	1.21883	0.00319	3.73684	0.02350
110	0.73825	0.00200	1.21316	0.00709	3.61805	0.00999

Table A11: Sample 1-2-4 resistance values for wide sensing electrodes

Sample 1-2-4						
Voltage (mA)	Top [Ω]		Bottom [Ω]		Oblique [Ω]	
	Resistance	Std dev	Resistance	Std dev	Resistance	Std dev
10	0.23990	0.00062	0.27234	0.00058	0.60022	0.00104
30	0.23264	0.00012	0.25836	0.00039	0.56660	0.00016
50	0.23139	0.00009	0.25770	0.00032	0.56159	0.00080
70	0.23104	0.00008	0.25590	0.00024	0.55940	0.00007
90	0.23053	0.00005	0.25535	0.00023	0.55878	0.00005
110	0.23041	0.00005	0.25452	0.00023	0.55856	0.00008

Table A12: Sample 1-3-7 resistance values for wide sensing electrodes

Sample 1-3-7						
Voltage (mA)	**Top [Ω]**		**Bottom [Ω]**		**Oblique [Ω]**	
	Resistance	**Std dev**	**Resistance**	**Std dev**	**Resistance**	**Std dev**
10	0.08285	0.00044	0.06650	0.00027	0.08763	0.00060
30	0.07860	0.00012	0.06266	0.00017	0.08411	0.00018
50	0.07937	0.00008	0.06326	0.00010	0.08419	0.00010
70	0.07910	0.00004	0.06273	0.00008	0.08395	0.00010
90	0.07886	0.00008	0.06267	0.00004	0.08364	0.00004
110	0.07853	0.00004	0.06249	0.00002	0.08340	0.00003

Table A13: Sample 2-1-0 resistance values for wide sensing electrodes

Sample 2-1-0						
Voltage (mA)	**Top [Ω]**		**Bottom [Ω]**		**Oblique [Ω]**	
	Resistance	**Std dev**	**Resistance**	**Std dev**	**Resistance**	**Std dev**
10	0.81931	0.00124	0.76343	0.00070	1.09914	0.00065
30	0.78300	0.00106	0.73379	0.00059	1.06070	0.00030
50	0.76992	0.00088	0.72779	0.00048	1.05648	0.00037
70	0.75859	0.00068	0.72120	0.00030	1.05252	0.00022
90	0.75060	0.00047	0.71772	0.00026	1.04972	0.00028
110	0.74295	0.00059	0.71362	0.00031	1.04675	0.00035

Table A14: Sample 2-2-4 resistance values for wide sensing electrodes

Sample 2-2-4						
Voltage (mA)	**Top [Ω]**		**Bottom [Ω]**		**Oblique [Ω]**	
	Resistance	**Std dev**	**Resistance**	**Std dev**	**Resistance**	**Std dev**
10	0.11240	0.00045	0.09951	0.00047	0.14663	0.00047
30	0.10919	0.00011	0.09640	0.00014	0.14188	0.00022
50	0.10857	0.00009	0.09632	0.00009	0.14140	0.00012
70	0.10766	0.00007	0.09501	0.00007	0.14098	0.00007
90	0.10760	0.00007	0.09476	0.00007	0.14094	0.00006
110	0.10707	0.00006	0.09451	0.00003	0.14078	0.00006

Table A15: Sample 2-3-7 resistance values for wide sensing electrodes

Sample 2-3-7						
Voltage (mA)	**Top [Ω]**		**Bottom [Ω]**		**Oblique [Ω]**	
	Resistance	**Std dev**	**Resistance**	**Std dev**	**Resistance**	**Std dev**
10	0.05290	0.00035	0.08724	0.00048	0.05736	0.00045
30	0.05007	0.00010	0.08334	0.00016	0.05471	0.00017
50	0.04983	0.00009	0.08330	0.00006	0.05509	0.00016
70	0.04998	0.00007	0.08272	0.00008	0.05468	0.00005
90	0.04975	0.00005	0.08230	0.00004	0.05475	0.00005
110	0.04972	0.00004	0.08174	0.00004	0.05442	0.00005

Table A16: Sample 3-1-0 resistance values for wide sensing electrodes

Sample 3-1-0						
Voltage (mA)	**Top [Ω]**		**Bottom [Ω]**		**Oblique [Ω]**	
	Resistance	**Std dev**	**Resistance**	**Std dev**	**Resistance**	**Std dev**
10	1.72431	0.00140	1.32650	0.00132	15.68973	0.00746
30	1.66819	0.00037	1.27775	0.00036	15.18064	0.00235
50	1.66645	0.00043	1.27396	0.00036	15.16484	0.00155
70	1.66240	0.00047	1.27741	0.00445	15.11891	0.00129
90	1.65973	0.00029	1.27530	0.00213	15.10116	0.00107
110	1.65619	0.00031	1.27043	0.00372	15.06130	0.00180

Table A17: Sample 3-2-4 resistance values for wide sensing electrodes

Sample 3-2-4						
Voltage (mA)	**Top [Ω]**		**Bottom [Ω]**		**Oblique [Ω]**	
	Resistance	**Std dev**	**Resistance**	**Std dev**	**Resistance**	**Std dev**
10	0.24115	0.00043	0.27880	0.00036	1.11131	0.00044
30	0.23400	0.00017	0.26657	0.00013	1.07587	0.00017
50	0.23268	0.00011	0.26651	0.00009	1.07457	0.00014
70	0.23231	0.00004	0.26514	0.00008	1.07207	0.00009
90	0.23231	0.00004	0.26533	0.00004	1.07176	0.00008
110	0.23193	0.00009	0.26476	0.00004	1.07086	0.00007

Table A18: Sample 3-2-4 resistance values for wide sensing electrodes

Sample 3-3-7						
Voltage (mA)	**Top [Ω]**		**Bottom [Ω]**		**Oblique [Ω]**	
	Resistance	**Std dev**	**Resistance**	**Std dev**	**Resistance**	**Std dev**
10	0.30987	0.00042	0.21972	0.00045	0.50208	0.00075
30	0.29557	0.00024	0.21353	0.00020	0.48143	0.00025
50	0.29540	0.00009	0.21239	0.00009	0.48078	0.00009
70	0.29385	0.00008	0.21233	0.00004	0.47969	0.00007
90	0.29397	0.00017	0.21178	0.00006	0.47940	0.00007
110	0.29367	0.00013	0.21195	0.00005	0.47900	0.00005

REFERENCES

Agilent Technologies. (2003, March). *"Agilent 34420A Nano Volt/Micro Ohm Meter User's Guide"* (Manual No. 34420-90001).

Agilent Technologies. (2004, March). *"USER'S GUIDE, Dynamic Measurement DC Source, Agilent Model 66312A, System DC Power Supply, Agilent 6611C, 6612C, 6613C, and 6614C"* (Manual No. 5962-8194).

Agilent Technologies. (2007, October). *"Agilent U2500A Series USB Simultaneous Sampling Multifunction Data Acquisition Devices"*.

Agilent Technologies. (2011, September). *"Agilent USB Modular Products".*

Andelidis N., Irving, P. (2007). *"Detection of impact damage in CFRp laminates by means of electrical potential techniques"*. Composites Science and Technology 67(2007), 594-604.

Angelidis, N., Wei, C., Irving, P. (2006). *"Respose to discussion of paper: The electrical resistance response of continuous carbon fibre composite laminates to mechanical strain".* Composites: Part A 37(2006), 1495-1499.

Ankara, A., Gokce Dara, B., Weisgerber, D. (2006). *"The Thermal Loading Response of CFRP Structures".* Journal of Thermoplastic Composite Materials 16 (2003), 317-331.

Anway, C., Day, A., Geis, J. (2010). *"Contact Resistance in Unidirectional Fiber Composite Materials as a Function of Force"*. SAMPE 2010.

Arby, J., Bochard, S., Chateauminois, A., Salvia, M., Giraud, G. (1998). *"In situ detection of damage in CFRP laminates by electrical resistance measurements".* Composites Science and Technology 59(1999), 925-935.

ASTM. (2006). "ASTM D 3763-06 Standard Test Method for High Speed Puncture Properties of Plastics Using Load and Displacement Sensors". ASTM International.

ASTM. (2007). "ASTM D 5728-07 Standard Test Method for Impact Resistance of Flat, Rigid Plastic Specimens by Means of a Falling Dart (Tup of Falling Mass)". ASTM International.

Axiom Test Equipment. (2011). *"Agilent/HP 6612C Power Supply, 20V, 2A, 40W"*.

Barakati, A., Zhupanska, O. (2011). *"Effects of Coupled Fields on the Mechanical Response of Electrically Conductive Composites"*. Procedia Engineering 10 (2011), 31-36.

Chung, D. (2000). *"Fibrous Composite Interfaces Studied by Electrical Resistance Measurement".* Advanced Engineering Materials 2(12).

Chung, D. (2010). "*Composite Materials: Science and Applications"*. London: Springer, 2010. Print.

Cotronics Corporation. (2008). *"DURALCO 120 500°F Electrically Conductive Adhesive"*.

Copper Development Association. (1997). *"Copper in Electrical Contacts"*. CDA Publication 23.

Deierling, P. (2010). "*Electrical and thermal behavior of IM7/977-3 Carbon fiber polymer matrix composites subjected to time-varying and steady electric currents*". Thesis. The University of Iowa. Print.

Demczyk, B.G., Wang, Y.M., Cumings, J., Hetman, M., Han, W., Zettl, A., and Ritchie, R.O. (2001). *"Direct mechanical measurement of the tensile strength and elastic modulus of multiwalled carbon nanotubes".* Materials Science and Engineering A334 (2002), 173-178.

Deo, R., Starnes, J., Holzwarth, R. (2001). *"Low-Cost Composite Materials and Structures for Aircraft Applications".* RTO-MP-069(II).

Ebbesen, T., Lezec, H., Hiura, H., Bennett, J., Ghaemi, H., Thio, T. (1996). *"Electrical conductivity of individual carbon nanotubes".* Nature 382 (1996), 54-56.

Ficher, J., Zhou, W., Vavro, J., Llaguno, M., Guthy, C., and Haggenmueller, R. (2002). *"Magnetically aligned single wall carbon nanotube films: Preferred orientation and anisotropic transport properties".* Journal of Applied Physics 93(4), 2157-2163.

Food and Agriculture Organization of the United Nations. (2003). *"Application of Natural Fibre Composites in the Development of Rural Societies".*

Fortress Stabilization Systems. (2011). "*Foundation Repair, Concrete Repair and Masonry Reinforcements, Bowed Basement Walls, Using Carbon Fiber Kevlar Technologies in Foundation, Concrete and Other Applications."*

Grimsley BW, Cano RJ, Johnston NJ, Loos AC, McMahon WM. (2010). "*Hybrid Composites for LH2 Fuel Tank Structure".* In: Proceedings of 33rd international SAMPE technical conference, November 4–8, Seattle, Washington, 2001.

Harris, P. (2009). *"Carbon Nanotube Science: Synthesis, properties and applications"*. New York, NY: Cambridge University Press. Print.

Hart, R. (2011). "*Characterization of Carbon Fiber Polymer Matrix Composites Subjected to Simultaneous Application of Electric Current Pulse and Low Velocity Impact*". Thesis. The University of Iowa. Print.

Hart, R., Deierling, P. (2011). *"Current Pulse Generator User Manual".*

Hexcel Corporation. (n.d.). *"Prepreg Technology".*

Hexcel Corporation. (2010). "*HexTow® Carbon Fiber, from Hexcel"*.

Hexcel Corporation. (2010). "*HexTow® IM7 Carbon Fiber, Product Data"*.

Hirano, Y., Katsumata, S., Iwahori, Y., and Todoroki, A. (2010). *"Artificial lightning testing on graphite/epoxy composite laminate".* Composites: Part A 41(2010), 1461-1470.

How Products are Made. (2011). *"How Carbon Fiber Is Made - Material, Making, Used, Processing, Parts, Components, Composition, Structure, Steps, Industry, Machine, Classification of Carbon Fibers, Raw Materials."*

Instron Corporation. (2004). *"Instron Dynatup Model 8200 Drop Weight Impact Testing Instrument: Operating Instructions"*. Serial number M14-14103-EN.

Iijima, S. (1991). *"Helical microtubules of graphitic carbon".* Nature 354 (1991), 56-58.

Iijima, S. (2002). *"Carbon nanotubes: past, present, and future".* Physica B 323 (2002), 1-5.

JCMA. (2011) "The Japan Carbon Fiber Manufacturers Association."

Jihua G. (2002) *"Single-walled carbon nanotube bucky paper/epoxy composites: molecular dynamics simulation and process development"*, FSU PHD Dissertation.

Jones, R. (2009). *"Mechanics of Composite Materials"*. Philadelphia, PA: Taylor & Francis. Print.

Koo, J., Pilato, L.A., Wissler, G., Lee, A., Abusafieh, A., and Weispfenning, J. (2004). *"Nanocomposites for carbon fiber reinforced polymer matrix composites".* AFRL contract number F49620-03-C-0093.

Lau, W. (1990). "*Pulsed Nd: YAG Laser Cutting of Carbon Fibre Composite Materials.*" CIRP Annals - Manufacturing Technology 39.1, 179-82. Print

LOCTITE. (2008, November). *"LOCTITE Hysol E-120HP Technical Data Sheet".* Web site: http://tds.loctite.com/tds5/docs/HYSAE-120HP-EN.PDF

McAndrew, J. (2009). *"Impact damage sensing in carbon fiber polymer-matrix composite plates via electrical resistance measurement".* Thesis. The University of Iowa. Print.

McCarvill, W., Strong, B. (2005). *"Epoxy Resin Formulation Made Simple: Case Studies".* Composites Manufacturing.

Morgan, P. (2005). *"Carbon Fibers and their Composites".* Philadelphia, PA: Taylor & Francis. Print.

Park, J., Hwang, T., Kim, H., Doh, Y. (2007). *"Experimental and numerical study of the electrical anisotropy in unidirectional carbon-fiber-reinforced polymer composites".* Smart Materials and structures 16 (2007), 57-66

Parkm J., Louis, J., Cheng, Q., Bao, J., Smithyman, J., Liang, R., Wang, B., Zhang, C., Brooks, J., Kramer, L., Franchasis, P., and Dorough, D. (2009). *"Electromagnetic interference shielding properties of carbon nanotube buckypaper composites".* Nanotechnology 20(2009).

Rahman, M., Ramakrishna, S., Prakash, J.R.S., and Tan, D.C.G. (1999)*"Machinability Study of Carbon Fiber Reinforced Composite."* Journal of Materials Processing Technology 89-90: 292-97. Science Direct. Web.

Rinzler, A., Liu, J., Dai, H., Nikolaev, P., Huffman, C., Rodriguez-Macias, F., Boul, P., Lu, A., Heymann, D., Colbert, D., Lee, R., Fischer, J., Rao, A., Eklund, P., and Smalley, R. (1998). *"Large-scale purification of single-wall carbon nanotubes: process, product, and characterization".* Applied Physics A: Materials Science and Processing 67 (1998), 29-37.

Schulte, K., Baron, Ch. (1988). *"Load and failure analyses of CFRP laminates by means of electrical resistivity measurements".* Composites Science and Technology 36(1989), 63-76.

Seidel, T.J., Galehdar, A., Rowe, W.S.T., John, S., Callus, P.J., Ghorbani, K. (2010). *"The anisotropic conductivity of unidirectional carbon fibre feinforced polymer laminates and its effect on microstrip antennas".* In the proceedings of Asia-Pacific Microwave Conference 2010.

Shaw, M. (2011) *"ATK Awarded Multi-million Dollar F-35 Contract."* Standard-Examiner - Top of Utah News & Multimedia. Web.

Sierakowski, R., Telitchev, I., Zhupanska, O. (2008). *"On the impact respose of electrified carbon fiber polymer matrix composites: Effects of electric current intensity and duration".* Composites Science and Technology 68 (2008), 639-649.

Snyder, D., Sierakowski, R., Chenette, E., Aus J. (2001). *"Preliminary assessment of electro-thermal-magnetically loaded composite panel impact resistance/crack propagation with high speed digital laser photography"*. Proceeding of SPIE 4183 (2001), 488-513.

SouthWest NanoTechnologies. (2010). *"SWeNT®SMW Technical Data Sheet Specialty Multiwall Carbon Nanotubes"*. Web.

Stenzenberger, H.D. (1993). *"Recent developments of thermosetting polymers for advanced composites".* Composite Structures, 24(1993), 219-231.

Structure Probe, Inc. (2005-2009). *"Properties of Cured Silver Films"*. Retrieved January 25, 2009.

Telitchev, I., Sierakowski, R., Zhupanska, O. (2008). *"Low-Velocity Impact Testing of Electrified Composites: Part I-Application of Electrical Current".* Experimental Techniques, 35-39.

Telitchev, I., Sierakowski, R., Zhupanska, O. (2008a). *"Low-Velocity Impact Testing of Electrified Composites: Part II-Experimental Setup and Prelimary Results".* Experimental Techniques, 53-57.

The University of Texas at Dallas. (2010). *"Nanotube Thermocells Hold Promise as Energy Source".*

Todoroki, A., Tanaka, M., Shimamura, Y. (2002). *"Measurement of orthotropic electric conductance of CFRP laminates and analysis of the effect on delamination monitoring with an electric resistance change method".* Composites Science and Technology, 62(2002), 619-628

Todoroki, A., Yoshida, J. (2004). *"Electrical Resistance Change of Unidirectional CFRP due to applied loads".* JSME Inernational Journal, 47(3), 357-363.

Top Shelf Sports. (2011). *"Hockey Stick Repair".*

Wang, D., Wang, S., Chung, D. D. L., & Chung, J. H. (2006). *"Comparison of the electrical resistance and potential techniques for the self-sensing of damage in carbon fiber polymer-matrix composites".* Journal of Intelligent Material Systems and Structures, 17(10), 853-861.

Wang, S. (2006). *"Characterization and Analysis of Electrical Conductivity Properties of Nanotube Composites".* Thesis. FAMU-FSU College of Engineering.

Water Jet Cutting World. (2011, Apr) *"What Is Water Jet Cutting."* Water Jet. 2.

Wazir, A., Kakakhel, L. (2009). *"Preparation and characterization of pitch-based carbon fibers".* New Carbon Materials, 24(1), 83-88.

Yeh, C., (2007). *"A Study of Nanostrucutre and Properties of Mixed nanotube Buckypaper Materials: Fabrication, Process Modeling Characterication, and Property Modeling".* Thesis. FAMU-FSU College of Engineering.

Zantout, A. (2009, May). *"Electrical and Impact Characterization of Carbon Fiber Polymer Matrix Composites".* Thesis. The University of Iowa. Print.

Zhupanska, O., Sierakowski, R. (2007). *"Effects of an electromagnetic field on the mechanical response of composites".* Journal of Composite Materials 41 (2007), 633-652.